UNIVERSIDADE FEDERAL DO RIO GRANDE DO SUL
FACULDADE DE MEDICINA

PROGRAMA DE PÓS-GRADUAÇÃO EM CIÊNCIAS DA SAÚDE:
CARDIOLOGIA E CIÊNCIAS CARDIOVASCULARES

TESE DE DOUTORADO

MÉTODOS DE IMAGEM NA AVALIAÇÃO VASCULAR

FELIPE SOARES TORRES

Orientador:
Dr. Miguel Gus

Porto Alegre, Dezembro de 2012

UNIVERSIDADE FEDERAL DO RIO GRANDE DO SUL
FACULDADE DE MEDICINA

PROGRAMA DE PÓS-GRADUAÇÃO EM CIÊNCIAS DA SAÚDE: CARDIOLOGIA E CIÊNCIAS CARDIOVASCULARES

TESE DE DOUTORADO

MÉTODOS DE IMAGEM NA AVALIAÇÃO VASCULAR

FELIPE SOARES TORRES

Tese de doutorado apresentada ao Programa de Pós-Graduação em Ciências da Saúde: Cardiologia e Ciências Cardiovasculares para obtenção do titulo de Doutor em Ciências Cardiovasculares.

Orientador:
Dr. Miguel Gus

Porto Alegre, Dezembro de 2012

FICHA CATALOGRÁFICA

Tese apresentada ao Curso de Pós-Graduação em Ciências da Saúde: Cardiologia e Ciências Cardiovasculares da Universidade Federal do Rio Grande do Sul em 13 de Dezembro de 2012, pela Comissão Examinadora constituída por:

Prof. Doutor Rogério E. G. Sarmento-Leite
Profa. Doutora Ticiana C. Rodrigues
Prof. Doutor Flávio D. Fuchs

CIP - Catalogação na Publicação

Torres, Felipe Soares
Métodos de Imagem na Avaliação Vascular / Felipe Soares Torres. -- 2012.
207 f.

Orientador: Miguel Gus.

Tese (Doutorado) -- Universidade Federal do Rio Grande do Sul, Faculdade de Medicina, Programa de Pós-Graduação em Ciências da Saúde: Cardiologia e Ciências Cardiovasculares, Porto Alegre, BR-RS, 2012.

1. Radiologia e Diagnóstico por Imagem. 2. Ultrassonografia. 3. Tomografia Computadorizada. 4. Ressonância Magnética. I. Gus, Miguel, orient. II. Título.

Elaborada pelo Sistema de Geração Automática de Ficha Catalográfica da UFRGS com os dados fornecidos pelo(a) autor(a).

DEDICATÓRIA

Aos meus pais, Jaime Torres Portos (*in memoriam*) e Sonia Elisabete Soares Kunzler. À minha esposa, Gabriela Pereira de Souza Favalli, e aos meu filhos Gustavo e Clarissa Favalli Torres.

AGRADECIMENTOS

Ao Programa de Pós Graduação em Ciências da Saúde Cardiologia e Ciências Cardiovasculares, pela oportunidade de poder conviver e aprender com pessoas de caráter, competência e dedicação extraordinários. Em especial, gostaria de agradecer de forma especial à Professora Doutora Sandra Costa Fuchs pela orientação, atenção e empenho para que esse momento pudesse se tornar realidade.

Ao meu Orientador, Doutor Miguel Gus, pela amizade, acessibilidade, interesse, disposição e incentivo constantes durante minha formação.

Aos amigos do Toronto General Hospital, em especial Narinder S. Paul, Andrew. M. Crean, Rachel M. Wald, Elsie T. Nguyen and Laura Jimenez-Juan. Aos amigos do Sunnybrook Health Sciences Centre, em especial ao colega e Chair of Radiology da Universidade de Toronto, Professor Alan Moody.

Ao grupo do Ambulatório de Hipertensão do Hospital de Clínicas de Porto Alegre, em especial ao Professor Doutor Flávio D. Fuchs, pela participação fundamental na sensibilização ao processo científico e pelo modelo de visão crítica da ciência.

Aos colegas e amigos do Serviço de Radiologia do Hospital de Clínicas de Porto Alegre, em particular aos Professores Álvaro P. A. Furtado e Luis A. Nasi.

À minha família, em especial a Sônia Elisabete Soares Kunzler, Jaime Torres Portos (*in memorian*), Caroline Torres Melo, Daniel Melo, Nicolas e Rafaela Torres Melo; a meus tios, Dionila e Félix Zanchet, e primos.

À minha amada esposa, Gabriela Favalli, pela companheirismo, paciência, compreensão e carinho imensuráveis. Aos meus filhos Gustavo e Clarissa, paixões de nossas vidas.

Esta tese de doutorado segue o formato proposto pelo Programa de Pós-Graduação em Ciências da Saúde: Cardiologia e Ciências Cardiovasculares da UFRGS, sendo apresentado na forma de Tese de Doutorado incluindo os artigos completos a serem submetidos para publicação, artigos já aceitos para publicação e já publicados.

SUMÁRIO

LISTA DE ABREVIATURAS EM PORTUGUÊS

ATCC – Angiotomografia Computadorizada Coronariana

AVC – Acidente Vascular Cerebral

CV - Cardiovascular

DAC – Doença Arterial Coronariana

DCV – Doença Cardiovascular

DP – Desvio Padrão

ECC – Escore de Cálcio Coronariano

EIM – Espessura das Camadas Íntima e Média

EIMC – Espessura das Camadas Íntima e Média das Artérias Carótidas

FC – Freqüência Cardíaca

HU – Unidades Hounsfield

IM – Infarto do Miocárdio

NIC – Nefropatia Induzida pelo Contraste

PC – Contraste de Fase (Angiografia por Contraste de Fase)

RM – Ressonância Magnética

TC – Tomografia Computadorizada

TGF – Taxa de Filtração Glomerular

TCMD - Tomografia Computadorizada de Múltiplas Fileiras de Detectores

US – Ultrassonografia

LISTA DE ABREVIATURAS EM INGLÊS

ABPM – Ambulatory Blood Pressure Monitoring

AHA – American Heart Association

BAV – Bicuspid Aortic Valve

CAD – Coronary Artery Disease

CCS – Coronary Calcium Score

CMR – Cardiovascular Magnetic Resonance

CoeffVi – Coefficient of Variance of an Individual

CoeffVp – Coefficient of Variance of the entire population

COPD – Chronic Obstructive Pulmonary Disease

CT – Computed Tomography

CTA – Coronary Computed Tomography Angiography

EBCT – Electrom Beam Computed Tomography

ECG – Electrocardiogram

ED – Effective Dose

FSE – Fast Spin Echo

HR – Hazard Ratio (introdução)

HR – Heart Rate (artigo original)

ICA – Invasive Coronary Angiography

ICC – Intraclass Correlatio Coefficient

IMT – Intima-media thickness

IQ – Image Quality

IV – Intravenous

LCC – Left Coronary Cusp

MDCT – Multidetector Computed Tomography

NCC – Non- Coronary Cusp

NPV – Negative Predictive Value

NR – Non-responders

PC – Phase Contrast

PPV – Positive Predictive Value

PW – Phase Window

R – Responders

RCC – Right Coronary Cusp

SSFP – Steady-State Free Precession

TOF – Time of Flight

TTE- Transthoracic Echocardiography

LISTA DE FIGURAS

LISTA DE TABELAS

1.Introdução

A doença cardiovascular (DCV) situa-se entre as principais causas de morte em todo o mundo. Estima-se que, ao nascimento, a probabilidade de morrer por DCV ao longo da vida seja de aproximadamente 47% e que, se todas as formas das principais doenças cardiovasculares fossem removidas, a expectativa de vida da população americana aumentaria em 7 anos (1). Em 2008, nos Estados Unidos, a DCV teve um custo estimado, direto e indireto, de 297.7 bilhões de dólares e foi responsável por 33.6% de todas as mortes, sendo a doença arterial coronariana (DAC) a causa de 1 em cada 6.6 mortes (1). Assim como nos Estados Unidos, as doenças do aparelho circulatório também são a principal causa de morte no Brasil, tendo sido responsáveis por cerca de 28.7% dos óbitos em 2010 (2).

O avanço tecnológico ocorrido na última metade do século XX permitiu o desenvolvimento de equipamentos capazes de adquirir imagens de alta qualidade e de fornecer importantes informações anatômicas e funcionais de forma não invasiva. Essas informações têm sido utilizadas no estudo das doenças do aparelho circulatório, em que os métodos de imagem têm desempenhado um papel tanto na estratificação de risco em pacientes assintomáticos quanto na avaliação de pacientes com doença cardiovascular estabelecida, estável ou não.

Diferentes métodos de imagem foram desenvolvidos e hoje se encontram disponíveis como ferramentas já estabelecidas na rotina de avaliação da DCV, destacando-se a ultrassonografia, a ressonância magnética e a tomografia computadorizada.

1.1 Ultrassonografia

A ultrassonografia (US), também conhecida como ecografia, utiliza as propriedades físicas das ondas sonoras para a geração de imagens de praticamente todas as estruturas do corpo humano com excelente resolução espacial e temporal. As ondas sonoras são distúrbios mecânicos que se propagam através de um meio (ondas sonoras não conseguem se propagar no vácuo) com determinada velocidade e número de oscilações por segundo, denominado de frequência (medida em Hertz, Hz). O som audível tem frequência entre 15 e 20.000 Hz (15-20 kHz). Já o ultrassom apresenta frequências maiores que 20 kHz e não pode ser percebido pelo ouvido humano. Em medicina, os equipamentos de US têm frequências que variam entre 1 e 20 MHz (1 Hertz = 1 ciclo por segundo; 1 MHz = 1 milhão de ciclos por segundo). O US utiliza as propriedades mecânicas das ondas sonoras e do meio onde a onda se propaga para gerar o chamado eco, o qual é utilizado para a formação da imagem utilizada clinicamente. Através da reflexão do pulso de US podemos determinar a posição, forma e velocidade de um objeto.

Para a formação da imagem utiliza-se o princípio pulso-eco através da utilização de um transdutor (em geral, transdutor é todo aquele dispositivo que converte energia de uma forma em outra). O transdutor do aparelho de US é a parte do equipamento que transforma energia elétrica em mecânica (ondas sonoras) e vice-versa. No transdutor, encontramos cristais

piezoelétricos, material com propriedade de gerar ondas sonoras com um estímulo elétrico (e reconhecer o estímulo mecânico, gerando sinais elétricos a partir do mesmo), os quais são responsáveis pela geração do pulso sonoro e pela detecção do eco. O pulso sonoro se propaga através do paciente, reflete nos tecidos interrogados e retorna em direção ao transdutor na forma de um eco. O eco é novamente transformado em sinais elétricos e a imagem é imediatamente formada e disponibilizada para o operador em tempo real.

A utilização dos dados (ecos) gerados pode ser realizada de diferentes maneiras para formação da imagem. A forma mais antiga, que não é mais utilizada clinicamente, utilizava o chamado modo A, ou modo de amplitude, na qual se usava um único gerador de pulso e eco que fornecia informações com relação à profundidade e amplitude do eco. O modo B, ou modo de brilho, permite a realização de uma varredura e a detecção de uma série de ecos, permitindo a formação de uma imagem tomográfica em tons de cinza de acordo com a intensidade do eco corrigida pelo tempo de retorno. O modo M, modo de movimento, utiliza o mesmo princípio do modo A e extrai continuamente, ao longo do tempo, informações sobre uma determinada fatia do corpo. O US de modo M é interpretado avaliando-se os padrões de movimento de refletores específicos e determinando as relações anatômicas de padrões característicos de movimento.

Uma outra forma de utilização do US é através do efeito Doppler, que descreve a mudança na frequência da onda sonora de um objeto em movimento em relação a um observador estacionário. No corpo humano, a ultrassonografia Doppler é muito útil para a avaliação do fluxo vascular, permitindo a detecção de fluxo sanguíneo (movimento), bem como as

alterações do fluxo causadas pela doença vascular. O US Doppler nos oferece a possibilidade de avaliação da velocidade do fluxo vascular através do Doppler de onda pulsada e da direção do fluxo sanguíneo através do Doppler colorido.

O US apresenta diversas vantagens em comparação com outros métodos de imagem disponíveis para a avaliação das doenças do aparelho circulatório.Trata-se de um método de custo relativamente baixo, amplamente disponível, que apresenta extensa experiência de uso e de risco praticamente inexistente. Por outro lado, é dependente da qualificação do operador, uma vez que cabe a ele o posicionamento do transdutor e a otimização dos parâmetros da imagem e documentação. Existe uma relação direta com a qualidade do equipamento utilizado e, notadamente, com as condições de propagação e reflexão da onda sonora no paciente. Por exemplo, a avaliação US das artérias renais depende da propagação do pulso sonoro através dos tecidos interpostos no abdômen e do retorno adequado do eco gerado. Na presença de distensão gasosa de alças intestinais interpondo-se entre o transdutor e o vaso retroperitonial, não será possível interrogar adequadamente as artérias renais utilizando-se o US. Da mesma forma, pacientes com doença pulmonar obstrutiva crônica e aumento do diâmetro da caixa torácica podem oferecer dificuldades quando da realização do ecocardiograma, tendo em vista a interposição dos pulmões entre o coração e o transdutor, que reduz o campo de interrogação pelo US (janela acústica). Quando aplicada à avaliação das doenças do aparelho circulatório, o US desponta como uma das principais ferramentas disponíveis para diagnosticar alterações vasculares e cardíacas, com inúmeras aplicações já presentes nos

algoritmos de avaliação, tratamento e seguimento de pacientes com DCV. Na investigação da doença vascular, em especial da doença do sistema carotídeo-vertebral, a US é considerada o método de escolha (indicação Classe I) para avaliação tanto de pacientes assintomáticos com suspeita de estenose carotídea como na avaliação de pacientes com sinais ou sintomas neurológicos potencialmente relacionados a evento isquêmico encefálico ou retiniano (3). Nas últimas décadas, diversos estudos com um grande número de pacientes estabeleceram a US como um método de imagem robusto para a avaliação da espessura das camadas íntima e média das artérias carótidas (4), medida que tem sido utilizada e recomendada para a estratificação de risco cardiovascular em pacientes assintomáticos (5, 6).

1.1.a Ultrassonografia das Camadas Íntima e Média das Artérias Carótidas

A US das artérias carótidas tem sido tradicionalmente utilizada na avaliação da doença cerebrovascular, em que a quantificação da velocidade de fluxo nesses vasos pelo estudo Doppler permite estratificar o risco de acidente vascular cerebral (AVC) e indicar a estratégia terapêutica mais adequada, tanto em pacientes sintomáticos (7, 8) quanto em assintomáticos (9). Mais recentemente, a US foi avaliada em estudos epidemiológicos e de estratificação de risco para a mensuração da espessura das camadas íntima e média (EIM) das artérias carótidas (EIMC) e para a determinação e caracterização de placas ateroscleróticas (10-23). Considerando que estenose significativa é aquela causada pela obstrução de pelo menos 50% da luz da carótida, não é surpresa o baixo rendimento do uso do Doppler em

estudos de base populacional e em pacientes assintomáticos, uma vez que a probabilidade pré-teste de doença carotídea obstrutiva significativa nesses pacientes é baixa (24).

Diversos estudos prospectivos demonstraram que um valor aumentado da EIM das artérias carótidas em pacientes sintomáticos e assintomáticos associa-se, independentemente de outros fatores de risco, à doença coronariana e cerebrovascular (11-16, 19-22).

Salonen e cols. (11), estudando prospectivamente 1257 homens finlandeses, demonstraram que o aumento de 0,19mm na EIM das artérias carótidas comuns associou-se de forma significativa e independente com o risco de desenvolvimento de infarto do miocárdio (IM), em um seguimento que variou de 1 mês a 3 anos, com um Razão de Risco (HR – "Hazard Ratio") de 1,22.

No estudo ARIC (12), para um aumento de 0,19mm na média da EIM das artérias carótidas (comum, bifurcação e interna), foi encontrado um HR para AVC, ajustado para sexo e idade, de 1,60 (IC95% 1,41 - 1,81) em mulheres e 1,31 (IC95% 1,15 - 1,49) em homens. O valor correspondente para o risco de IM foi de 1,69 (IC95% 1,50 - 1,90) em mulheres e 1,36 (IC95% 1,23 - 1,51) em homens.

No estudo de Rotterdam (13), para um aumento na EIM das artérias carótidas comuns de 0,163mm (um desvio padrão, DP), os HRs para AVC e IM, ajustados para sexo e idade, foram de 1,41 (IC95% 1,25 a 1,82) e 1,43 (IC95% 1,16 a 1,78) respectivamente. O ajuste para outros fatores de risco cardiovasculares mostrou os respectivos valores de 1,34 (IC95% 1,08 – 1,67) e 1,25 (IC95% 0,91 – 1,72).

O “Cardiovascular Health Study” (15) demonstrou que um aumento de 0,2mm (1 DP) na medida da EIM das artérias carótidas comuns de pacientes com idade maior que 65 anos resultou em um HR, ajustado para sexo, idade e diversos fatores de risco, de 1,24 (IC95% 1,12 - 1,38) e de 1,28 (IC95% 1,16 - 1,42) para IM e AVC respectivamente.

Kitamura e cols. (19) estudaram a associação entre a EIM das carótidas comuns e a incidência de AVC em 1289 homens idosos japoneses durante um seguimento médio de 4,5 anos. O risco relativo, ajustado para múltiplos fatores de risco, de pacientes no quartil de espessura mais alto (EIM maior ou igual a 1,07mm) comparado àqueles no quartil mais baixo (EIM menor ou igual a 0,7mm) foi de 3,0 (IC95% 1,1 -8,3).

O estudo CAPS (20) avaliou 5056 indivíduos em uma ampla faixa etária por um período médio de 4,2 anos. Para o desfecho combinado de IM, AVC ou morte por qualquer causa, um aumento de 1 DP na medida da EIM da carótida comum (0,16mm) e da bifurcação carotídea (0,34mm) correspondeu a um HR de 1,17 (IC95% 1,08 a 1,26) e 1,14 (IC95% 1,05 a 1,24), respectivamente, ajustados para sexo, idade e múltiplos fatores de risco. Além disso, o HR para cada aumento de 1 DP foi consideravelmente maior em pacientes mais jovens (<50 anos).

O estudo SMART (21) avaliou a associação entre a EIM das artérias carótidas comuns e a incidência de eventos vasculares (morte, IM não fatal ou AVC) em 2374 indivíduos com doença arterial manifesta ou fatores de risco cardiovasculares. O HR associado com a ocorrência de um evento vascular, ajustado para idade e sexo, para um aumento de 1 DP na EIM

(0,32mm), foi de 1,18 (IC95% 1,04 -1,32). O HR associado com a ocorrência de AVC isquêmico foi de 1,35 (IC95% 1,16 - 1,59).

Considerando-se a capacidade da EIM das artérias carótidas em predizer eventos cardiovasculares futuros em pacientes assintomáticos e a performance variável dos escores clínicos de predição de risco, como o escore de Framingham (25), considerou-se a possibilidade de investigar o benefício adicional da medida da EIM das artérias carótidas na estratificação de risco cardiovascular além daquele fornecido pelos fatores de risco tradicionais e escores clínicos atualmente utilizados (26-31).

O estudo GENIC (32) comparou o escore de Framingham com a EIM e ocorrência de placas ateroscleróticas nas artérias carótidas comuns de 510 indivíduos com AVC com os de 510 controles. Houve significativa correlação entre as variáveis medidas, sendo que o uso da medida da EIM e da presença de placas nas artérias carótidas comuns complementou a avaliação de risco cardiovascular oferecida pelo escore de Framingham.

O estudo PARC-AALA (33), estudo observacional com 2634 indivíduos, demonstrou significativa correlação entre o escore de Framingham e a EIM das artérias carótidas comuns em uma população que incluía pessoas de diversas regiões geográficas do mundo, incluindo 692 indivíduos da América Latina. Entretanto, houve uma grande dispersão da distribuição do escore individual de acordo com a medida da EIM das carótidas, indicando que o escore de risco de Framingham e a medida da EIM das carótidas podem não refletir exatamente o mesmo componente de risco cardiovascular. Isto vai ao encontro dos estudos previamente mencionados que demonstraram que a EIM das carótidas é um marcador de

risco cardiovascular, independente de fatores de risco cardiovasculares modificáveis e não modificáveis.

O estudo observacional PARC (34), que incluiu 5199 indivíduos com idade entre 30 a 79 anos, igualmente demonstrou significativa correlação entre o escore de Framingham e a medida da EIM das artérias carótidas comuns.

Baldassarre e cols. (23) acompanharam 248 pacientes com escore de risco de Framingham <20% (baixo ou intermediário) por mais de 5 anos. A utilização da medida máxima da EIM das artérias carótidas melhorou significativamente o valor preditivo do escore de Framingham. Pacientes com escore estimado entre 10 e 20% (tradicionalmente considerados como de risco intermediário) e que apresentavam EIM das carótidas acima do percentil 60 para homens e 80 para mulheres passaram a fazer parte da mesma categoria de risco de pacientes com escore de Framingham entre 20 e 30%, o que claramente implica em uma mudança na estratégia terapêutica desses indivíduos.

Bard e cols. (29) estudaram o efeito da mensuração da EIM das artérias carótidas na estratificação de risco de 95 pacientes com risco cardiovascular intermediário estimado pelo escore de Framingham. Com a utilização de pontos de coorte tradicionalmente utilizados na literatura, mais de 65% dos pacientes tiveram seu risco cardiovascular reajustado. Ou seja, a avaliação da aterosclerose carotídea através do exame de US teria um valor adicional na estratificação de risco além daquele fornecido pelas variáveis tradicionalmente utilizadas, como o escore de Framingham.

Assim, em pacientes classificados como de risco cardiovascular baixo ou intermediário pelo escore de Framingham, a medida da EIM das carótidas pode ser clinicamente útil como um suplemento ao escore de Framingham nas decisões de modificação de risco cardiovascular (28), fato recomendado pela Associação Americana de Cardiologia em 2001 (27). Além disso, a identificação de indivíduos assintomáticos com doença arterial subclínica pode ser considerada como o melhor teste de rastreamento para predizer a ocorrência de eventos coronarianos e para que possa ser oferecido um tratamento agressivo de redução de risco (31). Em 2003, o relatório da 34ª Conferência de Bethesda concluiu que pacientes classificados como de risco intermediário para eventos cardiovasculares totais possivelmente se beneficiariam de estratificação de risco adicional por um teste não invasivo, como a medida da EIM das artérias carótidas ou do escore de cálcio coronariano (35). Em 2007, a força tarefa para o manejo da hipertensão arterial da Sociedade Europeia de Hipertensão e Sociedade Europeia de Cardiologia recomendou o uso do US carotídeo em pacientes hipertensos tanto para reestratificação do risco cardiovascular como para avaliação de lesão em órgão alvo (36). Relatório de consenso da Sociedade Americana de Ecocardiografia (2008) para o uso da US de carótidas como método de rastreamento de doença aterosclerótica subclínica recomenda o uso em pacientes com risco intermediário de DCV sem doença CVD estabelecida ou diabetes (37). Nessa mesma linha, a diretriz da “Society for Heart Attack Prevention and Eradication” (SHAPE) recomenda avaliação periódica da EIM das artérias carótidas em todos os pacientes assintomáticos do sexo masculino com idade entre 45-75 anos e femininos entre 55-75 anos (38).

Novos estudos, entretanto, têm trazido controvérsia sobre a real utilidade da utilização da medida da EIM das artérias carótidas na estratificação de risco cardiovascular, particularmente à luz de outros métodos de avaliação da doença arterial subclínica (39). Uma recente metanálise concluiu que o uso de métodos de imagem, incluindo a medida da EIM das artérias carótidas, para a avaliação da doença aterosclerótica subclínica pode resultar em melhora na estratificação de risco cardiovascular (5). No entanto, outra metanálise utilizando dados individuais de mais de 45.000 pacientes de 14 estudos de coorte demonstrou apenas uma pequena melhora na predição do risco cardiovascular em 10 anos, quando a medida da EIM das artérias carótidas foi adicionada ao escore de risco de Framingham (40). Mais recentemente, o estudo multicêntrico IMPROVE demonstrou que a medida da EIM das artérias carótidas em 3703 indivíduos teve valor aditivo com relação à acurácia do escore de risco de Framingham na predição de risco cardiovascular (41). Os autores concluíram que uma estratégia de estratificação de risco baseada na EIM das artérias carótidas como um adjunto do escore de risco de Framingham parece ser uma abordagem racional na prevenção de doença cardiovascular.

1.1.b. Técnica da Medida Ultrassonográfica das Camadas Íntima e Média das Artérias Carótidas

Nas artérias carótidas, o US permite a visualização de duas linhas ecogênicas (brilhantes) criadas pela interface entre a luz arterial e a camada íntima e entre a camada média e a adventícia (42-46). O espaço compreendido entre essas duas linhas corresponde à soma das camadas

íntima e média (43) e pode ser identificado tanto na parede anterior (mais próxima ao transdutor) quanto na posterior (mais afastada do transdutor) do vaso examinado.

Para fins de avaliação do risco cardiovascular não está claramente estabelecido se a parede do vaso a ser medida é a mais próxima ou a mais distal ao transdutor (47) (11-15, 19-21, 23). A medida da parede proximal é, na melhor das hipóteses, uma aproximação da real EIMC (44) e é muito dependente da qualidade e dos ajustes técnicos do aparelho de US (11, 14, 19, 23, 47, 48). Por outro lado, tem sido demonstrado que a medida da EIMC da parede proximal pode ser obtida em uma considerável proporção dos indivíduos com boa reprodutibilidade, não devendo ser, portanto, menosprezada. No entanto, alguns autores sugerem que seja analisada separadamente (49, 50). Parece, assim, que a medida da EIMC da parede distal é a preferida (28, 50, 51), uma vez que estudos que compararam os achados de US com a histologia indicam que as medidas da parede distal são mais indicativas da real espessura da parede do vaso (43-46), além de serem mais reprodutíveis (49).

Diferentes segmentos das artérias carótidas podem ser estudados, incluindo a carótida comum, a bifurcação carotídea, o bulbo e a carótida interna. Sabe-se que a doença aterosclerótica tem maior manifestação no bulbo e bifurcação carotídeos, mas, são nestes setores onde se encontram as maiores dificuldades para o examinador (17, 48, 49, 52). No estudo ARIC, a medida da EIMC na carótida comum foi obtida em 91,4% dos pacientes, comparativamente a somente 48,6% na carótida interna (10). Em uma tentativa de padronizar as medidas, o “Mannhein Intima-Media Thickness

Consensus" sugeriu que a medida da carótida comum é a ideal (50). Com relação à capacidade de predição de eventos futuros, parece que todos os segmentos apresentam capacidade semelhante (10, 17, 51, 52), embora alguns autores considerem que a adição dos valores encontrados no bulbo e carótida interna aumenta a força da associação com aterosclerose coronariana (15, 53, 54). O recente estudo IMPROVE (41) demonstrou que, para todos os segmentos carotídeos (comum, bifurcação e carótida interna), um valor aumentado da EIMC se associa com aumento de risco cardiovascular e que não parece haver diferenças importantes na capacidade da medida dos diferentes segmentos em refletir risco, sugerindo que a medida da EIMC da carótida comum seja tão boa quanto uma medida mais elaborada incluindo outros segmentos (55).

A reprodutibilidade das medidas da EIMC depende do segmento avaliado (49), da espessura total medida (49) e do tipo de aferição realizada, automática ou manual (56). Tem sido sugerido que a variabilidade da medida é menor quando se determina a espessura média do segmento distal da artéria carótida comum em mais de uma direção (48). Além disso, grande parte da variabilidade na medida é causada por diferenças entre observadores, enquanto que a intraobservador parece ser menor (48, 49). Estudos que utilizaram detectores automáticos através de softwares específicos também parecem demonstrar menor variabilidade na medida (42, 56). Mesmo assim, a medida manual da parede posterior da artéria carótida interna, quando comparada com a medida semiautomática, também demonstra boa reprodutibilidade (57).

Um fator importante a ser considerado na mensuração da EIMC é a presença de placa aterosclerótica no segmento avaliado, uma vez que é um achado frequente na população dentro da faixa etária de maior risco cardiovascular (58). A definição de placa e sua inclusão no relatório é consenso nos diferentes estudos (19, 23, 48, 49, 59, 60), sendo que alguns autores recomendam considerar a presença de placa aterosclerótica de forma separada da EIMC (50, 51, 61), já que poderiam representar indivíduos com perfis de risco cardiovascular diferentes (50, 61). O "Mannhein Intima-Media Thickness Consensus" definiu placa aterosclerótica como uma alteração focal que protrui para a luz arterial em pelo menos 0,5mm ou 50% do valor adjacente da EIMC ou uma medida da EIMC > 1,5mm (50).

Portanto, parece que a medida da espessura das camadas íntima e média da parede posterior da porção distal da carótida comum é a mais fácil e mais reprodutível dentre todas as opções. Além disso, apresenta associação definida com maior incidência de doença cerebrovascular e coronariana. Quando for realizada a mensuração no bulbo e carótida interna, os valores podem ser avaliados separadamente, não incluindo na medida placas ateroscleróticas, as quais também devem ser descritas de forma distinta.

1.1.c Recomendações de Diretrizes

Em 2008, a Sociedade Americana de Ecocardiografia publicou um documento de consenso a respeito do uso da EIM das artérias carótidas na avaliação de doença vascular subclínica e na estratificação de risco cardiovascular (37). O documento indica que a medida da EIM das artérias

carótidas e a identificação de placa aterosclerótica pelo US são mais úteis para o refinamento da avaliação de risco CV em pacientes com risco intermediário (6 a 20%, de acordo com o escore de risco de Framingham e sem evidência de DAC, doença arterial periférica, doença cerebrovascular, diabete melitus ou aneurisma de aorta abdominal). Em contrapartida, Força Tarefa da US Preventive Services, em 2009, considerou serem insuficientes as evidências disponíveis para que se pudesse fazer uma recomendação específica com relação ao uso de fatores de risco não tradicionais na avaliação de risco CV, incluindo a medida da EIM das artérias carótidas (62). A diretriz mais recente da American Heart Association e American College of Cardiology Foundation (AHA/ACCF) para a avaliação de risco cardiovascular em adultos assintomáticos considera que a avaliação de risco que utiliza os modelos de predição de risco vigentes se estende com a informação de história familiar de DCV como um primeiro passo (6). Indivíduos considerados de risco baixo ou alto, de acordo com essa avaliação inicial, não requerem testes adicionais. Entretanto, testes adicionais, incluindo a medida da EIM das artérias carótidas, poderiam ser úteis para guiar a terapia para aqueles de risco intermediário. Nesse cenário, a AHA/ACCF considera a medida da EIM das artérias carótidas como razoável (Recomendação classe IIa, nível de evidência B) (6). Mais recentemente, a Society of Atherosclerosis Imaging and Prevention publicou critérios de uso apropriado para a medida da EIM das artérias carótidas em que considerou como apropriado o uso da medida para a detecção inicial de risco cardiovascular em pacientes considerados de risco intermediário (63). Ainda, em pacientes sem doença CV estabelecida, o uso também foi considerado apropriado para aqueles com síndrome

metabólica e com idade ≥30 anos, com diabete melitus, com risco CV intermediário e história familiar de doença CV prematura e para pacientes com risco cardiovascular intermediário e escore de cálcio coronariano igual a zero (63).

1.2 Tomografia Computadorizada

A tomografia computadorizada (TC) é um método que utiliza os raios-X para a formação da imagem e que foi desenvolvido no início da década de 70, mas somente na década de 80 seu uso se expandiu de forma significativa para praticamente todas as áreas da medicina.

Os raios-X são uma forma de radiação eletromagnética que se propaga através do espaço e interage com os átomos da matéria. Eles são fótons originados na eletrosfera de um átomo, diferindo dos raios gama, os quais, apesar de também serem fótons, se originam do núcleo do átomo. Os raios-X são produzidos dentro do tubo de raio-X, uma cápsula blindada com uma abertura para onde os fótons produzidos são direcionados. Dentro dessa cápsula, filamentos emissores de elétrons localizados no cátodo são excitados por uma corrente elétrica e criam uma nuvem de elétrons. No lado oposto ao cátodo, localiza-se o ânodo, estrutura giratória que contém uma placa metálica. Criando-se uma diferença de potencial entre o cátodo e o ânodo, os elétrons localizados no cátodo irão se deslocar em alta velocidade em direção ao ânodo e se chocar com a placa metálica, gerando os raios-X, os quais serão direcionados pela angulação do ânodo, em sua maioria, para a abertura do tubo. Após deixar o tubo, os fótons atravessarão o objeto de

interesse (paciente), posicionado entre o tubo e o detector, e atingirão o detector do equipamento de TC. A atenuação do feixe de energia causada durante a passagem através dos tecidos do paciente e registrada pelo detector vai permitir a avaliação da composição física desses tecidos, assim formando a imagem.

No raio-X convencional, um feixe de energia uniforme é direcionado ao paciente e sai na superfície oposta do mesmo codificado com as variações da intensidade que resultam das diferentes atenuações que o feixe de raio-X sofre ao longo do seu trajeto através do paciente. Na TC, diferentemente do sistema convencional em que o padrão de atenuação é gravado em uma superfície bidimensional (o receptor da imagem - filme), há a informação de múltiplos feixes de raios-X que atravessam os tecidos do paciente em diferentes angulações e são detectados à medida que o tubo e o conjunto de detectores giram ao redor do paciente. Desta forma, a TC é capaz de gerar uma imagem transversal eliminando a superposição de estruturas que ocorre no exame convencional, em que há a compressão de uma estrutura tridimensional em um sistema detector bidimensional.

A primeira geração de equipamentos de TC foi introduzida no mercado no início da década de 70. Nesse tipo de equipamento, a fonte de raios-X (o tubo) movia-se em paralelo e em conjunto com um único detector localizado do outro lado do paciente. O movimento do conjunto era em linha reta e produzia uma única projeção. Após a aquisição de pelo menos 180 projeções, com diferenças de angulação de 1 grau, uma imagem transversal era produzida, o que demorava cerca de 4 a 5 minutos. A colocação de mais de um detector no conjunto caracterizou a segunda geração de TC,

permitindo reduzir o tempo de aquisição de uma imagem transversal proporcionalmente ao número de detectores adicionados. A terceira geração de equipamentos permitiu um grande salto tecnológico e o advento da TC helicoidal, uma vez que uma fileira de detectores foi colocada em forma de arco no lado oposto ao da fonte de raios-X, permitindo um movimento rotacional ao invés de em linha reta como até então. O desenvolvimento em conjunto de tubos de alta energia, da tecnologia chamada “slip-ring”, em que a transmissão de energia e dados de forma contínua permitia a rotação ininterrupta do conjunto fonte-detector, e de novos algoritmos de reconstrução da imagem forneceu o substrato para o lançamento da tomografia helicoidal. Nesse método, o conjunto tubo-detector gira ao redor do paciente, e a mesa onde o paciente está posicionado desloca-se de forma contínua até que a anatomia de interesse seja coberta de forma integral. Com o advento da tomografia de múltiplas fileiras de detectores (TCMD), no início da década de 90, foi possível reduzir o tempo de aquisição de imagem de forma significativa, permitindo estudar de maneira rápida estruturas em movimento como o coração e as artérias coronárias. Ao invés de o feixe de raios-X incidir sobre somente uma fileira de detectores posicionada em forma de arco em torno do paciente (e, assim, gerar somente uma imagem transversal por rotação), múltiplas fileiras foram adicionadas ao longo do eixo longitudinal do paciente, permitindo que, com uma circunvolução do conjunto tubo-detectores, múltiplas imagens transversais pudessem ser geradas ao mesmo tempo. Inicialmente, 2 fileiras de detectores foram desenvolvidas (1992), subsequentemente passando a 4, 6, 8, 16, 32, 64, 128 e 320 (2008). Tecnologias mais atuais permitem a aquisição de 640 imagens transversais

por rotação do tubo com 0.5 mm de espessura cada. Ainda, alguns fabricantes desenvolveram equipamentos com 2 tubos de raios-X angulados e que atuam ao mesmo tempo, permitindo a redução no tempo de aquisição de uma imagem (reduzindo a resolução temporal). Todas essas evoluções tecnológicas (64) resultaram na capacidade da TC de adquirir imagens de forma muito rápida (alta resolução temporal) e com alta definição (alta resolução espacial e resolução de contraste), permitindo o uso desse equipamento na avaliação de vasos de grande, médio e pequeno calibre, incluindo as artérias coronárias.

1.2.a. Escore de Cálcio Coronariano

O escore de cálcio coronariano (ECC) é gerado a partir de imagens tomográficas das artérias coronárias sem a necessidade de utilização de meio de contraste intravenoso. Inicialmente desenvolvido com base na TC por feixe de elétrons, há mais de 20 anos, atualmente é realizado utilizando-se a TCMD (65). O método mais utilizado e difundido foi desenvolvido por Arthur Agatston e colaboradores (66) e é conhecido pelo escore de Agatston. Nesse escore, quando há pelo menos 3 elementos de imagem (chamados de pixels) dispostos lado a lado e com atenuação de pelo menos 130 unidades Hounsfield (HU), esses pixels são identificados como pertencentes a uma placa aterosclerótica calcificada. A multiplicação do número de pixels (área) pela atenuação máxima dessa região (representado por um fator de densidade) fornece um número que, somado a todos os outros números representando todas as placas ateroscleróticas coronarianas, resulta no escore de cálcio das artérias coronárias (escore de Agatston ou somente

ECC). A forte correlação entre a quantidade de cálcio coronariano detectado através do ECC e a presença e extensão de placa aterosclerótica em análise histológica foi demonstrada por Rumberger e colaboradores (67, 68). Posteriormente, Baumgart e colaboradores (69) e Schmermund e colaboradores (70) confirmaram a associação direta, in vivo, da localização e extensão da placa aterosclerótica detectada pelo ECC e pelo US intravascular.

O ECC é um método robusto, reprodutível e que demonstra, de forma não invasiva, a carga aterosclerótica nas artérias coronárias (65). O ECC se estabeleceu como o preditor mais forte de DAC em pacientes assintomáticos, superando e demonstrando valor aditivo aos escores de risco tradicionais tal como o Escore de Risco de Framingham.

Raggi e colaboradores (71) compararam a habilidade do ECC e dos fatores de risco CV tradicionais para a predição de infarto do miocárdio e morte em 676 pacientes com risco CV intermediário em seguimento de 3 anos. O ECC ajustado para sexo e idade forneceu os modelos com melhor capacidade de predição de risco para a ocorrência de eventos duros e incrementou a informação prognóstica fornecida pelos fatores de risco tradicionais (71).

Shaw e colaboradores (72) avaliaram mortalidade por todas as causas em 10377 indivíduos assintomáticos com uma probabilidade pré-teste intermediária para DAC seguidos por 5 ± 3,5 anos. Em ambos os sexos, o ECC se mostrou um preditor independente de morte. A inclusão do ECC em modelos multivariados que utilizavam os fatores de risco CV aumentou de forma significativa a capacidade de predição de mortalidade total (72).

Greenland e colaboradores (73) avaliaram a ocorrência de desfechos CV maiores em 1312 pacientes com idade > 45 anos, sem diabetes e com pelo menos um fator de risco tradicional em um seguimento de 7 anos (mediana). A presença de cálcio detectado através do ECC foi preditora de eventos e incrementou a informação prognóstica fornecida pelos fatores de risco tradicionais. O benefício do uso do ECC foi marcado, entretanto, somente em pacientes com risco cardiovascular intermediário de acordo com o escore de risco de Framingham (risco de eventos duros em 10 anos entre 10 e 20%) (73).

Detrano e colaboradores (74) avaliaram a capacidade do ECC em predizer eventos em 6722 indivíduos de diversas etnias e sem doença CV prévia, em um seguimento de 3,8 anos (mediana). Os autores demonstraram que o ECC é um forte preditor de DAC e que oferece informação prognóstica adicional àquela oferecida pelos fatores de risco tradicionais (74).

Polonsky e colaboradores (75), avaliando 5878 participantes do estudo MESA (Multi-Ethnic Study of Atherosclerosis), investigaram se a adição do ECC a um modelo de predição de risco baseado nos fatores de risco tradicionais melhora a classificação de risco CV. Após um seguimento de 5.8 anos (mediana), a adição do ECC aos fatores de risco tradicionais resulta em uma significativa melhora na classificação de risco para a predição de DCV, achado que se reproduz em diferentes grupos étnicos, em homens e mulheres (75). Indivíduos com risco CV intermediário obtiveram o maior benefício com o uso do ECC para reclassificação de risco. Resultados semelhantes foram obtidos nas coortes de Rotterdam (76) e Heinz Nixdorf

(77), em que foram estudados 2028 indivíduos seguidos por 9,2 anos e 4487 indivíduos seguidos por 5 anos, respectivamente.

Recentemente, Yeboah e colaboradores (39) avaliaram a capacidade de diversos marcadores de risco, incluindo o ECC, em melhorar a predição de risco cardiovascular em pacientes com risco intermediário (entre 5 e 20%) pelo escore de risco de Framingham. Após um seguimento de 7,6 anos (mediana), o ECC se associou de forma independente com DCV incidente e determinou o maior aumento da área sob a curva ROC (receiver operator characteristic curve) dentre todos os marcadores estudados (39).

O valor prognóstico da ausência de calcificação coronariana foi sumarizado em uma revisão sistemática que incluiu 13 estudos e mais de 29.000 pacientes (78). Em um seguimento médio de 50 meses, a incidência de eventos cardiovasculares em indivíduos com ECC = 0 foi de 0,47% (78), o que demonstra um excelente prognóstico na ausência de calcificações coronarianas em indivíduos assintomáticos.

1.2.a.1 Recomendações de Diretrizes

O ECC já é considerado por diretrizes nacionais e internacionais como um método para a estratificação do risco cardiovascular em pacientes assintomáticos e de risco cardiovascular intermediário (6, 38, 79, 80). Recente recomendação de consenso de diversas entidades médicas internacionais considerou apropriado o uso do ECC para avaliação de pacientes assintomáticos e com risco cardiovascular intermediário e para pacientes com risco cardiovascular baixo, mas com história familiar de DCV prematura (81). O valor do uso do ECC para avaliação de DAC em pacientes

sintomáticos ainda é motivo de debate, tendo em vista os resultados conflitantes quando utilizado para excluir DAC obstrutiva (82). Mesmo assim, diretrizes britânicas recomendam a realização de ECC em pacientes com dor torácica e baixa probabilidade pré-teste de DAC (83). A American Heart Association considera razoável o uso do ECC em pacientes sintomáticos (65).

1.2.b Angiotomografia Computadorizada Coronariana

A angiotomografia computadorizada coronariana (ATCC) utiliza meio de contraste iodado intravenoso para gerar imagens com alta definição das artérias coronárias. Alguns pré-requisitos, entretanto, devem ser observados para que o exame possa ser realizado e forneça qualidade de imagem diagnóstica, incluindo uma frequência cárdica regular e idealmente baixa (<60 bpm) (84), ausência de alergia ao contraste iodado (sempre necessário para contrastar o lúmen vascular) e função renal que permita a utilização do meio de contraste intravenoso. Além disso, um equipamento com no mínimo 64 fileiras de detectores é necessário (considerado adequado) para a realização do exame (81). Para a otimização da qualidade da imagem, certas intervenções frequentemente são necessárias antes e durante o exame (85), como por exemplo o uso de betabloqueadores para o controle da frequência cardíaca e de nitrato sublingual para provocar vasodilatação e melhorar a visualização das artérias coronárias. Após a aquisição das imagens, lança-se mão de técnicas de pós-processamento através de softwares específicos para a reconstrução das imagens das artérias coronárias em diferentes

planos, curvos ou retilíneos, e dimensões (2 ou 3 dimensões), com o objetivo de otimizar a avaliação anatômica do vaso.

A ATCC tem se estabelecido como método para a avaliação de pacientes com suspeita de DAC, fornecendo valiosa informação diagnóstica (86) e prognóstica (87) em pacientes sintomáticos com suspeita de DAC obstrutiva. Em 2008, o resultado de três estudos multicêntricos que avaliaram a sensibilidade e especificidade da ATCC, em comparação com a angiografia coronariana convencional, foi publicado e demonstrou excelente sensibilidade e moderada especificidade para a detecção de DAC obstrutiva (estenose luminal ≥ 50%) (88-90). Revisão sistemática com metanálise incluindo 28 estudos com 1286 pacientes foi publicada no mesmo ano, com resultados semelhantes (86). Na avaliação por paciente, a sensibilidade, especificidade, valor preditivo positivo e valor preditivo negativo encontrados foram de 99% (IC95%: 97-99%), 89% (IC95%: 83-94%), 93% (IC95%: 64-100%) e 100% (IC95%: 86-100%) respectivamente. Na avaliação por segmento coronariano (n=14199), a sensibilidade, especificidade, valor preditivo positivo e valor preditivo negativo encontrados foram de 90% (IC95%: 85-94%), 97% (IC95%: 95-98%), 76% (IC95%: 44-93%) e 99% (IC95%: 95-100%) respectivamente (86).

Recentemente, importantes estudos demonstraram a capacidade de a ATCC fornecer informações de valor prognóstico. Em uma revisão sistemática com metanálise, Bamberg e colaboradores (87) avaliaram a capacidade da ATCC em predizer eventos cardiovasculares em 11 estudos totalizando 7335 pacientes. A presença e a extensão de DAC obstrutiva demonstraram valor preditivo independente para eventos cardiovasculares

maiores, inclusive após ajuste para o ECC (87). Hulten e colaboradores (91) realizaram uma revisão sistemática com metanálise de 18 estudos prospectivos envolvendo 9592 pacientes e seguimento de 20 meses (mediana) para avaliar o valor prognóstico da ATCC. A taxa anual de eventos CV maiores (morte, infarto do miocárdio e revascularização) foi de 8,8% em pacientes com estenose luminal > 50% em comparação com 0,17% em pacientes com ATCC normal. A razão de verossimilhança negativa para eventos CV maiores após uma ATCC normal foi de 0,008 (IC95% 0,0004 a 0,17, p<0,001) (91).

A publicação de resultados de estudos envolvendo o registro internacional CONFIRM (Coronary CT Angiography Evaluation for Clinical Outcomes: An International Multicenter Registry) solidificou a ATCC como método para a avaliação de pacientes com probabilidade pré-teste baixa ou intermediária e com suspeita de DAC obstrutiva. Min e colaboradores (92) avaliaram mais de 24.000 pacientes consecutivos, sem evidência de DAC estabelecida, referidos para realização de ATCC por suspeita de DAC entre 2005 e 2009. Após seguimento de 2,3 ± 1,1 anos, os autores demonstraram significativa associação entre risco de morte (ajustado) e a presença de doença aterosclerótica obstrutiva (Hazard Ratio [HR]: 2.6; IC95%: 1.94 - 3.49) e não obstrutiva (Hazard Ratio [HR]: 1.6; IC95%: 1.18 - 2.16), em comparação com pacientes sem evidência de DAC. Além disso, observou-se uma nítida curva dose-resposta, com aumento progressivo do risco de morte em pacientes com doença não obstrutiva, doença obstrutiva de 1 vaso, 2 vasos e 3 vasos ou tronco da coronária esquerda (92).

Lin e colaboradores (93) avaliaram prospectivamente 2583 pacientes com evidência de aterosclerose coronariana não obstrutiva (sem estenose luminal ≥ 50%) na ATCC. Em um seguimento médio de 3,1 ± 0,5 anos e após ajuste para fatores de risco para DAC, a presença de placa aterosclerótica não obstrutiva se associou com aumento da mortalidade (HR: 1,98, IC95%: 1,06 - 3,69, p = 0,03), sendo que a maior extensão da aterosclerose, avaliada por DAC não obstrutiva em 3 vasos, se associou com maior risco de morte (HR: 5,12, IC95%: 2,16 - 12,10, p = 0,0002).

Além da avaliação de pacientes estáveis com suspeita de DAC, a ATCC tem demonstrado utilidade na avaliação de pacientes com dor torácica classificada como de risco baixo a intermediário na sala de emergência. Estudos observacionais prospectivos e ensaios clínicos randomizados têm demonstrado que a ATCC permite uma rápida estratificação de risco, excluindo a presença de síndrome coronariana aguda com elevado valor preditivo negativo.

O ROMICAT (Rule Out Myocardial Infarction Using Computer Assisted Tomography) foi um estudo observacional em pacientes com dor torácica de risco baixo a intermediário para síndrome coronariana aguda (SCA) (94). Todos os 368 pacientes realizaram ATCC, sendo que os resultados não foram revelados aos médicos assistentes ou pacientes. Este estudo demonstrou que 50% dos pacientes não apresentavam evidência de DAC e não desenvolveram SCA durante a hospitalização ou eventos cardiovasculares maiores em 6 meses de seguimento (94). Seguimento de 90.5% desses pacientes em 2 anos demonstrou taxa de eventos cardiovasculares maiores de 0%, 4,6% e 30,3% em indivíduos sem evidência

de aterosclerose na ATCC, com doença não obstrutiva e com DAC obstrutiva, respectivamente (95).

No estudo multicêntrico CT-STAT (Coronary Computed Tomographic Angiography for Systematic Triage of Acute Chest Pain patients to treatment), 699 pacientes com dor torácica na sala de emergência foram randomizados para avaliação com ATCC ou com cintilografia miocárdica com protocolo de repouso e estresse (96). O desfecho primário do estudo, tempo para o diagnóstico, foi significativamente menor no braço que utilizou ATCC, sendo reduzido em 54% em comparação com o braço que utilizou a cintilografia (mediana 2,9 versus 6,3 horas; p< 0,0001), sem diferença na taxa de eventos entre os grupos (96).

Uma metanálise que avaliou a utilidade clínica da ATCC na avaliação diagnóstica de pacientes com dor torácica atendidos na emergência foi recentemente publicada e incluiu 9 estudos com um total de 1349 pacientes (97). Os autores encontraram uma sensibilidade de 95% (IC95%: 88-100), especificidade de 87% (IC95%: 83-92) e razão de verossimilhança negativa de 0,06 (IC95%: 0-0,14) e positiva de 7,4 (IC95%: 4,8-10) para o diagnóstico de SCA nessa população de probabilidade pré-teste baixa a intermediária (97).

No estudo ROMICAT II, 1000 pacientes com dor torácica de baixo risco foram randomizados para uma estratégia que incluiu ATCC precoce ou atendimento usual (98). O desfecho primário, tempo de internação hospitalar, foi reduzido em 7,6h com a estratégia baseada na TC (p<0,001), sem diferença na taxa de eventos cardiovasculares.

Litt e colaboradores (99), em um ensaio clínico randomizado e multicêntrico, randomizaram 1370 pacientes que procuraram salas de emergência por dor torácica de risco baixo a intermediário para duas estratégias de avaliação: usual versus baseada na ATCC. Nenhum paciente com ATCC negativa morreu ou teve infarto do miocárdio em seguimento de 30 dias. Pacientes randomizados para ATCC tiveram maior taxa de alta da emergência (49,6% versus 22,7%; diferença, 26,8%; CI95%: 21,4 a 32,2) e menor tempo de internação hospitalar (mediana de18,0 horas versus 24,8 horas; P<0.001) em comparação com a estratégia de avaliação usual (99).

1.2.b.1 Recomendações de Diretrizes

A ATCC tem sua utilização endossada por sociedades internacionais em uma ampla gama de situações clínicas dentro da avaliação de doença arterial coronariana (81). Dentre essas indicações destaca-se a de avaliação de pacientes com suspeita de DAC e probabilidade pré-teste baixa ou intermediária, ou com resultado de exames anteriores duvidosos ou contraditórios (81). Alem disso, a ATCC foi recentemente incorporada em diretrizes europeias como alternativa à angiografia invasiva para a exclusão de SCA em pacientes avaliados na sala de emergência com dor torácica aguda e probabilidade pré-teste baixa a intermediária (Classe de recomendação IIa, Nível de evidência B) (100). Salienta-se que a AHA/ACCF considera inadequada a utilização da ATCC para a avaliação de risco cardiovascular em pacientes assintomáticos (Classe de recomendação III, Nível de evidência C) (6).

1.2.c. Riscos e Limitações Associados à Tomografia Computadorizada

A TC não é um método isento de limitações. Exposição à radiação ionizante, proveniente dos Raios-X, é uma questão a ser sempre considerada quando da utilização do exame. Recente estudo internacional demonstrou grande variação na dose de radiação de exames de ATCC, dependendo dos parâmetros de aquisição da imagem utilizados (101). Diversas adaptações dos protocolos de aquisição têm sido sugeridas para minimizar a dose mantendo a qualidade da imagem obtida (85). Salienta-se que a dose de radiação recebida pelo paciente quando da realização do ECC é similar à dose a que estamos expostos ao longo de um ano proveniente do meio-ambiente (102). No caso da ATCC, o tipo de equipamento utilizado e o controle rigoroso dos parâmetros de exposição quando da realização do exame são elementos determinantes da dose de radiação que o paciente irá receber (85). Tendo em vista que os efeitos da radiação ionizante a longo prazo (efeitos estocásticos) são cumulativos, um dos principais fatores determinantes da maior exposição populacional à radiação é o uso inadequado dos métodos diagnósticos. Indicação precisa e adequada permite a otimização da relação risco/benefício do exame. A repetição de estudos em um mesmo indivíduo, incluindo exames de TC, cintilografia miocárdica ou tomografia por emissão de pósitrons, pode, a longo prazo, determinar uma relação risco/benefício desfavorável. Nesse contexto, estratégias que utilizam métodos dependentes da radiação ionizante para rastreamento em um grande número de indivíduos assintomáticos já foram questionadas pelo mesmo motivo (103).

Tendo em vista a ainda insuficiente resolução temporal (rapidez da aquisição da imagem) da maioria dos equipamentos disponíveis (64), faz-se necessário o controle medicamentoso da frequência cardíaca (FC) do paciente para a realização da ATCC. O insucesso da redução da frequência cardíaca geralmente se traduz em um exame de baixa qualidade, por vezes não permitindo uma avaliação diagnóstica confiável (85). Os medicamentos mais frequentemente utilizados para reduzir a FC são os betabloqueadores, particularmente o metoprolol por via oral e/ou intravenosa, devido à segurança e ampla experiência de uso (104). Não se sabe, entretanto, qual a melhor estratégia para o controle da FC quando da realização da ATCC (105). Em pacientes com contraindicação ao uso de betabloqueadores, bloqueadores do canal de cálcio (106) e, mais recentemente, ivrabadina (107), podem ser utilizados, porém a experiência com o uso desses agentes, particularmente do último, ainda é limitada.

Por último, a ATCC requer o uso de meio de contraste iodado intravenoso. Em pacientes com déficit de função renal, deve ser avaliada a relação risco/benefício da realização do exame, uma vez que pode haver agravamento da função renal devido à utilização do contraste intravenoso, a chamada nefropatia induzida pelo contraste (NIC) (108). A definição de NIC tem variado na literatura, sendo que alguns autores sugerem o uso de valores relativos de aumento da creatinina sérica e outros, absolutos. A Sociedade Europeia de Urorradiologia (ESUR) define NIC como uma alteração na função renal com aumento de mais de 25% (ou 44 µmol/l) da creatinina basal que ocorre nos primeiros 3 dias após a administração de contraste intravascular na ausência de etiologia alternativa (108). O risco de

desenvolvimento de NIC depende fundamentalmente da função renal do paciente, sendo progressivamente maior nos indivíduos com taxa de filtração glomerular (TFG) estimada abaixo de 60 e particularmente abaixo de 45 mL/min/1.73m2 (108, 109). A maioria da evidência disponível com relação à incidência de NIC é referente ao uso intra-arterial em procedimentos de hemodinâmica, o qual parece conferir um maior risco em comparação ao uso intravenoso (108). Em pacientes que receberam contraste intravenoso para exame de TC, a incidência de NIC depende da função renal, sendo estimada em 0,0%, 2,9% e 12,1% em pacientes com TFG estimada de 45-59, 30-44 e <30 mL/min/1.73m2, respectivamente (110). Em pacientes sob risco de desenvolvimento de NIC, a avaliação cuidadosa da relação risco/benefício do uso de meio de contraste intravenoso deve ser a regra. Naqueles em que haja a necessidade de utilização de contraste intravenoso, expansão vascular com hidratação utilizando solução salina, ou solução de bicarbonato alternativamente, é recomendada para reduzir o risco de NIC (108).

Ainda, o uso de contraste iodado está associado com risco de desenvolvimento de reações adversas agudas (até 1 hora após a administração) ou tardias (entre 1 e 7 dias da administração) de graus variados, relacionadas a reações idiossincrásicas ou quimiotóxicas (111). A ESUR relata que reações leves podem ser encontradas em até 15% dos pacientes após o uso de meio de contraste de alta osmolalidade, em comparação com 3% de incidência após a utilização de contraste de baixa osmolalidade (111). Reações tardias, que envolvem principalmente a pele, têm incidência que pode atingir cerca de 15% dos indivíduos, dependendo do tipo de contraste utilizado (112). Reações agudas graves são mais raras, com

incidência de 0,22% com a utilização de meio de contraste de alta osmolalidade em comparação com 0,04% com o uso de contrastes de baixa osmolalidade (113). Pacientes com fatores de risco para o desenvolvimento de reações adversas podem necessitar de preparo medicamentoso. Quanto ao uso de esquemas profiláticos com corticóides (113), o uso de corticóide em esquema profilático demonstrou redução de cerca de 30% na incidência de reações em pacientes que utilizaram meio de contraste iônico (113).

1.3 Ressonância Magnética

Apesar de ser um método que já vinha sendo utilizado no estudo das doenças cardiovasculares desde o começo da década de 80, somente com o avanço tecnológico ocorrido no início dos anos 90 e, principalmente, na década passada, a ressonância magnética (RM) começou a ser utilizada de forma mais sólida na rotina da investigação da doença vascular.

Os equipamentos de ressonância magnética fazem uso das propriedades eletromagnéticas dos prótons presentes no núcleo dos átomos (ressonância nuclear magnética). Por serem amplamente presentes no corpo humano, os prótons de hidrogênio são os mais frequentemente utilizados. Embora o campo magnético de um único próton de hidrogênio seja minúsculo, o efeito agrupado de todos os prótons no corpo é mensurável. A geração das imagens pode ser compreendida em termos de manipulação da magnetização dos prótons de hidrogênio. Cada átomo de hidrogênio se comporta como um pequeno ímã que contém seu próprio, e minúsculo, campo magnético. Quando exposto a um campo magnético externo

extremamente potente, o campo magnético de cada hidrogênio individualmente tende a se orientar de acordo com o campo externo. Assim, os pequenos campos magnéticos individuais acabam se alinhando e formando uma magnetização conjunta. Através da aplicação de pulsos de radiofrequência em frequências determinadas, fazendo com que os prótons entrem em ressonância, é possível modificar a orientação do campo magnético agrupado dos prótons de hidrogênio. Essa modificação pode ser detectada com o auxílio de bobinas localizadas dentro do equipamento ou colocadas na superfície do paciente, próximas à região anatômica de interesse. A manipulação adicional do campo magnético através da criação de gradientes (variação na força do campo magnético no interior do magneto) permite a localização, espacial e temporal, e consequente captação seletiva dessa alteração do campo magnético em regiões específicas do corpo (anatomia de interesse). Quando esse processo se repete de forma ordenada, o sinal captado é transformado em uma imagem a qual é utilizada para fins diagnósticos.

A utilização das propriedades físicas dos prótons de hidrogênio fez da RM um método aplicável a praticamente todos os indivíduos, sem limitações decorrentes de janela acústica ou exposição à radiação ionizante. Devido a sua grande capacidade de caracterização tecidual, de quantificação do fluxo vascular e de avaliação funcional de diferentes estruturas e órgãos do corpo humano, a RM despontou como um dos principais métodos de imagem de avaliação não invasiva em praticamente todas as áreas da medicina. No aparelho circulatório, a RM desempenha um papel singular no estudo dos

vasos, centrais e periféricos, e do coração, com amplas possibilidades de aplicação clínica.

1.3.a Ressonância Magnética da Aorta Torácica

A RM é um método de imagem estabelecido na investigação de patologias da aorta torácica e abdominal, tendo em vista sua excelente resolução espacial e a capacidade de gerar imagens em múltiplos planos. Na avaliação das doenças da aorta, diversas técnicas de geração da imagem têm sido empregadas e oferecem uma série de alternativas dependendo das características clínicas do paciente e do tipo de alteração que se deseja investigar.

O método mais utilizado é a angiografia por RM com utilização de meio e contraste intravenoso (gadolínio). Diferentemente do meio de contraste iodado quando utilizado em exames de TC, o gadolínio não é diretamente visualizado pela RM. As moléculas do gadolínio provocam uma alteração na magnetização dos tecidos e estruturas adjacentes, aumentando o sinal desses tecidos e estruturas em determinados tipos de sequências de pulso (chamadas de sequências ponderadas ou pesadas em T1) e facilitando a visualização dessa anatomia. Quando os compostos contendo gadolínio são injetados dentro de vasos sanguíneos, há um grande aumento do sinal do sangue em comparação com as estruturas extravasculares, permitindo uma visualização preferencial da anatomia vascular. Diversos avanços tecnológicos, como a realização de aquisições em múltiplas estações utilizando o movimento da mesa do exame (114, 115), redução do tempo de aquisição com métodos aceleração da imagem (parallel imaging) (116) e a

utilização de métodos de compartilhamento do espaço K (time-resolved) (117), favoreceram a expansão e grande aceitação dessa modalidade na avaliação da doença vascular.

O uso de meio de contraste contendo gadolínio, entretanto, é limitado pela função renal do paciente, tendo em vista o risco de desenvolvimento de fibrose sistêmica nefrogênica naqueles com TFG estimada abaixo de 30 e, particularmente, abaixo de 15 mL/min/1.73m2. Assim, grande ênfase tem se colocado na avaliação da aorta sem a necessidade da utilização de meio de contraste. Diversas técnicas foram desenvolvidas, incluindo a angiografia por tempo de vôo (Time of Flight, TOF), a angiografia por contraste de fase (Phase Contrast, PC) e a angiografia baseada no tempo de decaimento T2. Essas técnicas não necessitam de meio de contraste para gerar imagens da anatomia vascular, mas apresentam vantagens e desvantagens dependendo da anatomia que necessita ser avaliada.

A técnica TOF utiliza o fluxo de sangue para dentro do plano de imagem (fatia), ou seja, os prótons do sangue que não tiveram sua magnetização manipulada por todos os pulsos de radiofrequência (ao contrário dos tecidos estacionários) para gerar as imagens (fenômeno chamado de tempo de vôo). As maiores limitações dessa técnica residem na perda de sinal quando o fluxo vascular não é laminar, ou seja, é complexo e turbulento, quando o fluxo é muito lento, ou quando ele é paralelo ao plano da imagem. Técnicas adicionais podem ser utilizadas para suprimir o sinal dos tecidos estacionários adjacentes, ou para avaliar seletivamente o fluxo venoso ou arterial, dependendo da orientação do fluxo sanguíneo. A angiografia por TOF geralmente é utilizada para a avaliação de vasos

intracranianos, carotídeos e de extremidade (118), não sendo utilizada para a avaliação da aorta.

A angiografia por contraste de fase (PC) se baseia na perda de sinal que ocorre com os prótons em movimento após a aplicação de gradientes bipolares (dois gradientes com polaridades opostas – chamados de codificadores de fluxo). Enquanto os prótons estacionários receberão os dois gradientes sem alteração em sua coerência de fase, prótons em movimento apresentarão perda de sinal proporcional à velocidade com que se movem. Após a codificação do fluxo nas 3 direções e a subtração das imagens estacionárias, somente o sinal proveniente dos vasos será demonstrado, gerando imagens angiográficas. Com essa técnica, tanto a velocidade como a direção do fluxo podem ser avaliadas. Essa técnica apresenta limitações quando o fluxo sanguíneo é turbulento ou complexo. A principal limitação desse método, entretanto, é o longo tempo de aquisição. Na avaliação da aorta torácica, a angiografia por PC é utilizada para a avaliação das velocidades e gradientes de pressão através de estenoses valvares (119), coarctação (120) na avaliação da dissecção aórtica (121).

A angiografia baseada no tempo de recuperação T2 utiliza a diferença no tempo de recuperação entre os tecidos para gerar imagens que destacam os tecidos contendo liquido e, assim, o sangue. Um método utilizado para a avaliação da aorta torácica é a angiografia com sincronização eletrocardiográfica baseada na sequência Fast Spin Echo (ECG-gated FSE). Essa sequência utiliza a rápida movimentação do sangue na sístole, com perda de sinal, e a lenta movimentação na diástole, com sinal mais intenso, para gerar as imagens através da subtração. Na aorta torácica, um estudo

prospectivo com 75 pacientes demonstrou qualidade de imagem ótima e satisfatória em 70 pacientes, sendo que, nos 34 pacientes com dissecção aórtica, o flap intimal foi consistentemente visualizado (122). Uma das limitações desse método é o tempo de aquisição ainda muito longo se comparado com a angiografia por RM que utiliza o gadolínio (1-3 minutos e 15-25 segundos respectivamente) (118).

Outro método de angiografia sem o uso de gadolínio que tem sido utilizado baseia-se na sequência Steady-State Free Precession (SSFP), em que o contraste tecidual gerado depende da relação entre a recuperação T2 e o decaimento T1 dos tecidos, o que produz imagens com alto sinal do sangue venoso e arterial (123). Tendo em vista o rápido movimento do sangue na aorta, sem a necessidade de supressão do sinal da gordura ou do sangue venoso, a angiografia SSFP tem ganho boa aceitação na avaliação da aorta torácica através de aquisições tridimensionais com uma relação sinal-ruído elevada (124, 125). Com o auxílio da sincronização eletrocardiográfica e de sincronização com o movimento respiratório, esse método pode adquirir imagens de muito boa qualidade em 5-10 minutos (118). Um estudo avaliou 50 pacientes consecutivos com suspeita de doença da aorta torácica e comparou a capacidade diagnóstica e qualidade da imagem da angiografia convencional com o uso do gadolínio e a angiografia SSFP (126). Não houve diferença na detecção de aneurisma, coarctação, dissecção, hematoma intramural e presença de trombo entre as técnicas, sendo que ambos os métodos demonstraram excelente qualidade de imagem. Da mesma forma, estudo retrospectivo com 21 pacientes comparou

as duas técnicas e demonstrou 100% de acurácia da angiografia SSFP para o diagnóstico de doenças da aorta (127).

A sequência com sincronização eletrocardiográfica cine-SSFP, em que as imagens são apresentadas como um filme (por isso o prefixo cine) através do ciclo cardíaco, também tem sido muito utilizada para a avaliação da aorta torácica. Este método permite uma avaliação anatômica com resolução espacial de poucos milímetros e resolução temporal (tempo de aquisição de uma imagem) bem abaixo dos 100 milissegundos. Cerca de 20-30 imagens podem ser adquiridas dentro de um ciclo cardíaco, utilizando-se uma aquisição multisegmentar que permite a visualização e aferição da distensibilidade do vaso durante a sístole e diástole (128). O alto contraste gerado entre o sangue e a parede do vaso permite também a medida do calibre vascular com precisão (129-131).

1.3.b Limitações da Ressonância Magnética

As limitações do método estão relacionadas a pacientes com implantes metálicos, incluindo certos clipes de aneurisma cerebral, marcapassos e desfibriladores implantáveis, que possam apresentar aumento da temperatura, alteração de funcionamento ou deslocamento decorrente da presença do campo magnético gerado pelo equipamento. Ainda, pacientes que possuem insuficiência renal de grau pelo menos moderado não devem receber o meio de contraste gadolínio devido ao risco aumentado de desenvolvimento de fibrose sistêmica nefrogênica (132). Pacientes com claustrofobia podem não tolerar a realização do exame de RM. Ainda, a baixa disponibilidade do equipamento e de pessoal capacitado

tecnicamente para a realização do exame têm limitado o crescimento dessa modalidade em algumas regiões do país.

1.3.b Recomendações de Diretrizes

Diretrizes internacionais para a avaliação e manejo das doenças da aorta torácica foram publicadas em 2010 (133). A avaliação por imagem é recomendada como Classe I para diversas patologias, incluindo síndromes genéticas, pacientes com válvula aórtica bicúspide e para a avaliação de risco e avaliação diagnóstica de dissecção de aorta em diferentes cenários clínicos. Ainda, o manejo cirúrgico de pacientes com aneurismas de aorta é baseado no diâmetro máximo da aorta torácica obtido por diferentes métodos de imagem, incluindo US, TC e RM (133).

2. Justificativa

Os métodos de imagem, incluindo a ultrassonografia vascular, a tomografia computadorizada coronariana e a ressonância magnética cardíaca ou vascular, são ferramentas muito utilizadas no estudo da anatomia, da função e da disfunção cardiovascular. Expande-se a utilização dos métodos de imagem para estratificação de risco cardiovascular a qual orientará a melhor estratégia de prevenção primária ou secundária. Neste cenário são amplas as possibilidades de pesquisa que envolvem métodos de imagem e a doença cardiovascular. Deve ser salientado que a contínua avaliação dos métodos disponíveis considerando-se diferentes aspectos faz-se necessária

para a quantificação formal do real benefício oferecido pelos mesmos, para definir a melhor estratégia de sua utilização e para desenvolver novas aplicações e tecnologias que possam aperfeiçoar a avaliação do paciente com DCV. A presente tese apresenta estudos que envolvem tal perspectiva, considerando a pesquisa em ultrassonografia vascular e espessura íntima de carótidas, angiotomografia de coronárias e escore de cálcio coronário e ressonância magnética de aorta.

3. Objetivos gerais :

Apresentar estudos que envolvem os diferentes métodos de imagem utilizados no estudo da doença vascular.

Serão apresentados quatro estudos a seguir:

1. **Torres FS**, Fuchs SC, Gus M *. Association between carotid intima-media thickness and retinal arteriolar and venular diameter in patients with hypertension: a cross-sectional study.
* Em nome dos coautores do Estudo Monitor-Retina.
Artigo em preparação para submissão para Atherosclerosis

2. **Torres FS**, Venkatesh V, Nguyen E, Jiménez-Juan L, Crean AM. Coronary Calcium Scan Aquisition Prior to Coronary CT Angiography: Limited Benefit or Useful Addition? AJR Am J Roentgenol. Jan 2013.
Artigo de revisão aceito para publicação no AJR Am J Roentgenol. (Fator de Impacto: 2.78)

3. Jiménez-Juan L, Nguyen ET, Wintersperger BJ, Moshonov H, Crean AM, Deva DP, Paul NS, **Torres FS**. Failed heart rate control with oral metoprolol prior to coronary CT angiography: effect of additional intravenous metoprolol on heart rate, image quality and radiation dose. Int J Cardiovasc Imaging. 2012. Apr 24.
Artigo publicado online no Int J Cardiovasc Imaging. (Fator de Impacto: 2.539)

4. **Torres FS**, Windram JD, Bradley TJ, Wintersperger BJ, Menezes R, Crean AM, Lay S, Colman JM, Silversides CK, Wald RM. Assessment of Aortic Root Dimensions in Patients with a Bicuspid Aortic Valve Using Cardiovascular Magnetic Resonance Imaging.

Artigo em preparação para submissão para Journal of Cardiovascular Magnetic Resonance

REFERÊNCIAS

1. Roger VL, Go AS, Lloyd-Jones DM, Benjamin EJ, Berry JD, Borden WB, et al. Heart disease and stroke statistics--2012 update: a report from the American Heart Association. Circulation. 2012;125(1):e2-e220.

2. Available from: http://www2.datasus.gov.br/DATASUS/index.php?area=0205&VObj=http://tabnet.datasus.gov.br/cgi/deftohtm.exe?sim/cnv/obt10.

3. Brott TG, Halperin JL, Abbara S, Bacharach JM, Barr JD, Bush RL, et al. 2011 ASA/ACCF/AHA/AANN/AANS/ACR/ASNR/CNS/SAIP/SCAI/SIR/SNIS/SVM/SVS guideline on the management of patients with extracranial carotid and vertebral artery disease. A report of the American College of Cardiology Foundation/American Heart Association Task Force on Practice Guidelines, and the American Stroke Association, American Association of Neuroscience Nurses, American Association of Neurological Surgeons, American College of Radiology, American Society of Neuroradiology, Congress of Neurological Surgeons, Society of Atherosclerosis Imaging and Prevention, Society for Cardiovascular Angiography and Interventions, Society of Interventional Radiology, Society of NeuroInterventional Surgery, Society for Vascular Medicine, and Society for Vascular Surgery. Circulation. 2011;124(4):e54-130.

4. O'Leary DH, Bots ML. Imaging of atherosclerosis: carotid intima-media thickness. Eur Heart J. 2011;31(14):1682-9.

5. Peters SA, den Ruijter HM, Bots ML, Moons KG. Improvements in risk stratification for the occurrence of cardiovascular disease by imaging subclinical atherosclerosis: a systematic review. Heart. 2012;98(3):177-84.

6. Greenland P, Alpert JS, Beller GA, Benjamin EJ, Budoff MJ, Fayad ZA, et al. 2010 ACCF/AHA guideline for assessment of cardiovascular risk in asymptomatic adults: a report of the American College of Cardiology Foundation/American Heart Association Task Force on Practice Guidelines. J Am Coll Cardiol. 2010;56(25):e50-103.

7. Johnston SC. Clinical practice. Transient ischemic attack. N Engl J Med. 2002;347(21):1687-92.

8. Sacco RL, Adams R, Albers G, Alberts MJ, Benavente O, Furie K, et al. Guidelines for prevention of stroke in patients with ischemic stroke or transient ischemic attack: a statement for healthcare professionals from the American Heart Association/American Stroke Association Council on Stroke: co-sponsored by the Council on Cardiovascular Radiology and Intervention: the American Academy of Neurology affirms the value of this guideline. Stroke. 2006;37(2):577-617.

9. Goldstein LB, Adams R, Alberts MJ, Appel LJ, Brass LM, Bushnell CD, et al. Primary prevention of ischemic stroke: a guideline from the American Heart Association/American Stroke Association Stroke Council: cosponsored by the Atherosclerotic Peripheral Vascular Disease Interdisciplinary Working Group; Cardiovascular Nursing Council; Clinical Cardiology Council; Nutrition, Physical Activity, and Metabolism Council; and the Quality of Care and Outcomes Research Interdisciplinary Working Group: the American Academy of Neurology affirms the value of this guideline. Stroke. 2006;37(6):1583-633.

10. Howard G, Sharrett AR, Heiss G, Evans GW, Chambless LE, Riley WA, et al. Carotid artery intimal-medial thickness distribution in general populations as evaluated by B-mode ultrasound. ARIC Investigators. Stroke. 1993;24(9):1297-304.

11. Salonen JT, Salonen R. Ultrasound B-mode imaging in observational studies of atherosclerotic progression. Circulation. 1993;87(3 Suppl):II56-65.

12. Chambless LE, Heiss G, Folsom AR, Rosamond W, Szklo M, Sharrett AR, et al. Association of coronary heart disease incidence with carotid arterial wall thickness and major risk factors: the Atherosclerosis Risk in Communities (ARIC) Study, 1987-1993. Am J Epidemiol. 1997;146(6):483-94.

13. Bots ML, Hoes AW, Koudstaal PJ, Hofman A, Grobbee DE. Common carotid intima-media thickness and risk of stroke and myocardial infarction: the Rotterdam Study. Circulation. 1997;96(5):1432-7.

14. Hodis HN, Mack WJ, LaBree L, Selzer RH, Liu CR, Liu CH, et al. The role of carotid arterial intima-media thickness in predicting clinical coronary events. Ann Intern Med. 1998;128(4):262-9.

15. O'Leary DH, Polak JF, Kronmal RA, Manolio TA, Burke GL, Wolfson SK, Jr. Carotid-artery intima and media thickness as a risk factor for myocardial infarction and stroke in older adults. Cardiovascular Health Study Collaborative Research Group. N Engl J Med. 1999;340(1):14-22.

16. Belcaro G, Nicolaides AN, Ramaswami G, Cesarone MR, De Sanctis M, Incandela L, et al. Carotid and femoral ultrasound morphology screening and cardiovascular events in low risk subjects: a 10-year follow-up study (the CAFES-CAVE study(1)). Atherosclerosis. 2001;156(2):379-87.

17. Iglesias del Sol A, Bots ML, Grobbee DE, Hofman A, Witteman JC. Carotid intima-media thickness at different sites: relation to incident myocardial infarction; The Rotterdam Study. Eur Heart J. 2002;23(12):934-40.

18. Hollander M, Hak AE, Koudstaal PJ, Bots ML, Grobbee DE, Hofman A, et al. Comparison between measures of atherosclerosis and risk of stroke: the Rotterdam Study. Stroke. 2003;34(10):2367-72.

19. Kitamura A, Iso H, Imano H, Ohira T, Okada T, Sato S, et al. Carotid intima-media thickness and plaque characteristics as a risk factor for stroke in Japanese elderly men. Stroke. 2004;35(12):2788-94.

20. Lorenz MW, von Kegler S, Steinmetz H, Markus HS, Sitzer M. Carotid intima-media thickening indicates a higher vascular risk across a wide age range: prospective data from the Carotid Atherosclerosis Progression Study (CAPS). Stroke. 2006;37(1):87-92.

21. Dijk JM, van der Graaf Y, Bots ML, Grobbee DE, Algra A. Carotid intima-media thickness and the risk of new vascular events in patients with manifest atherosclerotic disease: the SMART study. Eur Heart J. 2006;27(16):1971-8.

22. Kuller LH, Arnold AM, Psaty BM, Robbins JA, O'Leary DH, Tracy RP, et al. 10-year follow-up of subclinical cardiovascular disease and risk of coronary heart disease in the Cardiovascular Health Study. Arch Intern Med. 2006;166(1):71-8.

23. Baldassarre D, Amato M, Pustina L, Castelnuovo S, Sanvito S, Gerosa L, et al. Measurement of carotid artery intima-media thickness in dyslipidemic patients increases the power of traditional risk factors to predict cardiovascular events. Atherosclerosis. 2007;191(2):403-8.

24. de Weerd M, Greving JP, de Jong AW, Buskens E, Bots ML. Prevalence of asymptomatic carotid artery stenosis according to age and sex: systematic review and metaregression analysis. Stroke. 2009;40(4):1105-13.

25. Brindle P, Beswick A, Fahey T, Ebrahim S. Accuracy and impact of risk assessment in the primary prevention of cardiovascular disease: a systematic review. Heart. 2006;92(12):1752-9.

26. Smith SC, Jr., Greenland P, Grundy SM. AHA Conference Proceedings. Prevention conference V: Beyond secondary prevention: Identifying the high-risk patient for primary prevention: executive summary. American Heart Association. Circulation. 2000;101(1):111-6.

27. Greenland P, Smith SC, Jr., Grundy SM. Improving coronary heart disease risk assessment in asymptomatic people: role of traditional risk factors and noninvasive cardiovascular tests. Circulation. 2001;104(15):1863-7.

28. Devine PJ, Carlson DW, Taylor AJ. Clinical value of carotid intima-media thickness testing. J Nucl Cardiol. 2006;13(5):710-8.

29. Bard RL, Kalsi H, Rubenfire M, Wakefield T, Fex B, Rajagopalan S, et al. Effect of carotid atherosclerosis screening on risk stratification during primary cardiovascular disease prevention. Am J Cardiol. 2004;93(8):1030-2.

30. Poredos P. Intima-media thickness: indicator of cardiovascular risk and measure of the extent of atherosclerosis. Vasc Med. 2004;9(1):46-54.

31. Simon A, Chironi G, Levenson J. Performance of subclinical arterial disease detection as a screening test for coronary heart disease. Hypertension. 2006;48(3):392-6.

32. Touboul PJ, Labreuche J, Vicaut E, Amarenco P. Carotid intima-media thickness, plaques, and Framingham risk score as independent determinants of stroke risk. Stroke. 2005;36(8):1741-5.

33. Touboul PJ, Hernandez-Hernandez R, Kucukoglu S, Woo KS, Vicaut E, Labreuche J, et al. Carotid artery intima media thickness, plaque and Framingham cardiovascular score in Asia, Africa/Middle East and Latin America: the PARC-AALA study. Int J Cardiovasc Imaging. 2007;23(5):557-67.

34. Touboul PJ, Vicaut E, Labreuche J, Belliard JP, Cohen S, Kownator S, et al. Correlation between the Framingham risk score and intima media thickness: the Paroi Arterielle et Risque Cardio-vasculaire (PARC) study. Atherosclerosis. 2007;192(2):363-9.

35. Wilson PW, Smith SC, Jr., Blumenthal RS, Burke GL, Wong ND. 34th Bethesda Conference: Task force #4--How do we select patients for atherosclerosis imaging? J Am Coll Cardiol. 2003;41(11):1898-906.

36. Mancia G, De Backer G, Dominiczak A, Cifkova R, Fagard R, Germano G, et al. 2007 Guidelines for the Management of Arterial Hypertension: The Task Force for the Management of Arterial Hypertension of the European Society of Hypertension (ESH) and of the European Society of Cardiology (ESC). J Hypertens. 2007;25(6):1105-87.

37. Stein JH, Korcarz CE, Hurst RT, Lonn E, Kendall CB, Mohler ER, et al. Use of carotid ultrasound to identify subclinical vascular disease and evaluate cardiovascular disease risk: a consensus statement from the American Society of Echocardiography Carotid Intima-Media Thickness Task Force.

Endorsed by the Society for Vascular Medicine. J Am Soc Echocardiogr. 2008;21(2):93-111; quiz 89-90.

38. Naghavi M, Falk E, Hecht HS, Jamieson MJ, Kaul S, Berman D, et al. From vulnerable plaque to vulnerable patient--Part III: Executive summary of the Screening for Heart Attack Prevention and Education (SHAPE) Task Force report. Am J Cardiol. 2006;98(2A):2H-15H.

39. Yeboah J, McClelland RL, Polonsky TS, Burke GL, Sibley CT, O'Leary D, et al. Comparison of novel risk markers for improvement in cardiovascular risk assessment in intermediate-risk individuals. JAMA. 2012;308(8):788-95.

40. Den Ruijter HM, Peters SA, Anderson TJ, Britton AR, Dekker JM, Eijkemans MJ, et al. Common carotid intima-media thickness measurements in cardiovascular risk prediction: a meta-analysis. JAMA. 2012;308(8):796-803.

41. Baldassarre D, Hamsten A, Veglia F, de Faire U, Humphries SE, Smit AJ, et al. Measurements of Carotid Intima-Media Thickness and of Interadventitia Common Carotid Diameter Improve Prediction of Cardiovascular Events: Results of the IMPROVE (Carotid Intima Media Thickness [IMT] and IMT-Progression as Predictors of Vascular Events in a High Risk European Population) Study. J Am Coll Cardiol. 2012;60(16):1489-99.

42. Selzer RH, Hodis HN, Kwong-Fu H, Mack WJ, Lee PL, Liu CR, et al. Evaluation of computerized edge tracking for quantifying intima-media thickness of the common carotid artery from B-mode ultrasound images. Atherosclerosis. 1994;111(1):1-11.

43. Pignoli P, Tremoli E, Poli A, Oreste P, Paoletti R. Intimal plus medial thickness of the arterial wall: a direct measurement with ultrasound imaging. Circulation. 1986;74(6):1399-406.

44. Wong M, Edelstein J, Wollman J, Bond MG. Ultrasonic-pathological comparison of the human arterial wall. Verification of intima-media thickness. Arterioscler Thromb. 1993;13(4):482-6.

45. Persson J, Formgren J, Israelsson B, Berglund G. Ultrasound-determined intima-media thickness and atherosclerosis. Direct and indirect validation. Arterioscler Thromb. 1994;14(2):261-4.

46. Wendelhag I, Gustavsson T, Suurkula M, Berglund G, Wikstrand J. Ultrasound measurement of wall thickness in the carotid artery: fundamental principles and description of a computerized analysing system. Clin Physiol. 1991;11(6):565-77.

47. Bots ML, Evans GW, Riley WA, Grobbee DE. Carotid intima-media thickness measurements in intervention studies: design options, progression rates, and sample size considerations: a point of view. Stroke. 2003;34(12):2985-94.

48. Kanters SD, Algra A, van Leeuwen MS, Banga JD. Reproducibility of in vivo carotid intima-media thickness measurements: a review. Stroke. 1997;28(3):665-71.

49. Stensland-Bugge E, Bonaa KH, Joakimsen O. Reproducibility of ultrasonographically determined intima-media thickness is dependent on arterial wall thickness. The Tromso Study. Stroke. 1997;28(10):1972-80.

50. Touboul PJ, Hennerici MG, Meairs S, Adams H, Amarenco P, Bornstein N, et al. Mannheim carotid intima-media thickness consensus

(2004-2006). An update on behalf of the Advisory Board of the 3rd and 4th Watching the Risk Symposium, 13th and 15th European Stroke Conferences, Mannheim, Germany, 2004, and Brussels, Belgium, 2006. Cerebrovasc Dis. 2007;23(1):75-80.

51. Roman MJ, Naqvi TZ, Gardin JM, Gerhard-Herman M, Jaff M, Mohler E. American society of echocardiography report. Clinical application of noninvasive vascular ultrasound in cardiovascular risk stratification: a report from the American Society of Echocardiography and the Society for Vascular Medicine and Biology. Vasc Med. 2006;11(3):201-11.

52. O'Leary DH, Polak JF. Intima-media thickness: a tool for atherosclerosis imaging and event prediction. Am J Cardiol. 2002;90(10C):18L-21L.

53. Crouse JR, 3rd, Craven TE, Hagaman AP, Bond MG. Association of coronary disease with segment-specific intimal-medial thickening of the extracranial carotid artery. Circulation. 1995;92(5):1141-7.

54. O'Leary DH, Polak JF, Kronmal RA, Savage PJ, Borhani NO, Kittner SJ, et al. Thickening of the carotid wall. A marker for atherosclerosis in the elderly? Cardiovascular Health Study Collaborative Research Group. Stroke. 1996;27(2):224-31.

55. Bots ML, den Ruijter HM. Should We Indeed Measure Carotid Intima-Media Thickness for Improving Prediction of Cardiovascular Events After IMPROVE? J Am Coll Cardiol. 2012;60(16):1500-2.

56. Graf S, Gariepy J, Massonneau M, Armentano RL, Mansour S, Barra JG, et al. Experimental and clinical validation of arterial diameter waveform

and intimal media thickness obtained from B-mode ultrasound image processing. Ultrasound Med Biol. 1999;25(9):1353-63.

57. Peters SA, den Ruijter HM, Palmer MK, Grobbee DE, Crouse JR, 3rd, O'Leary DH, et al. Manual or semi-automated edge detection of the maximal far wall common carotid intima-media thickness: a direct comparison. J Intern Med. 2012;271(3):247-56.

58. Li R, Duncan BB, Metcalf PA, Crouse JR, 3rd, Sharrett AR, Tyroler HA, et al. B-mode-detected carotid artery plaque in a general population. Atherosclerosis Risk in Communities (ARIC) Study Investigators. Stroke. 1994;25(12):2377-83.

59. Ebrahim S, Papacosta O, Whincup P, Wannamethee G, Walker M, Nicolaides AN, et al. Carotid plaque, intima media thickness, cardiovascular risk factors, and prevalent cardiovascular disease in men and women: the British Regional Heart Study. Stroke. 1999;30(4):841-50.

60. Polak JF, Shemanski L, O'Leary DH, Lefkowitz D, Price TR, Savage PJ, et al. Hypoechoic plaque at US of the carotid artery: an independent risk factor for incident stroke in adults aged 65 years or older. Cardiovascular Health Study. Radiology. 1998;208(3):649-54.

61. Mancini GB, Dahlof B, Diez J. Surrogate markers for cardiovascular disease: structural markers. Circulation. 2004;109(25 Suppl 1):IV22-30.

62. Using nontraditional risk factors in coronary heart disease risk assessment: U.S. Preventive Services Task Force recommendation statement. Ann Intern Med. 2009;151(7):474-82.

63. Society of Atherosclerosis Imaging and Prevention Developed in collaboration with the International Atherosclerosis Society. Appropriate use

criteria for carotid intima media thickness testing. Atherosclerosis. 2011;214(1):43-6.

64. Halliburton S, Arbab-Zadeh A, Dey D, Einstein AJ, Gentry R, George RT, et al. State-of-the-art in CT hardware and scan modes for cardiovascular CT. J Cardiovasc Comput Tomogr. 2012;6(3):154-63.

65. Budoff MJ, Achenbach S, Blumenthal RS, Carr JJ, Goldin JG, Greenland P, et al. Assessment of coronary artery disease by cardiac computed tomography: a scientific statement from the American Heart Association Committee on Cardiovascular Imaging and Intervention, Council on Cardiovascular Radiology and Intervention, and Committee on Cardiac Imaging, Council on Clinical Cardiology. Circulation. 2006;114(16):1761-91.

66. Agatston AS, Janowitz WR, Hildner FJ, Zusmer NR, Viamonte M, Jr., Detrano R. Quantification of coronary artery calcium using ultrafast computed tomography. J Am Coll Cardiol. 1990;15(4):827-32.

67. Rumberger JA, Schwartz RS, Simons DB, Sheedy PF, 3rd, Edwards WD, Fitzpatrick LA. Relation of coronary calcium determined by electron beam computed tomography and lumen narrowing determined by autopsy. Am J Cardiol. 1994;73(16):1169-73.

68. Rumberger JA, Simons DB, Fitzpatrick LA, Sheedy PF, Schwartz RS. Coronary artery calcium area by electron-beam computed tomography and coronary atherosclerotic plaque area. A histopathologic correlative study. Circulation. 1995;92(8):2157-62.

69. Baumgart D, Schmermund A, Goerge G, Haude M, Ge J, Adamzik M, et al. Comparison of electron beam computed tomography with intracoronary

ultrasound and coronary angiography for detection of coronary atherosclerosis. J Am Coll Cardiol. 1997;30(1):57-64.

70. Schmermund A, Baumgart D, Gorge G, Seibel R, Gronemeyer D, Ge J, et al. Coronary artery calcium in acute coronary syndromes: a comparative study of electron-beam computed tomography, coronary angiography, and intracoronary ultrasound in survivors of acute myocardial infarction and unstable angina. Circulation. 1997;96(5):1461-9.

71. Raggi P, Cooil B, Callister TQ. Use of electron beam tomography data to develop models for prediction of hard coronary events. Am Heart J. 2001;141(3):375-82.

72. Shaw LJ, Raggi P, Schisterman E, Berman DS, Callister TQ. Prognostic value of cardiac risk factors and coronary artery calcium screening for all-cause mortality. Radiology. 2003;228(3):826-33.

73. Greenland P, LaBree L, Azen SP, Doherty TM, Detrano RC. Coronary artery calcium score combined with Framingham score for risk prediction in asymptomatic individuals. JAMA. 2004;291(2):210-5.

74. Detrano R, Guerci AD, Carr JJ, Bild DE, Burke G, Folsom AR, et al. Coronary calcium as a predictor of coronary events in four racial or ethnic groups. N Engl J Med. 2008;358(13):1336-45.

75. Polonsky TS, McClelland RL, Jorgensen NW, Bild DE, Burke GL, Guerci AD, et al. Coronary artery calcium score and risk classification for coronary heart disease prediction. JAMA. 2010;303(16):1610-6.

76. Elias-Smale SE, Proenca RV, Koller MT, Kavousi M, van Rooij FJ, Hunink MG, et al. Coronary calcium score improves classification of coronary

heart disease risk in the elderly: the Rotterdam study. J Am Coll Cardiol. Oct 19;56(17):1407-14.

77. Erbel R, Mohlenkamp S, Moebus S, Schmermund A, Lehmann N, Stang A, et al. Coronary risk stratification, discrimination, and reclassification improvement based on quantification of subclinical coronary atherosclerosis: the Heinz Nixdorf Recall study. J Am Coll Cardiol. 2010;56(17):1397-406.

78. Sarwar A, Shaw LJ, Shapiro MD, Blankstein R, Hoffmann U, Cury RC, et al. Diagnostic and prognostic value of absence of coronary artery calcification. JACC Cardiovasc Imaging. 2009;2(6):675-88.

79. Greenland P, Bonow RO, Brundage BH, Budoff MJ, Eisenberg MJ, Grundy SM, et al. ACCF/AHA 2007 clinical expert consensus document on coronary artery calcium scoring by computed tomography in global cardiovascular risk assessment and in evaluation of patients with chest pain: a report of the American College of Cardiology Foundation Clinical Expert Consensus Task Force (ACCF/AHA Writing Committee to Update the 2000 Expert Consensus Document on Electron Beam Computed Tomography). Circulation. 2007;115(3):402-26.

80. Rochitte CE, Pinto IM, Fernandes JL, Filho CF, Jatene A, Carvalho AC, et al. [Cardiovascular magnetic resonance and computed tomography imaging guidelines of the Brazilian Society of Cardiology]. Arq Bras Cardiol. 2006;87(3):e60-100.

81. Taylor AJ, Cerqueira M, Hodgson JM, Mark D, Min J, O'Gara P, et al. ACCF/SCCT/ACR/AHA/ASE/ASNC/NASCI/SCAI/SCMR 2010 Appropriate Use Criteria for Cardiac Computed Tomography. A Report of the American College of Cardiology Foundation Appropriate Use Criteria Task Force, the

Society of Cardiovascular Computed Tomography, the American College of Radiology, the American Heart Association, the American Society of Echocardiography, the American Society of Nuclear Cardiology, the North American Society for Cardiovascular Imaging, the Society for Cardiovascular Angiography and Interventions, and the Society for Cardiovascular Magnetic Resonance. J Cardiovasc Comput Tomogr. 2010;4(6):407 e1-33.

82. Gottlieb I, Miller JM, Arbab-Zadeh A, Dewey M, Clouse ME, Sara L, et al. The absence of coronary calcification does not exclude obstructive coronary artery disease or the need for revascularization in patients referred for conventional coronary angiography. J Am Coll Cardiol. 2010;55(7):627-34.

83. Skinner JS, Smeeth L, Kendall JM, Adams PC, Timmis A. NICE guidance. Chest pain of recent onset: assessment and diagnosis of recent onset chest pain or discomfort of suspected cardiac origin. Heart. 2010;96(12):974-8.

84. Abbara S, Arbab-Zadeh A, Callister TQ, Desai MY, Mamuya W, Thomson L, et al. SCCT guidelines for performance of coronary computed tomographic angiography: a report of the Society of Cardiovascular Computed Tomography Guidelines Committee. J Cardiovasc Comput Tomogr. 2009;3(3):190-204.

85. Torres FS, Crean AM, Nguyen ET, Paul N. Strategies for radiation-dose reduction and image-quality optimization in multidetector computed tomographic coronary angiography. Can Assoc Radiol J. 2010;61(5):271-9.

86. Mowatt G, Cook JA, Hillis GS, Walker S, Fraser C, Jia X, et al. 64-Slice computed tomography angiography in the diagnosis and assessment of

coronary artery disease: systematic review and meta-analysis. Heart. 2008;94(11):1386-93.

87. Bamberg F, Sommer WH, Hoffmann V, Achenbach S, Nikolaou K, Conen D, et al. Meta-analysis and systematic review of the long-term predictive value of assessment of coronary atherosclerosis by contrast-enhanced coronary computed tomography angiography. J Am Coll Cardiol. 2011;57(24):2426-36.

88. Budoff MJ, Dowe D, Jollis JG, Gitter M, Sutherland J, Halamert E, et al. Diagnostic performance of 64-multidetector row coronary computed tomographic angiography for evaluation of coronary artery stenosis in individuals without known coronary artery disease: results from the prospective multicenter ACCURACY (Assessment by Coronary Computed Tomographic Angiography of Individuals Undergoing Invasive Coronary Angiography) trial. J Am Coll Cardiol. 2008;52(21):1724-32.

89. Miller JM, Rochitte CE, Dewey M, Arbab-Zadeh A, Niinuma H, Gottlieb I, et al. Diagnostic performance of coronary angiography by 64-row CT. N Engl J Med. 2008;359(22):2324-36.

90. Meijboom WB, Meijs MF, Schuijf JD, Cramer MJ, Mollet NR, van Mieghem CA, et al. Diagnostic accuracy of 64-slice computed tomography coronary angiography: a prospective, multicenter, multivendor study. J Am Coll Cardiol. 2008;52(25):2135-44.

91. Hulten EA, Carbonaro S, Petrillo SP, Mitchell JD, Villines TC. Prognostic value of cardiac computed tomography angiography: a systematic review and meta-analysis. J Am Coll Cardiol. 2011;57(10):1237-47.

92. Min JK, Dunning A, Lin FY, Achenbach S, Al-Mallah M, Budoff MJ, et al. Age- and sex-related differences in all-cause mortality risk based on coronary computed tomography angiography findings results from the International Multicenter CONFIRM (Coronary CT Angiography Evaluation for Clinical Outcomes: An International Multicenter Registry) of 23,854 patients without known coronary artery disease. J Am Coll Cardiol. 2011;58(8):849-60.

93. Lin FY, Shaw LJ, Dunning AM, Labounty TM, Choi JH, Weinsaft JW, et al. Mortality risk in symptomatic patients with nonobstructive coronary artery disease: a prospective 2-center study of 2,583 patients undergoing 64-detector row coronary computed tomographic angiography. J Am Coll Cardiol. 2011;58(5):510-9.

94. Hoffmann U, Bamberg F, Chae CU, Nichols JH, Rogers IS, Seneviratne SK, et al. Coronary computed tomography angiography for early triage of patients with acute chest pain: the ROMICAT (Rule Out Myocardial Infarction using Computer Assisted Tomography) trial. J Am Coll Cardiol. 2009;53(18):1642-50.

95. Schlett CL, Banerji D, Siegel E, Bamberg F, Lehman SJ, Ferencik M, et al. Prognostic value of CT angiography for major adverse cardiac events in patients with acute chest pain from the emergency department: 2-year outcomes of the ROMICAT trial. JACC Cardiovasc Imaging. 2011;4(5):481-91.

96. Goldstein JA, Chinnaiyan KM, Abidov A, Achenbach S, Berman DS, Hayes SW, et al. The CT-STAT (Coronary Computed Tomographic Angiography for Systematic Triage of Acute Chest Pain Patients to Treatment) trial. J Am Coll Cardiol. 2011;58(14):1414-22.

97. Samad Z, Hakeem A, Mahmood SS, Pieper K, Patel MR, Simel DL, et al. A meta-analysis and systematic review of computed tomography angiography as a diagnostic triage tool for patients with chest pain presenting to the emergency department. J Nucl Cardiol. 2012;19(2):364-76.

98. Hoffmann U, Truong QA, Schoenfeld DA, Chou ET, Woodard PK, Nagurney JT, et al. Coronary CT angiography versus standard evaluation in acute chest pain. N Engl J Med. 2012;367(4):299-308.

99. Litt HI, Gatsonis C, Snyder B, Singh H, Miller CD, Entrikin DW, et al. CT angiography for safe discharge of patients with possible acute coronary syndromes. N Engl J Med. 2012;366(15):1393-403.

100. Hamm CW, Bassand JP, Agewall S, Bax J, Boersma E, Bueno H, et al. ESC Guidelines for the management of acute coronary syndromes in patients presenting without persistent ST-segment elevation: The Task Force for the management of acute coronary syndromes (ACS) in patients presenting without persistent ST-segment elevation of the European Society of Cardiology (ESC). Eur Heart J. 2011;32(23):2999-3054.

101. Hausleiter J, Meyer T, Hermann F, Hadamitzky M, Krebs M, Gerber TC, et al. Estimated radiation dose associated with cardiac CT angiography. JAMA. 2009;301(5):500-7.

102. Mettler FA, Jr., Huda W, Yoshizumi TT, Mahesh M. Effective doses in radiology and diagnostic nuclear medicine: a catalog. Radiology. 2008;248(1):254-63.

103. Kim KP, Einstein AJ, Berrington de Gonzalez A. Coronary artery calcification screening: estimated radiation dose and cancer risk. Arch Intern Med. 2009;169(13):1188-94.

104. Mahabadi AA, Achenbach S, Burgstahler C, Dill T, Fischbach R, Knez A, et al. Safety, efficacy, and indications of beta-adrenergic receptor blockade to reduce heart rate prior to coronary CT angiography. Radiology. 2010;257(3):614-23.

105. Torres FS, Jeddiyan S, Jimenez-Juan L, Nguyen ET. Beta-blockers to control heart rate during coronary CT angiography. Radiology. 2011;259(2):615-6; author reply 6-7.

106. Roberts WT, Wright AR, Timmis JB, Timmis AD. Safety and efficacy of a rate control protocol for cardiac CT. Br J Radiol. 2009;82(976):267-71.

107. Adile KK, Kapoor A, Jain SK, Gupta A, Kumar S, Tewari S, et al. Safety and efficacy of oral ivabradine as a heart rate-reducing agent in patients undergoing CT coronary angiography. Br J Radiol. 2012;85(1016):e424-8.

108. Stacul F, van der Molen AJ, Reimer P, Webb JA, Thomsen HS, Morcos SK, et al. Contrast induced nephropathy: updated ESUR Contrast Media Safety Committee guidelines. Eur Radiol. 2011;21(12):2527-41.

109. Murakami R, Hayashi H, Sugizaki K, Yoshida T, Okazaki E, Kumita S, et al. Contrast-induced nephropathy in patients with renal insufficiency undergoing contrast-enhanced MDCT. Eur Radiol. 2012;22(10):2147-52.

110. Kim SM, Cha RH, Lee JP, Kim DK, Oh KH, Joo KW, et al. Incidence and outcomes of contrast-induced nephropathy after computed tomography in patients with CKD: a quality improvement report. Am J Kidney Dis. 2010;55(6):1018-25.

111. Thomsen HS. European Society of Urogenital Radiology (ESUR) guidelines on the safe use of iodinated contrast media. Eur J Radiol. 2006;60(3):307-13.

112. Loh S, Bagheri S, Katzberg RW, Fung MA, Li CS. Delayed adverse reaction to contrast-enhanced CT: a prospective single-center study comparison to control group without enhancement. Radiology. 2010;255(3):764-71.

113. Iyer RS, Schopp JG, Swanson JO, Thapa MM, Phillips GS. Safety Essentials: Acute Reactions to Iodinated Contrast Media. Can Assoc Radiol J. May 5, 2012. (epub ahead of print)

114. Ho KY, Leiner T, de Haan MW, Kessels AG, Kitslaar PJ, van Engelshoven JM. Peripheral vascular tree stenoses: evaluation with moving-bed infusion-tracking MR angiography. Radiology. 1998;206(3):683-92.

115. Meaney JF, Ridgway JP, Chakraverty S, Robertson I, Kessel D, Radjenovic A, et al. Stepping-table gadolinium-enhanced digital subtraction MR angiography of the aorta and lower extremity arteries: preliminary experience. Radiology. 1999;211(1):59-67.

116. Sodickson DK, McKenzie CA, Li W, Wolff S, Manning WJ, Edelman RR. Contrast-enhanced 3D MR angiography with simultaneous acquisition of spatial harmonics: A pilot study. Radiology. 2000;217(1):284-9.

117. Korosec FR, Frayne R, Grist TM, Mistretta CA. Time-resolved contrast-enhanced 3D MR angiography. Magn Reson Med. 1996 Sep;36(3):345-51.

118. Miyazaki M, Lee VS. Nonenhanced MR angiography. Radiology. 2008;248(1):20-43.

119. Defrance C, Bollache E, Kachenoura N, Perdrix L, Hrynchyshyn N, Bruguiere E, et al. Evaluation of aortic valve stenosis using cardiovascular magnetic resonance: comparison of an original semiautomated analysis of

phase-contrast cardiovascular magnetic resonance with Doppler echocardiography. Circ Cardiovasc Imaging. 2012;5(5):604-12.

120. Julsrud PR, Breen JF, Felmlee JP, Warnes CA, Connolly HM, Schaff HV. Coarctation of the aorta: collateral flow assessment with phase-contrast MR angiography. AJR Am J Roentgenol. 1997;169(6):1735-42.

121. Silverman JM, Raissi S, Tyszka JM, Trento A, Herfkens RJ. Phase-contrast cine MR angiography detection of thoracic aortic dissection. Int J Card Imaging. 2000;16(6):461-70.

122. Urata J, Miyazaki M, Wada H, Nakaura T, Yamashita Y, Takahashi M. Clinical evaluation of aortic diseases using nonenhanced MRA with ECG-triggered 3D half-Fourier FSE. J Magn Reson Imaging. 2001;14(2):113-9.

123. Morita S, Masukawa A, Suzuki K, Hirata M, Kojima S, Ueno E. Unenhanced MR angiography: techniques and clinical applications in patients with chronic kidney disease. Radiographics. 2011;31(2):E13-33.

124. Amano Y, Takahama K, Kumita S. Non-contrast-enhanced MR angiography of the thoracic aorta using cardiac and navigator-gated magnetization-prepared three-dimensional steady-state free precession. J Magn Reson Imaging. 2008;27(3):504-9.

125. Krishnam MS, Tomasian A, Deshpande V, Tran L, Laub G, Finn JP, et al. Noncontrast 3D steady-state free-precession magnetic resonance angiography of the whole chest using nonselective radiofrequency excitation over a large field of view: comparison with single-phase 3D contrast-enhanced magnetic resonance angiography. Invest Radiol. 2008;43(6):411-20.

126. Krishnam MS, Tomasian A, Malik S, Desphande V, Laub G, Ruehm SG. Image quality and diagnostic accuracy of unenhanced SSFP MR angiography compared with conventional contrast-enhanced MR angiography for the assessment of thoracic aortic diseases. Eur Radiol. 2010;20(6):1311-20.

127. Srichai MB, Kim S, Axel L, Babb J, Hecht EM. Non-gadolinium-enhanced 3-dimensional magnetic resonance angiography for the evaluation of thoracic aortic disease: a preliminary experience. Tex Heart Inst J. 2010;37(1):58-65.

128. Dogui A, Kachenoura N, Frouin F, Lefort M, De Cesare A, Mousseaux E, et al. Consistency of aortic distensibility and pulse wave velocity estimates with respect to the Bramwell-Hill theoretical model: a cardiovascular magnetic resonance study. J Cardiovasc Magn Reson. 2011;13:11.

129. Burman ED, Keegan J, Kilner PJ. Aortic root measurement by cardiovascular magnetic resonance: specification of planes and lines of measurement and corresponding normal values. Circ Cardiovasc Imaging. 2008;1(2):104-13.

130. Groth M, Henes FO, Mullerleile K, Bannas P, Adam G, Regier M. Accuracy of thoracic aortic measurements assessed by contrast enhanced and unenhanced magnetic resonance imaging. Eur J Radiol. 2012;81(4):762-6.

131. Potthast S, Mitsumori L, Stanescu LA, Richardson ML, Branch K, Dubinsky TJ, et al. Measuring aortic diameter with different MR techniques: comparison of three-dimensional (3D) navigated steady-state free-precession (SSFP), 3D contrast-enhanced magnetic resonance angiography (CE-MRA),

2D T2 black blood, and 2D cine SSFP. J Magn Reson Imaging. 2010;31(1):177-84.

132. Thomsen HS, Morcos SK, Almen T, Bellin MF, Bertolotto M, Bongartz G, et al. Nephrogenic systemic fibrosis and gadolinium-based contrast media: updated ESUR Contrast Medium Safety Committee guidelines. Eur Radiol. Aug 4, 2012. (epub ahead of print)

133. Hiratzka LF, Bakris GL, Beckman JA, Bersin RM, Carr VF, Casey DE, Jr., et al. 2010 ACCF/AHA/AATS/ACR/ASA/SCA/SCAI/SIR/STS/SVM Guidelines for the diagnosis and management of patients with thoracic aortic disease. A Report of the American College of Cardiology Foundation/American Heart Association Task Force on Practice Guidelines, American Association for Thoracic Surgery, American College of Radiology,American Stroke Association, Society of Cardiovascular Anesthesiologists, Society for Cardiovascular Angiography and Interventions, Society of Interventional Radiology, Society of Thoracic Surgeons,and Society for Vascular Medicine. J Am Coll Cardiol. 2010;55(14):e27-e129.

5. Artigo Original em Inglês:

Association between carotid intima-media thickness and retinal arteriolar and venular diameter in patients with hypertension: a cross-sectional study.

Felipe Soares Torres MD[1,2], Sandra Costa Fuchs MD, PhD[1], Miguel Gus MD PhD[3], on behalf of co-authors of Monitor-Retina Study.

1. Postgraduate Studies Program in Cardiology, School of Medicine, Universidade Federal do Rio Grande do Sul, Porto Alegre, Brazil
2. Division of Radiology, Hospital de Clínicas de Porto Alegre, Porto Alegre, RS, Brazil
3. Division of Cardiology, Hospital de Clinicas de Porto Alegre, Porto Alegre, Brazil

Address for Correspondence:

Felipe Soares Torres

Postgraduate Studies Program in Cardiology, School of Medicine, Universidade Federal do Rio Grande do Sul

Ramiro Barcelos, 2600

CEP: 90.035-003, Porto Alegre-RS, Brazil

Phone: 55-51-3316 5604

Fax : 55-51-3316 5614

E-mail: felipesoarestorres@gmail.com

Abstract

Background: retinal vessel changes are common in hypertensive patients, but its association with abnormalities in other vascular sites has been poorly investigated. The aim of this study was to examine the association between ultrasound-measured carotid intima-media thickness (IMT) and retinal arteriolar and venular diameters in hypertensive patients.

Methods: In this cross-section study, 173 hypertensive patients had both retinography taken and digitized to determine vessel diameters by an edge-detecting computerized method and carotid ultrasound for semi-automated carotid IMT measurement. The association between the mean common carotid IMT and retinal arteriolar and venular diameters was assessed by using multiple linear regression models.

Results: The mean (±SD) arteriolar and venular diameters were 102. 8 (±11.6) μm and 128.9 (±15.5) μm, respectively, and common carotid IMT was 0.87 (±0.19) mm. A significant and independent association was demonstrated for carotid IMT and retinal arteriolar caliber (adjusted β -0.235, p = 0.001) and for carotid IMT and retinal venular caliber (adjusted β 0.184, p = 0.011) after controlling for age, sex, systolic blood pressure, total cholesterol, prior cardiovascular disease and the retinal fellow vessel.

Conclusion: in patients with hypertension, carotid intima-media thickness, a marker of macrovascular damage, is significantly and independently correlated with microvascular damage represented by retinal arteriolar and venular calibers.

Keywords: Hypertension, retinal arteriolar narrowing, microdensitometric method, carotid intima-media thickness

Introduction

Ultrasound-measured carotid intima-media thickness (IMT) is associated with multiple clinical atherosclerotic risk factors (1-3) and it is a predictor of future cardiovascular events (4-7). Measurement of carotid IMT is considered reasonable for risk assessment in asymptomatic patients at the intermediate risk range, as assessed by clinical risk scores (8). In patients with hypertension, carotid IMT has also been defined as a predictor of cardiovascular events in patients with established cardiovascular disease (9). Little is known, however, about the association between microvascular retinal changes and abnormalities in medium sized vessels, such as the carotid arteries.

The direct visualization of retinal vessels offers the opportunity to noninvasively assess the microvasculature and it has been incorporated in the evaluation of target organ damage in patient with hypertension (10). The development of computer-assisted measurement of retinal arteriolar and venular diameters has allowed reproducible documentation of vascular damage in these patients (11-13). Although retinal vessel caliber has been associated with the incidence of hypertension (14), coronary heart disease (15), stroke (16) and cardiovascular mortality (17), other non-invasive tools are usually employed to assess in cardiovascular risk stratification (8, 18, 19).

We hypothesize that, in patients with hypertension, there is an inverse association between retinal arteriolar diameter and a direct association between retinal venular caliber and carotid intima-media thickness. The purpose of this study is, therefore, to assess the association between the

retinal arteriolar and venular diameters, as assessed by a semi-automated microdensitometric method (13), and the common carotid intima-media thickness, as assessed by carotid ultrasound.

Patients and Methods

This cross-sectional study was conducted in the Hypertension Clinic of the Division of Cardiology of Hospital de Clínicas de Porto Alegre (Porto Alegre, Brazil). The study was approved by the Ethics Committee of our Institution, which is accredited by the Office of Human Research Protections as an Institutional Review Board, and all patients signed a written informed consent for participation.

The study population was selected from a consecutive sample of patients screened for participation in a randomized clinical trial of approaches to improve adherence in patients with hypertension (20). Patients were included in this analysis if they had: [1] history of hypertension and were aged between > 18 years; [2] absence of clinical suspicion or laboratory evidence of secondary hypertension; [3] agreed to participate in the study and had the ability to provide informed consent.

Patients underwent to an extensive demographic and clinical baseline data collection. Patients with a history of percutaneous coronary intervention or coronary revascularization, carotid endarterectomy, myocardial infarction, angina, heart failure, stroke, and transient ischemic attack were considered as having cardiovascular disease. Diabetes mellitus was defined as fasting plasma glucose of at least 126 mg/dl or use of antidiabetic drugs. Blood pressure was measured with an office aneroid sphygmomanometer and the

mean values were estimated after an average of 6 measures in 3 different visits according to guidelines (10, 21). Patients with BP within normal values but taking BP drugs and those with severe hypertension (180/110 mmHg) or evidence of clinical disease were classified on the occasion of the first visit. In addition, all patients underwent 24-h ambulatory blood pressure monitoring (ABPM) using a monitor (Spacelabs 90207; Spacelabs Healthcare, Redmond, Washington, USA) programmed to take measurements every 15 min from 0700 to 2300h and every 20 min from 2300 to 0700h. Office hypertension was defined as a mean blood pressure 140/90 mm Hg or use of antihypertensive medications and 24-h ABPM hypertension as blood pressure of at least 130/80 mmHg (22).

Retinography was obtained using Topcon TVR-50 retinal camera (Topcon, Japan) in a 35- degree angle focusing in the posterior polo and the four quadrants (superior-nasal, inferior-nasal, superior-temporal, and inferior-temporal) after pharmacologic pupil dilation (20 min after instillation of tropicamine). The color slides were digitized in a 35-mm film scanner Hewlett Packard model Photo Smart 20S (Hewlett Packard, Andover, MA) with a resolution of 600 dots per inch. Images were stored in 24 bits (true color). To enhance contrast of the retinal vessels against the retinal pigment epithelium, the green channel of the bitmap was selected. Details of the microdensitometric method, which is based on the subpixel resolution to identify vessels edge, were reported (13). The inner zone, which corresponds to the distance between one half of the optic disc diameter to one full disc diameter, was used for measurement of retinal and venular caliber (13).

Measurements of carotid IMT were performed with patients in the supine position using an EnVisor HD (Philips Medical, Andover, MA, USA) ultrasound system, equipped with a 5–12 MHz linear probe, according to standard recommendations (23, 24). The carotid arteries were segmented in carotid bulb (1 cm proximal to the flow divider), internal carotid artery (1cm distal to the flow divider) and common carotid artery (between 1 and 2 cm proximal to the tip of the flow divider). Initially, a longitudinal and cross-sectional review of all three carotid segments was performed in order to document the presence of carotid plaques, defined as a focal structure that encroaches into the arterial lumen of at least 0.5 mm or 50% of the surrounding intima-media thickness or demonstrated a thickness of greater than or equal to 1.5 mm (24). Carotid IMT was then measured in the far wall of both right and left common carotid arteries, using an optimal angle of incidence, with at least one complimentary projection. Longitudinal static images were analyzed using an automated software (Carotid Analyzer for Research, Medical Imaging Applications, Medical Imaging Applications LLC, USA). Carotid IMT value was calculated by averaging the left and right mean common carotid IMT (24). A single investigator, blinded to patient's clinical characteristics and retinal measurements, acquired and analyzed all carotid measurements.

Statistical Analysis

Values were described as mean (± standard deviation) or number of patients (percentage). Correlation between the arteriolar and venular caliber and carotid IMT was tested using Pearson product moment correlation (r).

The association between the arteriolar and venular caliber and carotid IMT was tested using multiple regression analysis. The multiple regression model included age, sex, blood pressure and also variables demonstrating a significant correlation with both retinal the arteriolar and venular caliber and carotid IMT in the univariate analysis. The fellow vessel caliber (i.e., venular caliber when the dependent variable was the arteriolar caliber, and vice-versa) was also included in the multiple regression model (25).

P values of less than 0.05 were considered significant, and all P values represent two-sided tests. The Statistical Program for Social Sciences, version 19.0 (SPSS Inc., Chicago, IL) was used for analysis.

Intra-class correlation coefficient was used to assess the intra-reader reproducibility of carotid IMT measurements in 32 consecutive patients. Excellent intra and inter-reader reproducibility of retinal vascular measurement using the microdensitometric method has been reported previously (13, 26).

Results

One hundred and seventy three patients had both retinograhy and carotid ultrasound done between April 2007 and April 2008. Participants were predominantly middle aged, females, and without previous cardiovascular disease (Table 1). The mean (± standard deviation, SD) retinal arteriolar and venous calibers were 102. 8 (11.6) μm and 128.9 (15.5) μm, respectively, and the mean (±SD) common carotid IMT was 0.87 (±0.19) mm (Table 2).

There was no statistically significant correlation between retinal arteriolar ($r = -0.117$, $p=0.13$) and venular ($r = 0.131$, $p=0.09$) diameters and

mean common carotid IMT prior of taking into account confounding factors. The association between retinal vessel caliber and carotid IMT became statistically significant after controlling for age, sex, systolic blood pressure, total cholesterol, prior cardiovascular disease, and the fellow vessel (Tables 3 and 4).

Mean common carotid IMT measurement showed excellent intra-reader reproducibility, with an intra-class correlation coefficient of 0.970 (95%CI 0.940 – 0.985).

Discussion

In the present study, we used a standardized and highly reproducible semi-automated method to assess for retinal vascular changes in a relatively large sample of patients with hypertension and we demonstrated an association between retinal vessel caliber and mean common carotid IMT. After adjusting for confounding factors, an inverse association was demonstrated between retinal arteriolar diameter and carotid IMT and a direct one between retinal venular caliber and carotid IMT.

Retinal arterial narrowing is considered an indicator of microvascular damage from aging, hypertension and other processes, and reflects intimal thickening and medial hyperplasia, hyalinization and sclerosis (27). Since similar pathological features are also seen in the coronary (28) and renal arterioles (29) of persons with hypertension, changes in the retinal arterioles may offer useful information regarding the state of the systemic microcirculation (30). The development of semi-automated methods for quantifying retinal vascular changes has allowed a more precise evaluation of

retinal microvascular disease and its association with cardiovascular events. Ultrasound evaluation of the carotid IMT is usually used to assess macrovascular damage. The correlation between IMT and traditional risk factors is well established as well as the association between IMT and hard cardiovascular outcomes (31). We hypothesized that this non-invasive method could also offer an opportunity to assess non-invasively the presence of microvascular damage. In this context, we sought to explore the correlation between signs of vascular damage in these two different vascular beds and we found an independent inverse association between the retinal arteriolar caliber and the IMT. Our results strengthen the link between elevated blood pressure and widespread vascular damage by demonstrating an independent association of markers of vasculopathy in the retina and in the carotid arteries. One must note that the strength of this association is modeled by a number of factors and it is difficult to predict damage in one vascular site exclusively based on the appearance of the other. This concept is mirrored by the slightly different predictive value of common and internal carotid IMT for stroke and for myocardial infarction (32). Therefore, although both retinal and carotid arterial abnormalities are markers of vascular damage, particularly regarding to hypertension, evidence of a decreased retinal arteriolar caliber does not necessarily means that an increased carotid IMT will be detected in the same patient.

A few studies have analyzed the association between retinal vascular abnormalities and markers of atherosclerosis in the carotid arteries in hypertensive patients. In a study including 437 never-treated hypertensive patients, Cuspidi and colleagues (33) examined the association between

evidence of target organ damage, including carotid ultrasound, with retinal microvascular changes, as assessed by non-mydriatic retinography. The authors found no association between IMT or carotid plaque with arteriovenous crossings, and concluded that fundoscopic examination has a limited clinical value to detect target organ damage in patients with grade 1 and 2 hypertension (33). Our study, on the other hand, assessed the presence of arteriolar narrowing and venous widening and we were able to demonstrate an independent association of both variables with carotid IMT. Patients with diffuse arteriolar narrowing, in the study by Cuspidi and colleagues, were included in the same group of patients with normal arteriolar-to-venous ratio and, therefore, the direct correlation between this parameter and carotid IMT could not be assessed. More recently, Song and colleagues (34) assessed the predictive value of retinal vascular findings for carotid artery atherosclerosis in 179 patients who received fundoscopic examination for different reasons. Patients with hypertensive retinopathy (n=26), according to Keith-Wagener-Baker stages I and II, had an increased IMT when compared to control subjects (n=44), but this association was not adjusted for confounding factors. In addition, details on how the optic fundus was examined and its reproducibility were not provided, limiting the applicability of the results. In the present study, we used a validated and highly reproducible semi-automated microdensitometric method (13, 26) to assess retinal vascular caliber, a method that has been shown to perform better that direct ophtalmoscopy for the detection of arteriolar narrowing (35).

Retinal arteriolar narrowing has been regarded as a marker of chronic vascular damage from elevated blood pressure (14). In the present study,

systolic blood pressure, as assessed by mean 24-hour ABPM, was not an independent predictor of retinal arteriolar diameter in the multiple linear regression model. Since 92% of our patients were taking anti-hypertensive medication and the mean 24-h blood pressure was approximately 131/78 mmHg, we may speculate that the vascular damage related to an elevated blood pressure in our sample may have been influenced by the pharmacological blood pressure therapy. Nonetheless, carotid IMT was found to be an independent and significant predictor of retinal arteriolar diameter, suggesting that the relationship between hypertension and vascular damage is indeed modeled by different factors depending on the vascular site. Retinal venular diameter, on the other hand, has been associated with obesity (36), the metabolic syndrome (37, 38) and other cardiovascular risk factors (37). In our study, in addition to male sex, carotid IMT remained a significant predictor of venular caliber in the multiple regression model, suggesting that venular caliber may also mirror widespread vascular damage in patients with hypertension. Taken together, these findings support the concept that retinal vessel diameter may reflect lifetime cumulative effects of various and different vascular process on the microvasculature (17).

The present investigation has some limitations. We used mean common carotid IMT because it is generally feasible to be used in clinical practice and its use has been recommended (24, 39). In addition, our sample included hypertensive patients screened for a randomized clinical trial and therefore our results may have limitations regarding its external validity.

In summary, in patients with hypertension, carotid intima-media thickness, a marker of macrovascular damage, is significantly and

independently correlated with microvasvular damage represented by retinal arteriolar and venular calibers. The utility of the detection of an abnormal carotid IMT to identify retinal microvascular changes should be explored in population-based studies.

Disclosure:

None.

Acknowledgements:

This work was supported, in part, by National Counsel of Technological and Scientific Development (CNPq) Grant 485831/2007-4, and Hospital de Clínicas de Porto Alegre-FIPE (Fundo de Incentivo a Pesquisa e Ensino); Protocols: GPPG 06142 and 04-465, RS, Brazil.

References

1. Heiss G, Sharrett AR, Barnes R, Chambless LE, Szklo M, Alzola C. Carotid atherosclerosis measured by B-mode ultrasound in populations: associations with cardiovascular risk factors in the ARIC study. Am J Epidemiol. 1991;134(3):250-6.

2. Ferrieres J, Elias A, Ruidavets JB, Cantet C, Bongard V, Fauvel J, et al. Carotid intima-media thickness and coronary heart disease risk factors in a low-risk population. J Hypertens. 1999;17(6):743-8.

3. Psaty BM, Arnold AM, Olson J, Saad MF, Shea S, Post W, et al. Association between levels of blood pressure and measures of subclinical disease multi-ethnic study of atherosclerosis. Am J Hypertens. 2006;19(11):1110-7.

4. Chambless LE, Heiss G, Folsom AR, Rosamond W, Szklo M, Sharrett AR, et al. Association of coronary heart disease incidence with carotid arterial wall thickness and major risk factors: the Atherosclerosis Risk in Communities (ARIC) Study, 1987-1993. Am J Epidemiol. 1997;146(6):483-94.

5. Hollander M, Hak AE, Koudstaal PJ, Bots ML, Grobbee DE, Hofman A, et al. Comparison between measures of atherosclerosis and risk of stroke: the Rotterdam Study. Stroke. 2003;34(10):2367-72.

6. Lorenz MW, von Kegler S, Steinmetz H, Markus HS, Sitzer M. Carotid intima-media thickening indicates a higher vascular risk across a wide age range: prospective data from the Carotid Atherosclerosis Progression Study (CAPS). Stroke. 2006;37(1):87-92.

7. Lorenz MW, Markus HS, Bots ML, Rosvall M, Sitzer M. Prediction of clinical cardiovascular events with carotid intima-media thickness: a systematic review and meta-analysis. Circulation. 2007;115(4):459-67.

8. Greenland P, Alpert JS, Beller GA, Benjamin EJ, Budoff MJ, Fayad ZA, et al. 2010 ACCF/AHA guideline for assessment of cardiovascular risk in asymptomatic adults: a report of the American College of Cardiology Foundation/American Heart Association Task Force on Practice Guidelines. J Am Coll Cardiol. 2010;56(25):e50-103.

9. Zielinski T, Dzielinska Z, Januszewicz A, Rynkun D, Makowiecka Ciesla M, Tyczynski P, et al. Carotid intima-media thickness as a marker of cardiovascular risk in hypertensive patients with coronary artery disease. Am J Hypertens. 2007;20(10):1058-64.

10. Chobanian AV, Bakris GL, Black HR, Cushman WC, Green LA, Izzo JL, Jr., et al. Seventh report of the Joint National Committee on Prevention, Detection, Evaluation, and Treatment of High Blood Pressure. Hypertension. 2003;42(6):1206-52.

11. Couper DJ, Klein R, Hubbard LD, Wong TY, Sorlie PD, Cooper LS, et al. Reliability of retinal photography in the assessment of retinal microvascular characteristics: the Atherosclerosis Risk in Communities Study. Am J Ophthalmol. 2002;133(1):78-88.

12. Sherry LM, Wang JJ, Rochtchina E, Wong T, Klein R, Hubbard L, et al. Reliability of computer-assisted retinal vessel measurementin a population. Clin Experiment Ophthalmol. 2002;30(3):179-82.

13. Pakter HM, Ferlin E, Fuchs SC, Maestri MK, Moraes RS, Nunes G, et al. Measuring arteriolar-to-venous ratio in retinal photography of patients with

hypertension: development and application of a new semi-automated method. Am J Hypertens. 2005;18(3):417-21.

14. Chew SK, Xie J, Wang JJ. Retinal arteriolar diameter and the prevalence and incidence of hypertension: a systematic review and meta-analysis of their association. Curr Hypertens Rep. 2012;14(2):144-51.

15. McGeechan K, Liew G, Macaskill P, Irwig L, Klein R, Klein BE, et al. Meta-analysis: retinal vessel caliber and risk for coronary heart disease. Ann Intern Med. 2009;151(6):404-13.

16. McGeechan K, Liew G, Macaskill P, Irwig L, Klein R, Klein BE, et al. Prediction of incident stroke events based on retinal vessel caliber: a systematic review and individual-participant meta-analysis. Am J Epidemiol. 2009;170(11):1323-32.

17. Wang JJ, Liew G, Klein R, Rochtchina E, Knudtson MD, Klein BE, et al. Retinal vessel diameter and cardiovascular mortality: pooled data analysis from two older populations. Eur Heart J. 2007;28(16):1984-92.

18. Naghavi M, Libby P, Falk E, Casscells SW, Litovsky S, Rumberger J, et al. From vulnerable plaque to vulnerable patient: a call for new definitions and risk assessment strategies: Part II. Circulation. 2003;108(15):1772-8.

19. Greenland P, Smith SC, Jr., Grundy SM. Improving coronary heart disease risk assessment in asymptomatic people: role of traditional risk factors and noninvasive cardiovascular tests. Circulation. 2001;104(15):1863-7.

20. Fuchs SC, Ferreira-da-Silva AL, Moreira LB, Neyeloff JL, Fuchs FC, Gus M, et al. Efficacy of isolated home blood pressure monitoring for blood

pressure control: randomized controlled trial with ambulatory blood pressure monitoring - MONITOR study. J Hypertens. 2012;30(1):75-80.

21. Sociedade Brasileira de Cardiologia-SBC; Sociedade Brasileira de Hipertensão-SBH; Sociedade Brasileira de Nefrologia-SBN. V Brazilian Guidelines in Arterial Hypertension. Arq Bras Cardiol. 2007;89(3):e24-79.

22. O'Brien E, Asmar R, Beilin L, Imai Y, Mallion JM, Mancia G, et al. European Society of Hypertension recommendations for conventional, ambulatory and home blood pressure measurement. J Hypertens. 2003;21(5):821-48.

23. Touboul PJ, Hennerici MG, Meairs S, Adams H, Amarenco P, Bornstein N, et al. Mannheim carotid intima-media thickness consensus (2004-2006). An update on behalf of the Advisory Board of the 3rd and 4th Watching the Risk Symposium, 13th and 15th European Stroke Conferences, Mannheim, Germany, 2004, and Brussels, Belgium, 2006. Cerebrovasc Dis. 2007;23(1):75-80.

24. Stein JH, Korcarz CE, Hurst RT, Lonn E, Kendall CB, Mohler ER, et al. Use of carotid ultrasound to identify subclinical vascular disease and evaluate cardiovascular disease risk: a consensus statement from the American Society of Echocardiography Carotid Intima-Media Thickness Task Force. Endorsed by the Society for Vascular Medicine. J Am Soc Echocardiogr. 2008;21(2):93-111; quiz 89-90.

25. Liew G, Sharrett AR, Kronmal R, Klein R, Wong TY, Mitchell P, et al. Measurement of retinal vascular caliber: issues and alternatives to using the arteriole to venule ratio. Invest Ophthalmol Vis Sci. 2007;48(1):52-7.

26. Pakter HM, Fuchs SC, Maestri MK, Moreira LB, Dei Ricardi LM, Pamplona VF, et al. Computer-assisted methods to evaluate retinal vascular caliber: what are they measuring? Invest Ophthalmol Vis Sci. 2011;52(2):810-5.

27. Tso MO, Jampol LM. Pathophysiology of hypertensive retinopathy. Ophthalmology. 1982;89(10):1132-45.

28. Mosseri M, Yarom R, Gotsman MS, Hasin Y. Histologic evidence for small-vessel coronary artery disease in patients with angina pectoris and patent large coronary arteries. Circulation. 1986;74(5):964-72.

29. Burchfiel CM, Tracy RE, Chyou PH, Strong JP. Cardiovascular risk factors and hyalinization of renal arterioles at autopsy. The Honolulu Heart Program. Arterioscler Thromb Vasc Biol. 1997;17(4):760-8.

30. Wong TY, Klein R, Sharrett AR, Duncan BB, Couper DJ, Tielsch JM, et al. Retinal arteriolar narrowing and risk of coronary heart disease in men and women. The Atherosclerosis Risk in Communities Study. JAMA. 2002;287(9):1153-9.

31. Den Ruijter HM, Peters SA, Anderson TJ, Britton AR, Dekker JM, Eijkemans MJ, et al. Common carotid intima-media thickness measurements in cardiovascular risk prediction: a meta-analysis. JAMA. 2012;308(8):796-803.

32. O'Leary DH, Bots ML. Imaging of atherosclerosis: carotid intima-media thickness. Eur Heart J. 2010;31(14):1682-9.

33. Cuspidi C, Meani S, Salerno M, Fusi V, Severgnini B, Valerio C, et al. Retinal microvascular changes and target organ damage in untreated essential hypertensives. J Hypertens. 2004;22(11):2095-102.

34. Song YJ, Cho KI, Kim SM, Jang HD, Park JM, Kim SS, et al. The predictive value of retinal vascular findings for carotid artery atherosclerosis: are further recommendations with regard to carotid atherosclerosis screening needed? Heart Vessels. 2012 Jun 9. (epub ahead of print)

35. Maestri MM, Fuchs SC, Ferlin E, Pakter HM, Nunes G, Moraes RS, et al. Detection of arteriolar narrowing in fundoscopic examination: evidence of a low performance of direct ophthalmoscopy in comparison with a microdensitometric method. Am J Hypertens. 2007;20(5):501-5.

36. Wang JJ, Taylor B, Wong TY, Chua B, Rochtchina E, Klein R, et al. Retinal vessel diameters and obesity: a population-based study in older persons. Obesity (Silver Spring). 2006;14(2):206-14.

37. Ikram MK, de Jong FJ, Vingerling JR, Witteman JC, Hofman A, Breteler MM, et al. Are retinal arteriolar or venular diameters associated with markers for cardiovascular disorders? The Rotterdam Study. Invest Ophthalmol Vis Sci. 2004;45(7):2129-34.

38. Wong TY, Duncan BB, Golden SH, Klein R, Couper DJ, Klein BE, et al. Associations between the metabolic syndrome and retinal microvascular signs: the Atherosclerosis Risk In Communities study. Invest Ophthalmol Vis Sci. 2004;45(9):2949-54.

39. Naghavi M, Falk E, Hecht HS, Jamieson MJ, Kaul S, Berman D, et al. From vulnerable plaque to vulnerable patient--Part III: Executive summary of the Screening for Heart Attack Prevention and Education (SHAPE) Task Force report. Am J Cardiol. 2006;98(2A):2H-15H.

Table 1. Characteristics of the patients studied. (mean (± SD) or *n* (%))

Characteristics	**Patients (*N* = 173)**
Age (years)	57.8 ± 11.7
Male sex	54 (31.2)
Caucasian	120 (69.4)
Body Mass Index (kg/m^2)	30.6 ± 5.5
Smoker	76 (43.9)
Total Cholesterol (mg/dL)	207.8 (45.6)
HDL Cholesterol (mg/dL)	55.4 (21.3)
Systolic Blood Pressure (mm Hg) [a]	130.9 ± 14.7
Diastolic Blood Pressure (mm Hg) [a]	77.6 ± 10.0
Use of anti-hypertensive drugs	160 (92.5)
Diabetes Mellitus	37 (21.4)
Prior CVD	40 (23.1)
Framingham Risk Score [b]	
Low	74 (42.8)
Intermediate	47 (27.2)
High	52 (30)

CVD, cardiovascular disease.

[a] mean 24h, according to ambulatory blood pressure monitoring

[b] Framingham Risk Score categories are defined according to the estimated 10-year cardiovascular risk, as follows: Low, < 10%;Intermediate, 10 to 20%; High, >20%.

Table 2. Retinal calibers assessed by microdensitometric method and carotid ultrasound measurement in 173 patients. (mean (± SD) or *n* (%))

Measurement	**Result**
Arteriolar diameter (μm)	102. 8 ± 11.6
25th percentile	95.1
50th percentile	102.2
75th percentile	109.5
Venous diameter (μm)	128.9 ±15.5
25th percentile	119.8
50th percentile	127.9
75th percentile	138.2
Mean common carotid IMT (mm)	0.87 ± 0.19
25th percentile	0.75
50th percentile	0.83
75th percentile	0.97
Carotid Plaque	88 (50.9)

IMT, intima-media thickness

Table 3. Multiple linear regression model of carotid IMT on retinal arteriolar caliber, adjusted by age, sex, systolic blood pressure, total cholesterol and prior cardiovascular disease

Characteristics	**Adjusted β**	***P* value**
Carotid IMT (mm)	-0.235	0.001
Age (years)	0.160	0.015
Sex (male)	-.097	0.104
Systolic Blood Pressure (mmHg) [a]	-0.079	0.184
Total cholesterol (mg/dL)	-0.014	0.808
Prior CVD	0.121	0.033
Retinal venular caliber (μm)	0.684	<0.001
Model	R^2=0.505	<0.001

CVD, cardiovascular disease; IMT, intima-media thickness.

[a] mean 24h, according to ambulatory blood pressure monitoring.

Table 4. Multiple linear regression model of carotid IMT on retinal venular caliber, adjusted by age, sex, systolic blood pressure, total cholesterol and prior cardiovascular disease

Characteristics	**Adjusted β**	***P* value**
Carotid IMT (mm)	0.184	0.011
Age (years)	-0.101	0.127
Sex (male)	0.118	0.049
Systolic Blood Pressure (mmHg)[a]	0.086	0.148
Total cholesterol (mg/dL)	0.106	0.071
Prior CVD	-0.090	0.117
Retinal arteriolar caliber (μm)	0.689	<0.001
Model	R^2=0.502	<0.001

CVD, cardiovascular disease; IMT, intima-media thickness.

[a], mean 24h, according to ambulatory blood pressure monitoring.

6. Artigo de Revisao em Inglês:

Artigo Aceito para Publicacão no

AJR American Journal of Roentgenology (Fator de Impacto: 2.78).

Data para publicação: Janeiro de 2013

Coronary Calcium Scan Acquisition Prior to Coronary CT Angiography: Limited Benefit or Useful Addition?

Felipe S. Torres [1], Vikram Venkatesh [2], Elsie T. Nguyen [3], Laura Jimenez-Juan [3], Andrew M. Crean [3]

[1] Postgraduate Studies Program in Cardiology, School of Medicine, Universidade Federal do Rio Grande do Sul, Porto Alegre, RS, Brazil

[2] Grand River and St. Mary's General Hospital, Kitchener, ON, Canada

[3] Department of Medical Imaging, Cardiothoracic Division, Toronto General Hospital, University Health Network, Toronto, ON, Canada

Corresponding Author:

Felipe S. Torres, MD

Postgraduate Studies Program in Cardiology, School of Medicine,

Universidade Federal do Rio Grande do Sul

Ramiro Barcelos 2400, 2nd floor, Porto Alegre, RS, Brazil. CEP 90035-003

Abstract

Objective: This article reviews the role of coronary calcium quantification in symptomatic patients and the pros and cons of acquiring a non-enhanced coronary calcium scan in every patient with suspected coronary artery disease referred for coronary CT angiography.

Conclusion: The acquisition of a coronary calcium scan in every symptomatic patient referred for coronary CT angiography requires a case-by-case approach.

Keywords: coronary artery disease; coronary artery calcium; CT angiography; MDCT angiography

Introduction

Quantification of the amount of calcium in the coronary arteries with computed tomography (CT) has emerged as a non-invasive marker of atherosclerotic disease and powerful independent predictor of cardiovascular events in asymptomatic populations (1). The risk assessment provided by coronary calcium score (CCS) extends beyond the standard risk prediction of the Framingham risk score and to populations with a wide range of ethnic backgrounds (1). The CCS has the ability to re-stratify individuals with intermediate cardiovascular risk into lower or higher risk groups (2), potentially changing the intensity of risk management (3). In addition, the inclusion of CCS as a screening tool has been advocated by the Screening for Heart Attack Prevention and Education (SHAPE) task force (4). Therefore, quantification of coronary calcium with CT has an established role in the identification and risk stratification of coronary artery disease (CAD) in asymptomatic individuals.

On the other hand, the available evidence supporting coronary calcium quantification for CAD risk assessment in symptomatic patients is less robust. In this population, coronary CT angiography (CTA) has become a popular non-invasive imaging modality for the evaluation of CAD, capable of not only excluding significant coronary stenosis with excellent negative predictive value (5), but also assessing non-calcified plaque burden and non-obstructive coronary disease that are important prognostic factors in the evaluation of coronary atherosclerosis (6). The UK National Institute for Health and Clinical Excellence (NICE) Guidelines recommends coronary calcium quantification

with CT for patients referred for evaluation of stable chest pain and a low likelihood of CAD (7). The Scientific Statement of the American Heart Association (AHA) on the assessment of coronary artery disease by cardiac CT states that “coronary calcium assessment may be reasonable for the assessment of symptomatic patients” (Class of Recommendation: IIb; Level of Evidence: B) (8). However, the 2010 Appropriate Use Criteria for Coronary Computed Tomography do not list the use of coronary calcium quantification as an appropriate test for symptomatic patients (9). Therefore, coronary calcium quantification has been an important component of risk stratification in asymptomatic individuals, while coronary CTA has been an emerging and now established non-invasive method for CAD assessment in symptomatic patients.

The purpose of this review is to summarize the role of coronary calcium quantification in the evaluation of stable CAD in symptomatic patients and to discuss the pros and cons of acquiring a non-enhanced coronary calcium scan in every patient with suspected CAD referred for coronary CTA. This review will not encompass patients evaluated in the emergency department with acute chest pain.

Role of coronary calcium quantification in symptomatic patients with suspected CAD

Since the primary goal in symptomatic patients is the inclusion or exclusion of obstructive CAD, the relationship between the amount of coronary calcium and the location and presence of hemodynamic significant stenosis has been the focus of many investigations.

1- Correlation between coronary calcium and presence of obstructive CAD by invasive coronary angiography (ICA)

It is well known that there is a relationship between the amount of coronary calcification detected by CT and the total atherosclerotic plaque burden, with the coronary calcium detected by CT defining on average only about one fifth of the total atherosclerotic plaque present at histological examination (10). Therefore, this means that the higher the CCS, the higher the total plaque burden and, consequently, the odds for detection of obstructive CAD (11).

Multiple studies from the last 2 decades, using mainly electron beam CT (ECBT) in patients undergoing ICA, addressed this issue and demonstrated that CCS has a high sensitivity but only moderate specificity for the detection of obstructive CAD (3, 11). The American College of Cardiology Foundation/American Heart Association 2007 Expert Consensus Document states that, in symptomatic patients, exclusion of measurable coronary calcium might be an effective filter before ICA or hospital admission (3). In this regard, the accuracy of a zero CCS to predict the absence of significant coronary stenosis by ICA was recently reviewed in a meta-analysis from Sarwar and colleagues (12). In 18 studies with > 10,000 symptomatic patients (56% prevalence of obstructive disease, defined as > 50% stenosis by ICA), the presence of calcium had a pooled sensitivity, specificity, negative predictive value (NPV) and positive predictive value (PPV) of 98%, 40%, 93% and 68%, respectively, for the prediction of a significant coronary stenosis. In

this population, a CCS of 0 was seen in 2% of patients in whom a > 50% coronary stenosis was detected on ICA (12). Conversely, recent studies have shown variable rates of obstructive CAD in patients with absent coronary calcification, ranging from 8%-19% (13, 14, 15) (Figure 1). This variability is due to the fact that the probability of obstructive CAD is driven in large part by the clinical pretest probability of disease (16, 17).

2- Correlation between the location of coronary calcification and the presence and severity of coronary stenosis

Coronary calcium has been considered a sensitive marker for the presence of significant stenosis in the coronary tree, but not in a particular coronary vessel or segment. In a study by Lau and colleagues (18), 50 patients referred for ICA for evaluation of suspected CAD underwent coronary CTA and coronary calcium quantification. Mean CCS was higher in segments, vessels, and patients with significant stenosis than in segments, vessels, and patients without stenosis. However, the ability of CCS to discriminate between the presence or absence of stenosis was greatest for patients and least for individual vessels and segments. (18). These results suggest that the presence of a large calcified plaque in a certain coronary segment does not necessarily mean that obstructive CAD will be detected in that particular segment on ICA or coronary CTA.

3- Prognostic value of zero coronary calcium score in symptomatic patients

The meta-analysis by Sarwar and colleagues also examined the prognosis of 3,924 symptomatic patients from 7 studies on the basis of absent coronary calcification (12). After a mean follow up of 42 months, 1.8% (17/921) of patients with no evidence of coronary calcium had a cardiovascular event in comparison to 9.0% (270/3,003) of patients with detectable coronary calcium. The number of events in patients with no detectable calcium in individual studies varied from 0 to 5.2% (12). More recently, the prognostic value of a CCS of 0 was assessed in the CONFIRM Registry (19), a large prospective multicenter cohort of symptomatic patients predominantly with intermediate pretest probability of CAD referred for coronary CTA. The prevalence of any major coronary artery with ≥50% stenosis on coronary CTA among patients with a CCS of 0 was 3.5%, and 82% of these patients had single-vessel disease, a cohort in which coronary revascularization has not been shown to improve survival. During a median follow-up of 2.1 years, there was no difference in all-cause mortality in patients without coronary calcification despite the presence of non-obstructive or obstructive CAD (figure 2).

In summary, there is a positive correlation between the amount of coronary calcification and the prevalence of obstructive CAD in symptomatic patients. The absence of coronary calcification, as demonstrated by CT, is also associated with a very good near term prognosis, particularly in patients in the low to intermediate risk category.

Coronary CT Angiography in the evaluation of symptomatic patients with suspected CAD

Coronary CTA plays an important role in the evaluation of symptomatic patients with low to intermediate risk of CAD. Numerous studies have demonstrated a high sensitivity and high NPV for ruling out obstructive coronary artery disease in stable symptomatic patients (5), providing important prognostic information (6). The ability to demonstrate obstructive and non-obstructive coronary disease cannot be overemphasized, since a dose response relationship between mortality and the presence of non-obstructive CAD, 1-vessel, 2-vessel and 3-vessel/left main obstructive CAD has been demonstrated by coronary CTA (20). In individuals in the low to intermediate risk categories, the use of coronary CTA has been considered appropriate for the evaluation of symptomatic patients with suspected stable CAD (9).

Role of Coronary Calcium Quantification Immediately Prior to Coronary CT Angiography

When considering the acquisition of a CCS prior to a coronary CTA, the information obtained may be useful to diagnose CAD and to establish the prognosis of the patient's disease. This additional information should be balanced against the risks of the test, mainly the radiation dose, and by the additional time required for immediate calculation and interpretation of the results prior to proceeding with the coronary CTA.

1- Influence of CCS in the decision on when to perform a coronary CTA

Coronary calcium score has been considered a possible gatekeeper for coronary CTA because the reliability of results of the coronary CTA is influenced by the presence and severity of coronary calcification (21). In this scenario, the decision to proceed with the coronary CTA acquisition after the results of the coronary calcium scan could be based on 2 categories: patients without evidence of coronary calcification (CCS = 0), and patients with a high coronary calcium score.

a) Absent Coronary Calcification (CCS = 0)

In low-risk symptomatic patients referred for coronary CTA, it has been proposed that a negative coronary calcium scan would suffice as a guarantor of an excellent prognosis in the evaluation of symptomatic patients with suspected CAD and that proceeding with the CTA acquisition might not be necessary (18). On the other hand, absence of coronary calcification may not be enough to exclude obstructive CAD (Figure 2), particularly in patients who present with typical angina or atypical chest pain (22). Dyspnea as a presenting symptom, smoking and family history of premature CAD in a first-degree relative were also factors associated with obstructive CAD in patients with CCS of 0 in a recent large registry study (19). Currently, there is no consensus regarding the usefulness of a negative CCS on deferring the coronary CTA in low to intermediate risk symptomatic patients (23). Nonetheless, the absence of coronary calcification is associated with low prevalence of obstructive CAD.

b) High Coronary Calcium Score

A high coronary calcium score is associated with a high prevalence of obstructive CAD, but the relation between coronary calcification and luminal narrowing at the same anatomic site is non-linear and has large confidence limits (11). Furthermore, it has been suggested that a high amount of coronary calcium concentrated in a single vessel may be more predictive of underlying obstructive disease than the overall amount of calcium in the entire coronary artery tree (24, 25). On the other hand, a recent analysis of the ACCURACY trial (26) demonstrated that coronary artery segments exhibiting calcified plaque were rarely associated with obstructive coronary stenosis.

Coronary calcification is also one of the factors associated with a non-diagnostic coronary CTA, particularly due to blooming artifact. Studies from patients with more extensive coronary calcification are more likely to present non-evaluable coronary segments (27, 28) (Figure 3) and result in false positive results (29, 30) (Figure 4). Some authors have even advocated not to proceed with the CTA when CCS levels are as low as 100 (21). However, as a determinant of poor image quality, the total CCS may be less important than the location and severity of the calcification within each vessel. Dewey and colleagues (31) suggested that, if a predefined upper limit of CCS were to be defined in order to perform coronary CTA, it would be more appropriate at a vessel level rather than at a patient level. In addition, the location of the calcification (i.e., the degree of circumferential compromise) may also be important, since completely circumferential calcified plaques tend to obscure the vessel lumen more often than eccentric calcified plaques (28). Nonetheless, data from the CORE 64 study (32) showed that the accuracy and NPV of coronary CTA to detect a ≥ 50% coronary stenosis in patients

referred to ICA is reduced when the CCS is ≥ 600. A recent meta-analysis from Abdulla and colleagues (25) on the influence of coronary calcification on diagnostic accuracy of 64-row MDCT suggested that, in patients with a CCS ≥400, a careful pre-angiographic evaluation based on patients total and arterial burden of calcified plaques should be considered before proceeding to angiography.

In summary, when a patient is referred for coronary CTA, there is no established upper limit of the total calcium score that could be used as a threshold above which a coronary CTA should not be performed. Nonetheless, one must keep in mind that the higher the CCS, the higher the prevalence of underlying obstructive CAD, the higher the number of non-evaluable segments and the lower the specificity of the coronary CTA. In this context, the 2010 Appropriateness Criteria for Cardiac Computed Tomography consider the performance of coronary CTA in patients with a CCS > 400 of uncertain value (9). Further studies are needed to investigate whether there is a threshold level of CCS either on a per-patient or per-segment level above which CTA should not be performed.

2- Influence of CCS in the interpretation of the coronary CTA results

In addition to the influence in the decision on when to proceed with the contrast-enhanced study, the CCS may also add to the interpretation of the coronary CTA. We may consider the results of the CCS in 3 different scenarios: negative, positive, or non-diagnostic coronary CTA.

a) Negative coronary CTA

Some authors (17) have suggested that, due to the high sensitivity of an elevated CCS, when a coronary CTA is negative for the presence of a significant stenosis in a patient with a CCS >400, the patient should be considered likely to have unrecognized obstructive CAD. On the other hand, applying the same criteria in a study by Leschka and colleagues (33), in which 74 patients referred for ICA also underwent coronary CTA and coronary calcium quantification, 6 patients (8.1%) would have been misclassified as having obstructive CAD on the basis of a CCS ≥ 400 despite being correctly classified by coronary CTA. These discrepant results are likely related to the pretest probability of obstructive CAD of the population studied, which should always be considered in the context of a negative coronary CTA. In patients with low to intermediate pretest probability, the populations for whom coronary CTA has been advocated (9), a negative coronary CTA shows very high NPV, independent of the CCS (5).

b) Positive coronary CTA

A coronary CTA indicating the presence of obstructive CAD is usually followed by a stress test or an invasive coronary angiogram, independent of the amount of coronary calcification. Therefore, the presence or absence of coronary calcium usually does not influence the result of a coronary CTA when it is considered positive for obstructive CAD.

c) Non-diagnostic coronary CTA

The utility of the CCS in the setting of a non-diagnostic CTA has not been formally evaluated, since patients with non-diagnostic studies usually undergo additional testing, such as a stress test or ICA. There are several possible causes for a non-diagnostic coronary CTA, one of the most common being severe coronary calcification. Since a non-evaluable coronary segment is usually considered positive for an obstructive coronary stenosis in research and clinical settings, the CCS is unlikely to change patient management in the majority of cases.

Another possible reason for a coronary CTA to be labeled as non-diagnostic is cardiac motion. In this setting, it has been proposed that the absence of coronary calcification would improve the diagnostic performance of the CTA alone and could exclude significant CAD with a high diagnostic accuracy, potentially avoiding unnecessary ICA examination in these patients (33). Nonetheless, as discussed previously, the NPV of absent coronary calcification is dependent on individual symptoms and pre-test clinical probability of CAD, which should always be considered when interpreting the coronary CTA and CCS in conjunction.

3- Comparative Prognostic Information

It is well known that the prognosis of patients with CAD is driven mainly by the presence of obstructive disease, with a progressively worse prognosis seen from 1-vessel, to 2-vessels and to 3-vessels disease (34). One of the strengths of coronary CTA is to demonstrate and quantify non-obstructive CAD. In this context, recent publications expanded the prognostic information provided by coronary CTA in patients with suspected CAD and non-

obstructive disease, confirming the dose-response relationship between the degree of coronary obstruction and adverse outcomes (6, 20, 35, 36).

Direct comparison between the prognostic information provided by these two tests when performed at the same time is limited to a small number of investigations. In the meta-analysis by Bamberg and colleagues (6), a pooled analysis of 3 studies with 3465 patients demonstrated that the association between the presence of significant coronary stenosis or any plaque and cardiovascular events remained highly significant after adjustment for coronary calcium. Since 2010, at least 6 other studies have been published comparing the prognostic information provided by CCS and coronary CTA in patients with suspected CAD (19, 37-41). In all studies but one (38), coronary CTA provided incremental prognostic information beyond the analysis of CCS.

3- Radiation Dose

The decision to perform a coronary calcium scan before every coronary CTA must balance the benefits, namely the added diagnostic and prognostic information, with the risks, namely the potential additional radiation dose.

The radiation dose of a coronary CTA, as shown by the multinational PROTECT I study (42), can be extremely variable, depending on the parameters used, in particular the scan mode and tube voltage. Many adaptations of the acquisition protocols have been suggested to minimize radiation dose while maintaining adequate image quality in coronary CTA (43). In this context, a strategy in which the coronary calcium scan was not performed, unless specifically requested by the referring physician, was put in

place and translated into a significant decrease in the radiation dose (44). In addition, despite efforts to standardize the acquisition protocol for coronary calcium scans (45), a wide spectrum of radiation doses (approximately 1-12 mSv) has been associated with this test (46, 47). On the other hand, with the development of newer technologies and optimized dose reduction protocols, a significant decrease in radiation dose for CCS is expected.

The manipulation of some acquisition parameters can have a profound impact on the radiation dose of the coronary calcium scan, and recommendations to minimize radiation exposure during acquisition of CCS have been recently published (48). Several studies have shown that the tube current can be adapted to patient's size without a significant effect on CCS results (49-51) and that prospective electrocardiographic (ECG)-triggering should be used to minimize radiation exposure (48). Although coronary calcium quantification with MDCT scanners at a peak tube voltage of 120 kVp is generally perceived as equivalent to electrom-beam CT calcium scores (52), CCS performed with a reduced tube voltage is feasible but requires modifications in the 130 Hounsfield units threshold used for calcium detection (53, 54). It is uncertain as to whether there is any significant effect of lower dose CCS acquisition combining all these modified parameters on the measured calcium score, and large prospectively recruited studies may be required to re-validate CCS prognostic information based on lower dose techniques.

One important parameter of the coronary CTA acquisition that can be directly determined by the CCS is the scan *z*-axis length, which has a direct effect on the radiation dose of the CT study (55, 56). When planning the z-

axis coverage of the coronary CTA acquisition by determining the limits of the craniocaudal extent of the coronary arteries, the use of the prospectively ECG-triggered coronary calcium images may reduce the total radiation dose of the combined CCS-CTA examination by allowing substantial z-axis radiation dose reduction for the CTA portion of the exam (57, 58).

Therefore, if the CCS is to be performed, a prospective ECG-triggered protocol must be used, along with a patient size-adjusted tube current, and the widest beam collimation that allows for reconstruction of 3-mm slices (48). In addition, the scan range of the coronary CTA should be guided by the non-enhanced acquisition, to minimize the scan *z*-axis length.

4- Additional Time Required for CCS Calculation before Coronary CTA Acquisition

In most centers, when CCS is performed prior to the coronary CTA, the interpretation of both tests is usually done after image acquisition. Depending on the number of studies performed per day, routine calculation of CCS immediately prior to every coronary CTA may not be practical and may potentially disrupt workflow and scanner throughput. Nonetheless, this is highly dependent on the structure and organization of each individual site.

Small Coronary Calcifications and Calcifications Elsewhere in the Chest

Very small coronary calcifications may be missed by the contrast enhanced CT angiography, since the degree of luminal attenuation may match the attenuation of small calcified plaques. Without the unenhanced

coronary calcium acquisition, a study may be mislabeled as normal (i.e., no evidence of coronary atherosclerosis) despite the presence of small atherosclerotic plaques. Although it has been shown that the prognosis of patients with non-obstructive CAD is worse when compared to patients without evidence of CAD on coronary CTA (36), the potential implications of this misinterpretation in terms of patient management and outcome is currently unknown. On the other hand, the reconstructed 2.5 to 3 mm thick images of CCS may obscure small calcified coronary plaques due to volume averaging (59), that may only be depicted in the contrast enhanced CTA reconstructed with thin slices (0.5 to 0.625 mm).

The acquisition of an unenhanced scan could provide additional information when characterizing cardiac non-coronary and non-cardiac structures. In such cases, the lack of an unenhanced acquisition could lead to reduced ability to recognize calcifications elsewhere in the heart, lungs or chest wall that might otherwise be confused with enhancing masses on the CTA. This hypothesis, however, has never been formally tested. Furthermore, it is preferable to deal with potentially important findings when detected instead of routinely performing an unenhanced acquisition that may rarely prove useful.

Coronary Calcium Quantification in Contrast-Enhanced Coronary CTA

Since the quantification of coronary calcium in contrast-enhanced studies could obviate the need for non-enhanced coronary calcium scans, there has been growing interest in calcium quantification using contrast-enhanced CT images. Different approaches have been compared to the

conventional coronary calcium scoring method and have demonstrated comparable results (60-64). However, these methods are dependent on datasets with very good to excellent image quality and are not as easy to calculate as the traditional CCS, requiring a variable amount of post-processing time and specific analysis software. Further studies with large numbers of patients are required to validate these techniques before its use could be recommended.

Conclusion

In conclusion, it is clear that both CCS and coronary CTA provide valuable information in the evaluation of CAD. The amount of data regarding the use of CCS in symptomatic patients is not as robust as in the asymptomatic population. The available evidence suggests that the diagnostic and prognostic information provided by coronary CTA in low to intermediate risk symptomatic patients evaluated for suspected CAD may exceed the information provided by the CCS. Nonetheless, the results of the CCS, when interpreted immediately, may serve as a gatekeeper for coronary CTA but this has its limitations both in practicality and efficacy. Also, the overall radiation dose impact of performing a prospectively triggered CCS is uncertain, and may actually reduce the total radiation depending on protocol chosen. There has been significant reduction in radiation dose associated with both tests (CCS and CTA) in recent years and the decision to routinely perform a CCS in symptomatic patients referred for coronary CTA should be individualized, requiring a case-by-case approach (Box). If a CCS is to be performed, several factors, such as clinical pretest probability of CAD and results of prior

diagnostic tests, must be considered before the decision to proceed with the coronary CTA.

References

1. Greenland P, LaBree L, Azen SP, Doherty TM, Detrano RC. Coronary artery calcium score combined with Framingham score for risk prediction in asymptomatic individuals. *JAMA* 2004;291:210-215.

2. Polonsky TS, McClelland RL, Jorgensen NW, et al. Coronary artery calcium score and risk classification for coronary heart disease prediction. *JAMA* 2010;303:1610-1616.

3. Greenland P, Bonow RO, Brundage BH, et al. ACCF/AHA 2007 clinical expert consensus document on coronary artery calcium scoring by computed tomography in global cardiovascular risk assessment and in evaluation of patients with chest pain: a report of the American College of Cardiology Foundation Clinical Expert Consensus Task Force (ACCF/AHA Writing Committee to Update the 2000 Expert Consensus Document on Electron Beam Computed Tomography). *Circulation* 2007;115:402-426.

4. Naghavi M, Falk E, Hecht HS, et al. From vulnerable plaque to vulnerable patient--Part III: Executive summary of the Screening for Heart Attack Prevention and Education (SHAPE) Task Force report. *Am J Cardiol* 2006;98:2H-15H.

5. Mowatt G, Cook JA, Hillis GS, et al. 64-Slice computed tomography angiography in the diagnosis and assessment of coronary artery disease: systematic review and meta-analysis. *Heart* 2008;94:1386-1393.

6. Bamberg F, Sommer WH, Hoffmann V, et al. Meta-analysis and systematic review of the long-term predictive value of assessment of coronary atherosclerosis by contrast-enhanced coronary computed tomography angiography. *J Am Coll Cardiol* 2011;57:2426-2436.

7. Skinner JS, Smeeth L, Kendall JM, Adams PC, Timmis A; Chest Pain Guideline Development Group. NICE guidance. Chest pain of recent onset: assessment and diagnosis of recent onset chest pain or discomfort of suspected cardiac origin. *Heart* 2010;96:974-978.

8. Budoff MJ, Achenbach S, Blumenthal RS, et al. Assessment of coronary artery disease by cardiac computed tomography: a scientific statement from the American Heart Association Committee on Cardiovascular Imaging and Intervention, Council on Cardiovascular Radiology and Intervention, and Committee on Cardiac Imaging, Council on Clinical Cardiology. *Circulation* 2006;114:1761-1791.

9. Taylor AJ, Cerqueira M, Hodgson JM, et al. ACCF/SCCT/ACR/AHA/ASE/ASNC/NASCI/SCAI/SCMR 2010 Appropriate Use Criteria for Cardiac Computed Tomography. A Report of the American College of Cardiology Foundation Appropriate Use Criteria Task Force, the

Society of Cardiovascular Computed Tomography, the American College of Radiology, the American Heart Association, the American Society of Echocardiography, the American Society of Nuclear Cardiology, the North American Society for Cardiovascular Imaging, the Society for Cardiovascular Angiography and Interventions, and the Society for Cardiovascular Magnetic Resonance.
J Cardiovasc Comput Tomogr 2010;4:407.e1-33.

10. Rumberger JA, Simons DB, Fitzpatrick LA, Sheedy PF, Schwartz RS. Coronary artery calcium area by electron-beam computed tomography and coronary atherosclerotic plaque area. A histopathologic correlative study. *Circulation* 1995;92:2157-2162.

11. O'Rourke RA, Brundage BH, Froelicher VF, et al. American College of Cardiology/American Heart Association Expert Consensus document on electron-beam computed tomography for the diagnosis and prognosis of coronary artery disease. *Circulation* 2000;102:126-140.

12. Sarwar A, Shaw LJ, Shapiro MD, et al. Diagnostic and prognostic value of absence of coronary artery calcification. *JACC Cardiovasc Imaging* 2009;2:675-688.

13. Akram K, O'Donnell RE, King S, Superko HR, Agatston A, Voros S. Influence of symptomatic status on the prevalence of obstructive coronary

artery disease in patients with zero calcium score. *Atherosclerosis* 2009;203:533-537.

14. Cademartiri F, Maffei E, Palumbo A, et al. Diagnostic accuracy of computed tomography coronary angiography in patients with a zero calcium score. *Eur Radiol* 2010;20:81-87.

15. Gottlieb I, Miller JM, Arbab-Zadeh A, et al. The absence of coronary calcification does not exclude obstructive coronary artery disease or the need for revascularization in patients referred for conventional coronary angiography. *J Am Coll Cardiol* 2010;55:627-634.

16. Blaha MJ, Blumenthal RS, Budoff MJ, Nasir K. Understanding the utility of zero coronary calcium as a prognostic test: a Bayesian approach. *Circ Cardiovasc Qual Outcomes* 2011;4:253-256.

17. van Werkhoven JM, de Boer SM, Schuijf JD, et al. Impact of clinical presentation and pretest likelihood on the relation between calcium score and computed tomographic coronary angiography. *Am J Cardiol* 2010;106:1675-1679.

18. Lau GT, Ridley LJ, Schieb MC, et al. Coronary artery stenoses: detection with calcium scoring, CT angiography, and both methods combined. *Radiology* 2005;235:415-422.

19. Villines TC, Hulten EA, Shaw LJ, et al. Prevalence and Severity of Coronary Artery Disease and Adverse Events Among Symptomatic Patients With Coronary Artery Calcification Scores of Zero Undergoing Coronary Computed Tomography Angiography Results From the CONFIRM (Coronary CT Angiography Evaluation for Clinical Outcomes: An International Multicenter) Registry. *J Am Coll Cardiol* 2011;58:2533-2540.

20. Min JK, Dunning A, Lin FY, et al. Age- and sex-related differences in all-cause mortality risk based on coronary computed tomography angiography findings results from the International Multicenter CONFIRM (Coronary CT Angiography Evaluation for Clinical Outcomes: An International Multicenter Registry) of 23,854 patients without known coronary artery disease. *J Am Coll Cardiol* 2011;58:849-860.

21. Palumbo AA, Maffei E, Martini C, et al. Coronary calcium score as gatekeeper for 64-slice computed tomography coronary angiography in patients with chest pain: per-segment and per-patient analysis. *Eur Radiol* 2009;19:2127-2135.

22. Akram K, O'Donnell RE, King S, Superko HR, Agatston A, Voros S. Influence of symptomatic status on the prevalence of obstructive coronary artery disease in patients with zero calcium score. *Atherosclerosis* 2009;203:533-537.

23. Nasir K, Blaha MJ, Kwon SW, Chang HJ. No Justification for Coronary CT Angiography in Low- to Intermediate-Risk Individuals with Coronary Artery Calcium Score of 0. *Radiology* 2011;261:663-664.

24. Thilo C, Gebregziabher M, Mayer FB, Zwerner PL, Costello P, Schoepf UJ. Correlation of regional distribution and morphological pattern of calcification at CT coronary artery calcium scoring with non-calcified plaque formation and stenosis. *Eur Radiol* 2010;20:855-861.

25. Abdulla J, Pedersen KS, Budoff M, Kofoed KF. Influence of coronary calcification on the diagnostic accuracy of 64-slice computed tomography coronary angiography: a systematic review and meta-analysis. *Int J Cardiovasc Imaging* 2011 Jun 12. [Epub ahead of print]

26. Min JK, Edwardes M, Lin FY,et al. Relationship of coronary artery plaque composition to coronary artery stenosis severity: Results from the prospective multicenter ACCURACY trial. *Atherosclerosis* 2011;219:573-578.

27. Stolzmann P, Scheffel H, Leschka S, et al. Influence of calcifications on diagnostic accuracy of coronary CT angiography using prospective ECG triggering. *AJR* 2008;191:1684-1689.

28. Vavere AL, Arbab-Zadeh A, Rochitte CE, et al. Coronary Artery Stenoses: Accuracy of 64-Detector Row CT Angiography in Segments with Mild,

Moderate, or Severe Calcification--A Subanalysis of the CORE-64 Trial. *Radiology* 2011;261:100-108.

29. Budoff MJ, Dowe D, Jollis JG, et al. Diagnostic performance of 64-multidetector row coronary computed tomographic angiography for evaluation of coronary artery stenosis in individuals without known coronary artery disease: results from the prospective multicenter ACCURACY (Assessment by Coronary Computed Tomographic Angiography of Individuals Undergoing Invasive Coronary Angiography) trial. *J Am Coll Cardiol* 2008;52:1724-1732.

30. Zhang S, Levin DC, Halpern EJ, Fischman D, Savage M, Walinsky P. Accuracy of MDCT in assessing the degree of stenosis caused by calcified coronary artery plaques. *AJR* 2008;191:1676-1683.

31. Dewey M, Vavere AL, Arbab-Zadeh A, et al. Patient characteristics as predictors of image quality and diagnostic accuracy of MDCT compared with conventional coronary angiography for detecting coronary artery stenoses: CORE-64 Multicenter International Trial. *AJR* 2010;194:93-102.

32. Arbab-Zadeh A, Miller JM, Rochitte CE, et al. Diagnostic Accuracy of Computed Tomography Coronary Angiography According to Pre-Test Probability of Coronary Artery Disease and Severity of Coronary Arterial Calcification The CORE-64 (Coronary Artery Evaluation Using 64-Row Multidetector Computed Tomography Angiography) International Multicenter Study. *J Am Coll Cardiol* 2012;59:379-387.

33.Leschka S, Scheffel H, Desbiolles L, et al. Combining dual-source computed tomography coronary angiography and calcium scoring: added value for the assessment of coronary artery disease. *Heart* 2008;94:1154-1161

34. Ringqvist I, Fisher LD, Mock M, et al. Prognostic value of angiographic indices of coronary artery disease from the Coronary Artery Surgery Study (CASS). *J Clin Invest* 1983;71:1854-1866.

35. Lin FY, Shaw LJ, Dunning AM, et al. Mortality risk in symptomatic patients with nonobstructive coronary artery disease: a prospective 2-center study of 2,583 patients undergoing 64-detector row coronary computed tomographic angiography. *J Am Coll Cardiol* 2011;58:510-519.

36. Hulten EA, Carbonaro S, Petrillo SP, Mitchell JD, Villines TC. Prognostic value of cardiac computed tomography angiography: a systematic review and meta-analysis. *J Am Coll Cardiol* 2011;57:1237-1247.

37. Kwon SW, Kim YJ, Shim J, et al. Coronary artery calcium scoring does not add prognostic value to standard 64-section CT angiography protocol in low-risk patients suspected of having coronary artery disease. *Radiology* 2011;259:92-99.

38. Schmermund A, Elsässer A, Behl M, et al. Comparison of prognostic usefulness (three years) of computed tomographic angiography versus 64-slice computed tomographic calcium scanner in subjects without significant coronary artery disease. *Am J Cardiol* 2010;106:1574-1579.

39. Russo V, Zavalloni A, Bacchi Reggiani ML, et al. Incremental prognostic value of coronary CT angiography in patients with suspected coronary artery disease. *Circ Cardiovasc Imaging* 2010;3:351-359.

40. Hadamitzky M, Distler R, Meyer T, et al. Prognostic value of coronary computed tomographic angiography in comparison with calcium scoring and clinical risk scores. *Circ Cardiovasc Imaging* 2011;4:16-23.

41. Petretta M, Daniele S, Acampa W, et al. Prognostic value of coronary artery calcium score and coronary CT angiography in patients with intermediate risk of coronary artery disease. *Int J Cardiovasc Imaging* 2011 Sep 16. [Epub ahead of print]

42. Hausleiter J, Meyer T, Hermann F, et al. Estimated radiation dose associated with cardiac CT angiography. *JAMA* 2009;301:500-507.

43. Torres FS, Crean AM, Nguyen ET, Paul N. Strategies for radiation-dose reduction and image-quality optimization in multidetector computed tomographic coronary angiography. *Can Assoc Radiol J* 2010;61:271-279.

44. Raff GL, Chinnaiyan KM, Share DA, et al. Radiation dose from cardiac computed tomography before and after implementation of radiation dose-reduction techniques. *JAMA* 2009;301:2340-2348.

45. McCollough CH, Ulzheimer S, Halliburton SS, Shanneik K, White RD, Kalender WA. Coronary artery calcium: a multi-institutional, multimanufacturer international standard for quantification at cardiac CT. *Radiology* 2007;243:527-538.

46. Mettler FA Jr, Huda W, Yoshizumi TT, Mahesh M. Effective doses in radiology and diagnostic nuclear medicine: a catalog. *Radiology* 2008;248:254-263.

47. Kim KP, Einstein AJ, Berrington de González A. Coronary artery calcification screening: estimated radiation dose and cancer risk. *Arch Intern Med* 2009;169:1188-1194.

48. Halliburton SS, Abbara S, Chen MY, et al; Society of Cardiovascular Computed Tomography. SCCT guidelines on radiation dose and dose-optimization strategies in cardiovascular CT. *J Cardiovasc Comput Tomogr* 2011;5:198-224.

49. Mahnken AH, Wildberger JE, Simon J, et al. Detection of coronary calcifications: feasibility of dose reduction with a body weight-adapted examination protocol. *AJR* 2003;181:533-538.

50. Newton TD, Mehrez H, Wong K, et al. Radiation dose threshold for coronary artery calcium score with MDCT: How low can you go? *Eur Radiol* 2011;21:2121-2129.

51. Dey D, Nakazato R, Pimentel R, et al. Low radiation coronary calcium scoring by dual-source CT with tube current optimization based on patient body size. *J Cardiovasc Comput Tomogr* 2012;6:113-120.

52. Daniell AL, Wong ND, Friedman JD, et al. Concordance of coronary artery calcium estimates between MDCT and electron beam tomography. *AJR* 2005;185:1542-1545.

53. Thomas CK, Mühlenbruch G, Wildberger JE, et al. Coronary artery calcium scoring with multislice computed tomography: in vitro assessment of a low tube voltage protocol. *Invest Radiol* 2006;41:668-673.

54. Nakazato R, Dey D, Gutstein A, et al. Coronary artery calcium scoring using a reduced tube voltage and radiation dose protocol with dual-source computed tomography. *J Cardiovasc Comput Tomogr* 2009;3:394-400.

55. Huda W, Mettler FA. Volume CT dose index and dose-length product displayed during CT: what good are they? *Radiology* 2011;258:236-242.

56. Khan A, Nasir K, Khosa F, Saghir A, Sarwar S, Clouse ME. Prospective gating with 320-MDCT angiography: effect of volume scan length on radiation dose. *AJR* 2011;196:407-411.

57. Gopal A, Budoff MJ. A new method to reduce radiation exposure during multi-row detector cardiac computed tomographic angiography. *Int J Cardiol* 2009;132:435-436.

58. Leschka S, Kim CH, Baumueller S, et al. Scan length adjustment of CT coronary angiography using the calcium scoring scan: effect on radiation dose. *AJR* 2010;194:W272-277.

59. Schlosser T, Hunold P, Voigtländer T, Schmermund A, Barkhausen J. Coronary artery calcium scoring: influence of reconstruction interval and reconstruction increment using 64-MDCT. *AJR* 2007;188:1063-1068.

60. Hong C, Becker CR, Schoepf UJ, Ohnesorge B, Bruening R, Reiser MF. Coronary artery calcium: absolute quantification in nonenhanced and contrast-enhanced multi-detector row CT studies. *Radiology* 2002;223:474-480.

61. Glodny B, Helmel B, Trieb T, Schenk C, Taferner B, Unterholzner V, Strasak A, Petersen J. A method for calcium quantification by means of CT coronary angiography using 64-multidetector CT: very high correlation with Agatston and volume scores. *Eur Radiol* 2009;19:1661-1668.

62. van der Bijl N, Joemai RM, Geleijns J, Bax JJ, Schuijf JD, de Roos A, Kroft LJ. Assessment of Agatston coronary artery calcium score using contrast-enhanced CT coronary angiography. *AJR* 2010;195:1299-1305.

63. Bischoff B, Kantert C, Meyer T, Hadamitzky M, Martinoff S, Schömig A, Hausleiter J. Cardiovascular risk assessment based on the quantification of coronary calcium in contrast-enhanced coronary computed tomography angiography. *Eur J Echocardiogr* 2011 Dec 13. [Epub ahead of print]

64. Otton JM, Lønborg JT, Boshell D, Feneley M, Hayen A, Sammel N, Sesel K, Bester L, McCrohon J. A method for coronary artery calcium scoring using contrast-enhanced computed tomography. *J Cardiovasc Comput Tomogr* 2012;6:37-44.

Figures Legends

Fig. 1 — All-cause mortality-free survival among patients according to coronary calcium score and the severety if coronary artery disease on coronary CTA (reproduced with permission from reference 19; Villines T, et al. J Am Coll Cardiol 2011).
CTA, computed tomography angiography.

Fig. 2 — 69 year old male with atypical chest pain.
A-C, Coronary computed tomography angiography cross-section (**A**) and curved plane reformatted (**B** and **C**) images of the right coronary artery showing a ≥ 50% stenosis (arrows) due to non-calcified plaque in a patient with a coronary calcium score = 0.

Fig. 3 — Bar graph shows influence of calcification on segment-level CT image quality (Reproduced with permission from reference 28;Vavere Al, et al. Radiology 2011:261:106. RSNA ©).

Fig. 4 — 65 year old male with atypical chest pain.
A, Transaxial coronary CTA image at the level of the mid left anterior descending coronary artery (LAD) shows a dense calcified plaque (white arrow) suspicious for a ≥ 50% stenosis.
B and **C**, Invasive coronary angiography images do not confirm the coronary CTA finding and showed only mild reduction in the caliber of the mid LAD (black arrows).

CTA, computed tomography angiography;

Box. Summary of the Role of Coronary Calcium Quantification Immediately Prior to Coronary CT Angiography *

Prior to Coronary CTA Acquisition

1. CCS may be used as a gatekeeper for coronary CTA when the CCS is very high, although there is no established upper limit of the total calcium score that could be used as a threshold above which a coronary CTA should not be performed.
2. The absence of coronary calcification is associated with a low prevalence of obstructive CAD and with a very good near term prognosis in symptomatic patients with a low to intermediate pretest probability of CAD. In these patients, additional information (symptoms, clinical risk factors and results of prior tests) should be entertained when considering deferring the coronary CTA based on a CCS = 0.
3. Radiation dose from CCS and coronary CTA may vary widely. Newer scanner technologies and the use of radiation dose reduction strategies have helped to significantly decrease the radiation dose of both tests. If CCS is to be acquired, much attention should be paid to minimize radiation exposure and to plan the scan range of the coronary CTA based on CCS images.

After Coronary CTA Acquisition and Interpretation

1. In patients with low to intermediate pretest probability of CAD (the categories for which coronary CTA has been endorsed), a negative coronary CTA shows a very high NPV, independent of the CCS.
2. The CCS does not influence the result of the coronary CTA when it is considered positive for obstructive CAD.
3. The utility of the CCS in the setting of a non-diagnostic CTA has not been formally evaluated, since patients with non-diagnostic studies usually undergo additional testing, such as a stress test or ICA.
4. The CCS should not be used *routinely* to detect small coronary calcified plaques that could potentially be obscured by the contrast-enhanced CTA acquisition or in an attempt to provide additional information when characterizing non-coronary structures.

* In patients with suspected stable CAD referred for coronary CTA.
CAD, coronary artery disease; CCS, coronary calcium score; CTA, computed tomography angiography; ICA, invasive coronary angiography; NPV, negative predictive value.

Figure 1

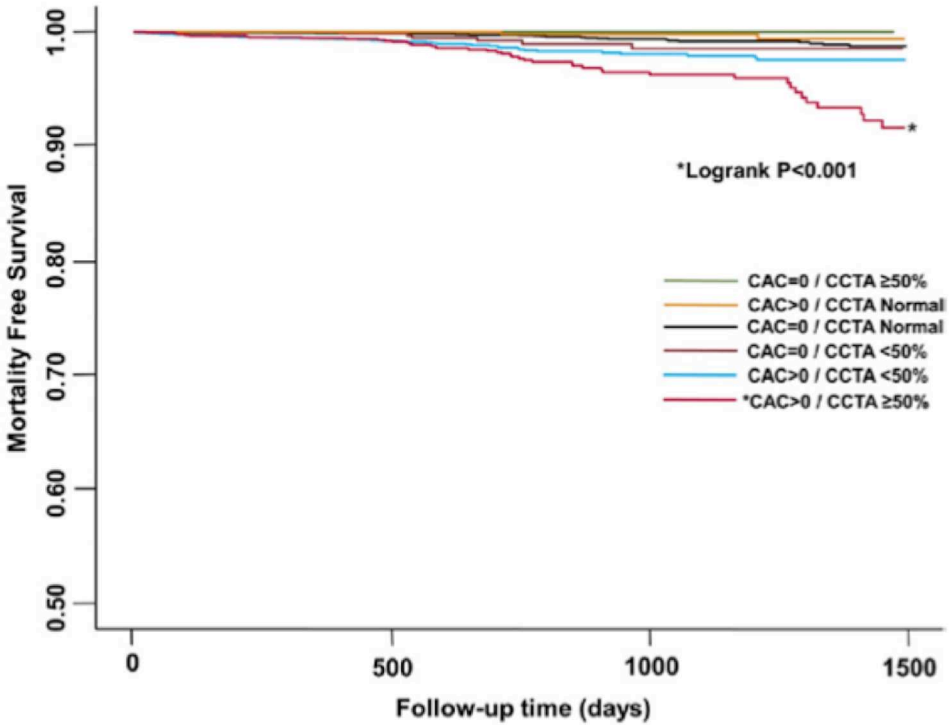
Mortality Free Survival
1.00
0.90
0.80
0.70
0.60
0.50
0
500
1000
1500
Follow-up time (days)
*Logrank P<0.001
CAC=0 / CCTA ≥50%
CAC>0 / CCTA Normal
CAC=0 / CCTA Normal
CAC=0 / CCTA <50%
CAC>0 / CCTA <50%
*CAC>0 / CCTA ≥50%

Figure 2

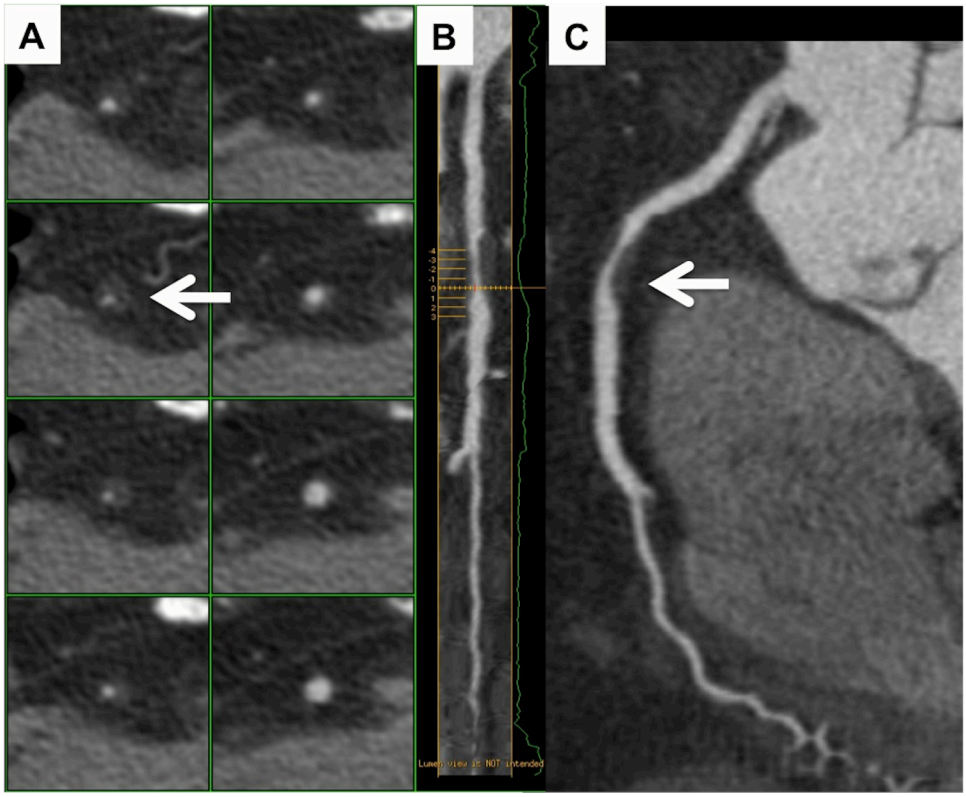

Figure 3

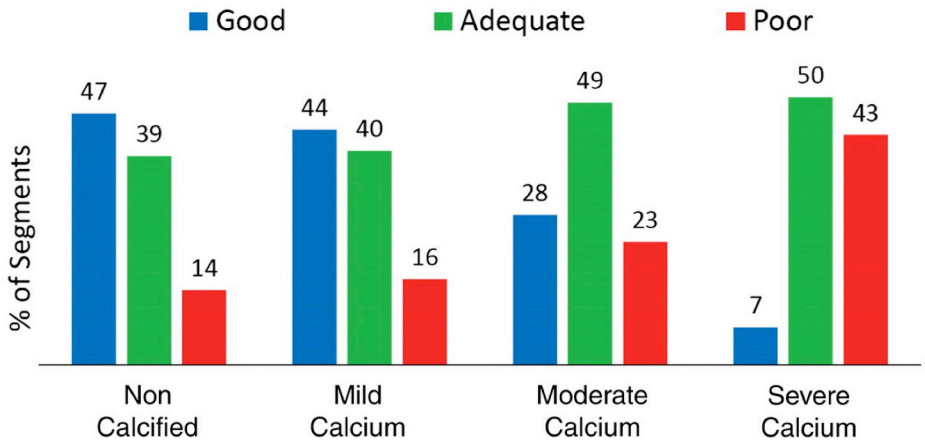
Good
Adequate
Poor
% of Segments
47
39
14
44
40
16
28
49
23
7
50
43
Non Calcified
Mild Calcium
Moderate Calcium
Severe Calcium

Figure 4a

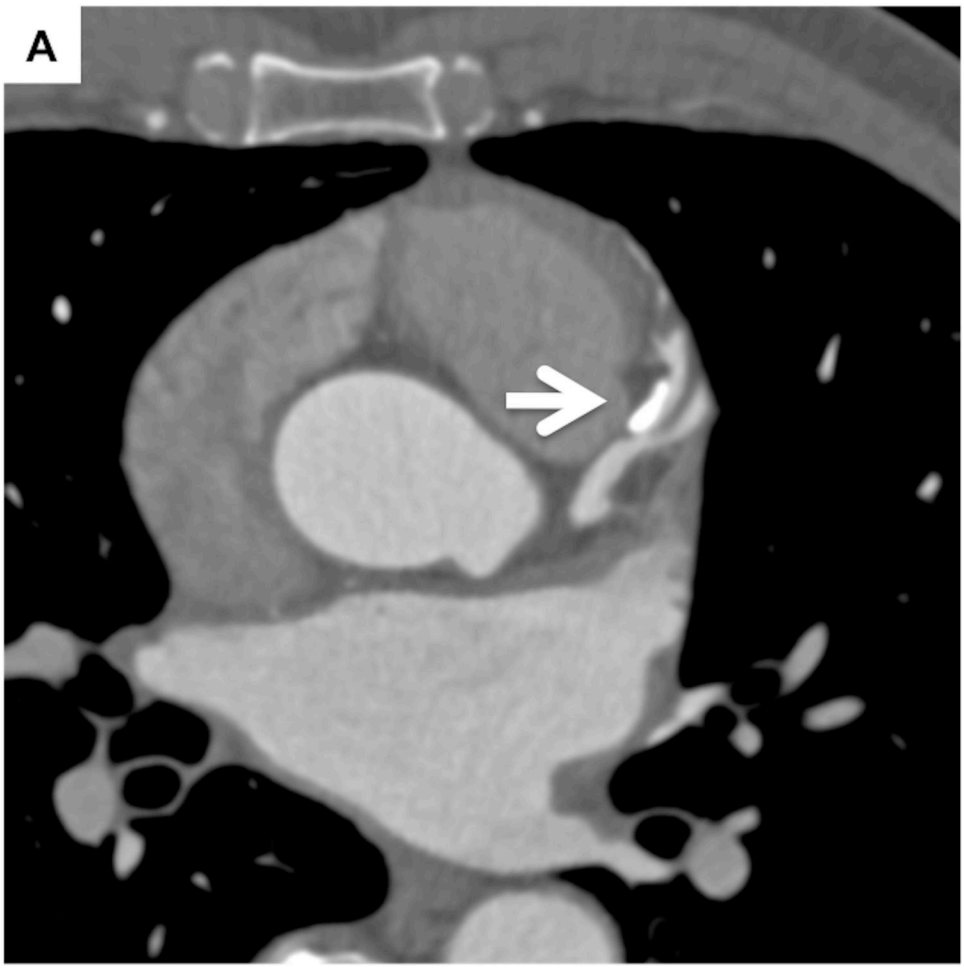

Figure 4b

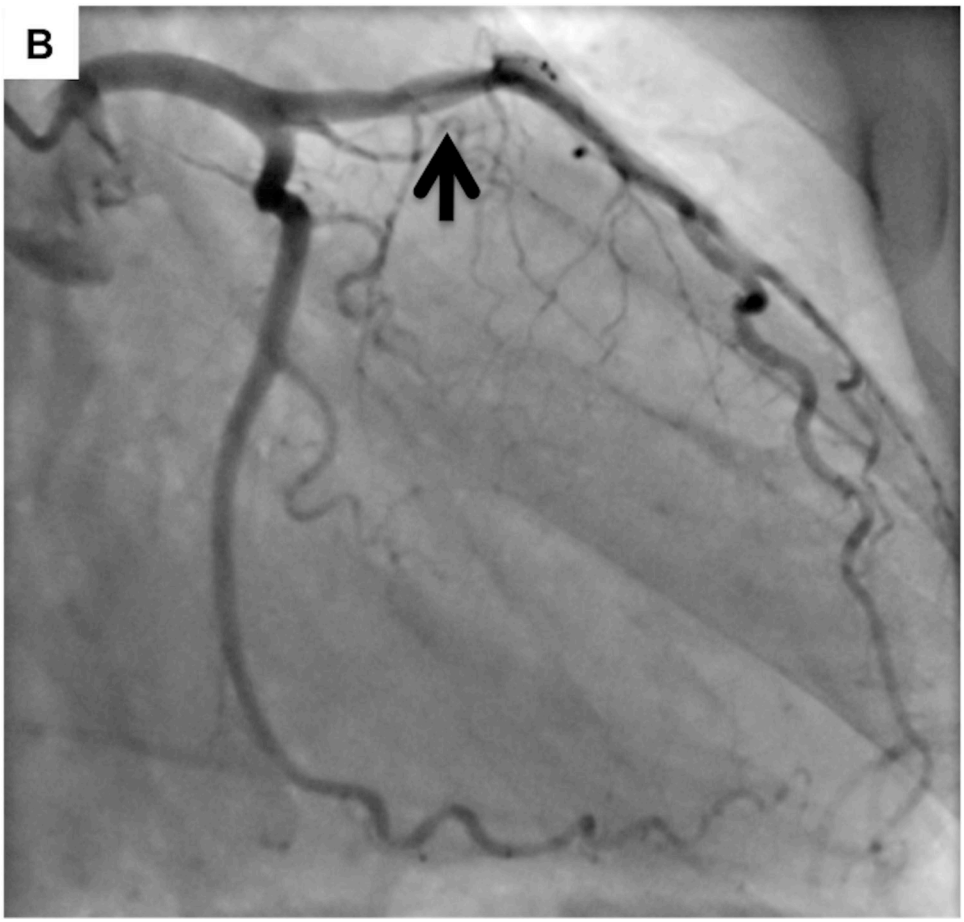

Figure 4c

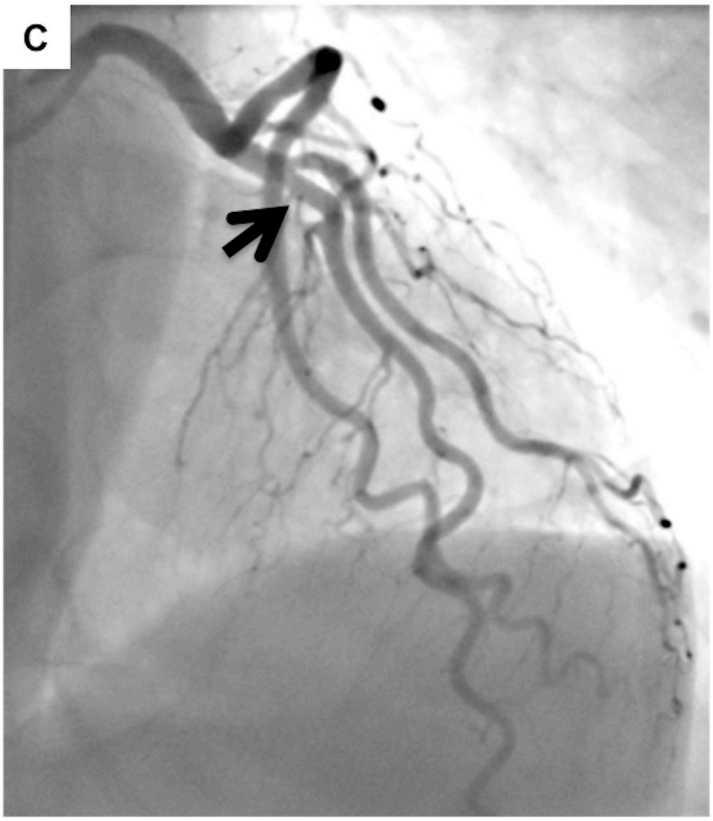

7. Artigo Original em Inglês:

Artigo publicado no

International Journal of Cardiovascular Imaging (Fator de Impacto: 2.539).

Publicado online em 24/04/2012. (DOI 10.1007/s10554-012-0049-x).

Título: Failed Heart Rate Control with Oral Metoprolol Prior to Coronary CT Angiography: Effect of Additional Intravenous Metoprolol on Heart Rate, Image Quality and Radiation Dose

Authors:

Laura Jimenez-Juan[1], Elsie T Nguyen[1], Bernd J Wintersperger[1], Hadas Monoshov[2], Andrew M Crean[1,3], Djeven P Deva[1], Narinder S Paul[1]

Felipe S Torres[4,5]

[1]Department of Medical Imaging, Cardiothoracic Division, Toronto General Hospital, University Health Network. Toronto, ON, Canada

[2]Joint Department of Medical Imaging, Mount Sinai Hospital, University Health Network and Women's College Hospital, Toronto, ON, Canada

[3]Department of Cardiology, Toronto General Hospital, University Health Network, Toronto, ON

[4]Department of Medical Imaging, Cardiothoracic Division, Sunnybrook Health Sciences Centre. Toronto, ON, Canada

[5]Postgraduate Studies Program in Cardiology, School of Medicine, Universidade Federal do Rio Grande do Sul, Porto Alegre, RS, Brazil

Corresponding author:

Felipe S. Torres

Postgraduate studies in Cardiology, School of Medicine, Universidade Federal do Rio Grande do Sul Ramiro Barcelos 2400, 2nd floor, Porto Alegre, RS, Brazil

90035-003

Phone: 55-51-3316.5604

Fax: 55-51-3316.5614

Email: felipesoarestorres@gmail.com

Abstract

Purpose: To evaluate the effect of intravenous (IV) metoprolol after a suboptimal heart rate (HR) response to oral metoprolol (75-150mg) on HR control, image quality (IQ) and radiation dose during coronary CTA using 320-MDCT.

Methods: Fifty-three consecutive patients who failed to achieve a target HR of <60 bpm after an oral dose of metoprolol and required supplementary IV metoprolol (5-20mg) prior to coronary CTA were evaluated. Patients with HR <60 bpm during image acquisition were defined as responders (R) and those with HR ≥ 60 bpm as non-responders (NR). Two observers assessed IQ using a 3-point scale (1-2, diagnostic and 3, non-diagnostic). Effective dose (ED) was estimated using dose-length product and a 0.014 mSV/mGy.cm conversion factor. Baseline characteristics and HR on arrival were similar in the two groups.

Results: 58% of patients didn't achieve the target HR after receiving IV metoprolol (NR). R had a significantly higher HR reduction after oral (mean HR 63.9 ± 4.5 bpm vs 69.6 ± 5.6 bpm) ($p < 0.005$) and IV (mean HR 55.4 ± 3.9 bpm vs 67.4 ± 5.3 bpm) ($p < 0.005$) doses of metoprolol. Studies from NR showed a significantly higher ED in comparison to R (8.0 ± 2.9 vs 6.1 ± 2.2 mSv) ($p=0.016$) and a significantly higher proportion of non-diagnostic coronary segments (9.2% vs 2.5%) ($p< 0.001$).

Conclusions: 58% of patients who do not achieve a HR of <60 bpm prior to coronary CTA with oral fail to respond to additional IV metoprolol and have studies with higher radiation dose and worse image quality.

Keywords

Heart rate; Beta-blocker; Coronary artery disease; Image quality; Radiation dose; 320 MDCT

Introduction

Coronary computed tomography angiography (CTA) is an important non-invasive modality for the evaluation of coronary artery disease (CAD). The high sensitivity and negative predictive value for excluding a significant coronary stenosis has led to the recognition of the value of this test in symptomatic patients with low to intermediate pretest probability of CAD [1]. The accuracy of this procedure is highly dependent on the image quality of the dataset and a robust heart rate (HR) control, ideally less than 60 beats per minute [bpm] [2], is essential for optimizing image quality and minimizing radiation dose [3].

Different medications have been used to achieve a slow and steady heart rate prior to coronary CTA, particularly β1cardioselective beta-blockers, such as metoprolol [4,5], atenolol [5] and, less frequently, esmolol [6]. A slow heart rate (< 65 bpm) has been demonstrated in approximately 35 - 81% of patients with the use of beta-blockers [7] and consistent results have been reported with metoprolol [5,8], the most frequently used medication prior to coronary CTA [4,7]. Since the plasma levels achieved after an oral dose of metoprolol can be variable [9] and the intravenous (IV) preparation achieves higher plasma concentrations as it bypasses the hepatic metabolism [4], IV metoprolol has been recommended as a supplement in patients in whom adequate HR control has not been achieved after an oral dose [7]. However, suboptimal results have been reported with this strategy [8] and the real additive effect of supplementary IV metoprolol in clinical practice has not been quantified [10].

We hypothesize that supplementary IV metoprolol has only limited additional effect in controlling heart rate of patients who had a suboptimal HR response to an oral dose. Therefore, the purpose of this study was to determine the efficacy of the sequential use of IV metoprolol after a suboptimal HR response to oral metoprolol in controlling heart rate prior to coronary CTA and to assess its effect on image quality and radiation dose.

Methods

Study Population

This retrospective observational study was approved by the local research ethics board and the need for patients' written informed consent was waived.

The study population comprised all consecutive patients clinically referred for coronary CTA at a tertiary academic medical center between October 2010 and March 2011 who required oral and IV metoprolol to achieve a target HR of < 60 bpm. During this period, a total of 370 coronary CTA were performed and 240 patients (65%) received oral metoprolol for HR control prior to the test. Of these 240 patients, 53 (22%) failed to reach the target HR of < 60 bpm with the oral metoprolol and received supplementary IV metoprolol (5 mg boluses, every 3-5 minutes, up to a maximum of 20 mg). These 53 patients were included in the present analysis. Clinical indications for coronary CTA included atypical chest pain or atypical symptoms (n=37, 70%), equivocal or positive results in a previous stress test with a low or

intermediate clinical suspicion of obstructive coronary artery disease (n=10, 20%), possible anomalous coronary artery (n=2, 4%), coronary stent evaluation (n=2, 4%) and other causes (evaluation of vasculitis [n=1, 2%] and cardiomyopathy to exclude ischemic origin [n=1, 2%]).

Demographics (age, sex), body mass index, ongoing pharmacological treatment, dose of metoprolol (oral and IV) and nitroglycerin received prior to coronary CTA scan as well as CT exposure parameters (tube voltage, tube current, scan length) were recorded. Potential-side effects related to beta-blocker administration were also recorded during 30 minutes after the study, while patient was held in the Medical Imaging Department. In preparation to the procedure, all patients received standard instructions, which included avoiding caffeine intake for 12 hours prior to the test and to refrain from food for 4 hours prior to the study [11].

Heart Rate Control and Monitoring

Patients with an initial HR ≥ 60 bpm received a single oral dose of metoprolol (75 mg if <70 kg or 150 mg if ≥ 70 kg of body weight) approximately 1 hour prior to coronary CTA in order to achieve a target HR of <60 bpm. Patients who failed to reach the target HR with oral metoprolol received supplementary IV metoprolol (5 mg boluses, every 3-5 minutes up, to a maximum of 20 mg) immediately prior to image acquisition. Contra-indications to beta-blocker administration included allergy to metoprolol, severe asthma or COPD (defined as daily use of medication, recent asthmatic crisis or worsening of dyspnea, or history of a previous severe crisis requiring

hospitalization), moderate to severe left ventricular global systolic dysfunction, severe aortic stenosis or left ventricular outflow tract obstruction, severe pulmonary hypertension, second or third degree atrioventricular block and systolic blood pressure of < 100 mmHg. In addition, all patients without contraindications received 0.3 mg of sublingual nitroglycerin 1 minute prior to the scan.

Heart rate during the following time-points prior to and during image acquisition were recorded by a dedicated cardiac CT nurse and technologist: 1) on patient's arrival, prior to beta-blocker administration (HR-1); 2) approximately 45 minutes after the administration of oral metoprolol, when the patient was transferred to the scanner suite (HR-2); 3) at the time of the breathing exercise, immediately after coronary artery calcium score acquisition, when the decision to give supplementary IV metoprolol was made, approximately 1 hour after oral dose administration (HR-3); 4) after each 5 mg dose of IV metoprolol, and 5) during CT image acquisition (HR-acq). Patients with a HR during image acquisition of < 60 bpm were classified as responders (R) and those with a HR ≥ 60 bpm were classified as non-responders (NR).

Scan Protocol

All coronary CTA studies were performed using a 320-MDCT (Aquilion ONE, Toshiba Medical Systems, Otawara, Japan) by using a minimum gantry rotation time of 350 milliseconds, a beam collimation of 320 x 0.5 millimeters, prospective electrocardiographic (ECG) triggering and a body mass index-

adapted tube potential (100-135 kVp) and tube current (370 mA-580 mA), according to the vendor's specifications. The whole heart was covered from below the level of the tracheal bifurcation to the diaphragm, based on the coronary calcium score acquisition. Two breath-hold calibrations were performed before contrast injection to achieve optimal synchronization of the CT gantry rotation to the patient's HR and to define the duration of X-ray tube exposure during the R-R interval (phase window, PW). The PW was stratified according to the HR as follows: HR ≥ 65 bpm, PW from 40% of the R-R interval to the next R wave (40%-R); HR at 60-64 bpm, PW from 60%-R, and HR < 60 bpm, PW from 70%-80%. In patients with a HR > 65 bpm or if the HR during data acquisition varied more than 20% from the breath-hold calibration, then the CT coronary angiography data were acquired over ≥ 2 heart beats to achieve a lower effective temporal resolution by using multisegment reconstruction.

A bolus-tracking technique was used to trigger image acquisition 5 seconds after the target attenuation threshold of 180 HU was reached in a prescribed region of interest within the descending thoracic aorta. A bolus of nonionic, isosmolar, iodinated contrast agent (Iodixanol 320 mg/mL, Visipaque 320, GE Healthcare, Princeton, NJ, USA) was injected trough an 18-gauge intravenous catheter inserted preferentially into the right antecubital vein with a dual power injector (Stellant D CT Injector, Medrad, Indianola, PA, USA) followed by 30 ml of saline chaser. The injection rate and the volume of injected contrast agent varied according to patient's body weight (4–7 mL/s and 60-105 ml respectively).

Image Reconstruction and Analysis

The raw data were reconstructed into transaxial 0.5-mm slices, with 0.25 mm overlap, within the selected PW and at a fixed temporal window at 75% of the R-R interval. Additional reconstructions (1%-5% intervals) were performed as necessary to achieve motion-free diagnostic images. In patients who underwent multibeat acquisitions, the slowest heartbeat was selected to allow for a half scan reconstruction, in addition to the multisegment reconstruction, in an attempt to obtain an optimal reconstruction phase. All images were reconstructed by using a 21.7 x 21.7-cm FOV and dedicated filter kernels for soft tissue or coronary stent evaluation depending on the indication.

All reconstructed images were stored in a digital picture archiving and communications system (Fusion eFilm v2.1, Merge Healthcare, Milwaukee, WI, USA) and were reviewed and post processed using a dedicated cardiac workstation (Vitrea2 FX, Vital Images, Plymouth, MN, USA).

The coronary arteries were systematically analyzed by using a 19-segment model, modified from the 15-segment model of the American Heart Association [12] by adding, when present, segment 16 for the distal half of the circumflex coronary artery; segment 17 for a ramus intermedius; and segments 18 and 19 for additional obtuse marginal branches. Anatomically absent segments were not included in the analysis. Two fellowship trained cardiac radiologists, blinded to clinical data, heart rate and dose of metoprolol received, evaluated the IQ of all coronary segments using a consensus review. Image quality was graded using a 3-point scale, where 1 was defined

as excellent IQ, 2 was defined as moderate but still diagnostic IQ and 3 was defined as poor, non-diagnostic IQ.

Radiation dose estimation

From each scan, the dose-length product was recorded from the scanner display. The effective dose was calculated by multiplying the dose-length product by a conversion factor of 0.014 mSv / mGy x cm [3] and expressed in millisieverts (mSv).

Statistical Analysis

Statistical analyses were performed using SPSS software version 18 (PASW Statistics 18, 2009).

Continuous variables were described using mean ± SD and categorical variables using frequency and percentage. Demographic data that was quantitative in nature, HR and radiation dose were compared between responders and non-responders using the pooled two-samples *t* test. The Chi-square test was used to compare the qualitative demographic data as well as oral and IV dose of metoprolol between the two groups. Image quality scores were compared between responders and non-responders using the Chi-square test. Statistical significance was set at a p-value less than 0.05.

Results

Patient characteristics and heart rate control

Of the 53 patients who had supplementary intravenous metoprolol, 22 (41.5%) patients achieved a heart rate <60 bpm during image acquisition and were classified as responders, while 31 (58.5%) patients remained with a HR ≥ 60 bpm and were classified as non-responders (Table 1). There was no statistically significant difference between R and NR regarding prior use of beta-blockers or in the initial dose of oral metoprolol used for coronary CTA. All patents received 0.3 mg of Nitroglycerin immediately prior to the study and none of the patients received anxiolityc medication in our department prior to the exam. No adverse effects were observed related to beta-blocker administration.

The HR of R and NR recorded on arrival (HR-1) (77.6 ± 10.5 bpm and 80.4 ± 11.1 bpm, respectively; p = 0.37) and 45 minutes post administration of oral metoprolol (HR-2) (68.7 ± 4.8 bpm and 71.3 ± 7.3 bpm, respectively; p = 0.16) were similar. Prior to administration of IV metoprolol (HR-3), there was a statistically significant difference between the mean HR of R in comparison to NR (63.9 ± 4.5 bpm and 69.6 ± 5.6 bpm; mean HR difference 5.8 [CI95% 2.8, 8.7], p < 0.005). Two patients classified as R had a HR < 60 bpm and received IV metoprolol due to occasional fluctuations of the HR to levels above 60 bpm at the breathing exercise after coronary calcium acquisition (HR-3). After receiving IV metoprolol, R showed a significantly higher HR reduction than NR, with a mean difference of 12 bpm (95%CI 9.4, 14.7) between the HR of R in comparison to NR (Fig1). In 59% of R, the target HR was achieved after receiving all four doses (20 mg) of IV metoprolol, while

90% of NR received four doses (Table 2). Three patients classified as NR received less than 20 mg of metoprolol. In these patients, the HR decreased to less than 60 bpm after the IV administration, but increased to above 60 bpm during image acquisition.

Image quality and radiation dose data

A total of 768 coronary segments were evaluated in 53 patients. In a per-segment analysis, R showed a statistically significant higher proportion of segments with excellent (grade 1) and moderate (grade 2) IQ and lower proportion of coronary segments graded as poor, non-diagnostic IQ (grade 3) (Table 3).

Table 4 shows the comparison of radiation dose between R and NR. The effective dose associated with the coronary CTA was significantly lower in R in comparison to NR, with a mean effective dose of 6.1 ± 2.2 mSv and 8.0 ± 2.9 mSv, respectively.

Discussion

In this study, we analyzed the effect of supplementary IV after a failed dose of oral metoprolol in achieving a HR of <60 bpm prior to coronary CTA. Our study adds to the current knowledge by showing the limited efficacy of additional IV metoprolol when the oral dose is insufficient. We have demonstrated that approximately 58% of the patients who fail to achieve the target HR of < 60 bpm after an oral dose of metoprolol prior to coronary CTA

do not achieve the target HR with supplementary IV metoprolol. In addition, in these patients, we showed that the radiation dose is increased and the image quality is worse in comparison to studies from patients in whom the target HR is reached.

There is substantial inter-subject variability in the efficacy of beta-blockers, particularly of metoprolol [13]. Certain ethnicities have shown to be more responsive than others when receiving the same dose of beta-blocker [14]. This variability in the heart rate response has been in part associated with genetic factors such as the polymorphisms of beta-adrenergic receptors, a potential cause for poor HR response observed in some patients [15]. Observational studies have confirmed this variability showing that, when used in isolation, either the oral or IV routes have generated mixed and suboptimal HR lowering effects [5,16-18]. A potential reason for failure of the oral dose of metoprolol is the magnitude of the hepatic metabolism of the drug, which can differ substantially between individuals [9]. In this context, the rationale for the sequential use of oral followed by IV metoprolol is very attractive, since the intravenous preparation bypasses the hepatic metabolism.

Previous studies have evaluated the efficacy of IV beta-blockers prior to coronary CTA, with substantial variation in HR response [5,18]. However, there is little data on the use of IV metoprolol as a supplement to an oral dose. In a study with 121 outpatients referred for coronary CTA, Roberts and colleagues [8] assessed the efficacy of a standardized HR control strategy including oral (100 mg) followed by IV (5-15 mg) metoprolol. The target HR of ≤ 60 bpm was achieved in only 65% of the 71 patients who received oral beta-blocker. In the small subset of 12 patients requiring supplementary IV

metoprolol, a HR ≤ 65 bpm was reached in only 3 [8]**.** In the present study, approximately 42% of patients achieved a HR < 60 bpm with the use of supplementary IV metoprolol in doses up to 20 mg. The improved HR lowering effect demonstrated in our study may be related to higher doses of oral and IV beta-blocker used [19]. Doses of oral metoprolol of up to 200 mg and intravenous doses of up to 30 mg have been recommended [7]. On the other hand, the excellent HR response achieved in R (mean HR 55.4 bpm during image acquisition) suggests that factors other than the dose of metoprolol may be responsible for the suboptimal HR reduction in NR. Therefore, these results highlight the necessity for the implementation of alternative HR control strategies for patients who do not respond adequately to the initial oral dose of beta-blocker.

A substantial number of R, approximately 59%, achieved the target HR after 20mg of IV metoprolol, while 90% of non-responders received the same dose without achieving the target HR. Therefore, it is not possible to predict which patients will respond to the IV preparation based on the HR response after the first or second supplementary IV doses, and one should not be discouraged by the lack of HR response after the injection of 5 or 10 mg of IV metoprolol. We have not evaluated if larger doses, up to 30 mg (7), would have been more effective in achieving the target HR and this remains to be tested. Despite the relatively large combined oral and IV dose administrated, none of our patients experienced side effects, which confirms the safety of this strategy. The combination of oral followed by IV beta-blockage offers an advantage over IV administration alone in terms workflow, since patients could be medicated outside the scanner suite without affecting the scanner

throughput. Since a large percentage of patients respond to the oral medication alone, this strategy would also reduce the use of the IV formulation, which is more expensive, in a large number of patients.

A difference in the heart rate lowering effect of the beta-blockade strategy used in our study between R and NR was noticed approximately 1h after the administration of oral metoprolol (HR-3). In addition, this difference was further increased after the administration of the IV metoprolol, again, while the patients were positioned in the CT scanner. These findings raise the possibility that, in susceptible individuals, acute anxiety may have been triggered when the patient was transferred to the CT scan room counteracting the heart rate lowering effects of the oral beta-blocker. Only one retrospective study has reported the effect of a short acting anxiolytic agent prior to coronary CTA and the results were disappointing [5]. In addition, the administration of these agents is usually guided by subjective evaluation, although objective anxiety screening tools are available and could be used in this setting [20].

Heart rate control remains necessary with current CT scan technology but may be omitted in case of substantially improved half-scan temporal resolution. Wang and colleagues [21] have shown the resting period of coronary arteries and their findings reinforce the need for a HR <60 bpm in case of >150 ms temporal resolution. With a minimum half-scan temporal resolution of 175 ms [22-24], heart rate control is required for coronary CTA performed in the current generation of 320-MDCT scanners in order to optimize image quality and radiation dose [23-25].

Previous studies have reported increased radiation dose in 320-MDCT coronary angiography performed in patients with HR above 65 bpm [24-26]. Similarly, in our study, the lowest doses were seen in studies from patients who achieved the target HR of <60 bpm in comparison to those who did not (mean ED 6.1 mSv vs 8.0 mSv, respectively). Adequate HR control is essential for minimizing radiation dose during coronary CTA when using a 320-MDCT because the HR directly determines the duration of the X-ray exposure during the cardiac cycle (PW) and also the number of heart beats exposed during image acquisition. A low and steady HR would enable image acquisition during only one heart beat and with narrow PW, translating into important radiation dose savings [23].

On the other hand, in patients with increased HR, extended PW and/or multibeat acquisition would be performed to increase the number of phases available for image reconstruction and to improve temporal resolution with multisegment reconstructions, in order to improve IQ, acknowledging the direct increase in radiation dose. In our study, NR showed a significantly higher proportion of non-diagnostic coronary segments when compared to R. In the study by Lee and colleagues [24], there was no significant difference in the number of evaluable coronary segments between patients who achieved and those who did not achieve the target HR of less than 65 bpm (96.9% vs 95.6%, respectively). However, in contrary to our study, retrospective ECG-gating was used in 77% of patients with HR > 65 bpm and, in many of these studies, full X-ray exposure during the entire R-R interval was performed, allowing for reconstruction of systolic phases in cases on inadequate IQ in diastolic phases. Our results indicate that adequate heart rate control is

important not only for radiation dose reduction but also for image quality optimization when using prospective ECG-triggering.

The present study has limitations. This is a single-center study with a relatively small number of patients but the largest study to evaluate the efficacy of supplementary IV dose of beta-blocker for HR reduction prior to coronary CTA. Nonetheless, the relative small sample size may have limited the power of our analysis to demonstrate baseline differences between groups that could have influenced the HR response to metoprolol. In addition, IV metoprolol was given while the patient was lying in the scanner table, until the target HR or the maximum dose of 20 mg was reached. Since the onset of action of IV metoprolol is usually 5-10 minutes after administration [4], it is possible that an insufficient time from IV injection to image acquisition could have affected the HR response observed in some patients. However, by spacing the boluses to every 3-5 min, by the time the fourth dose was administered, which was the case in 90% of NR, a minimum of 12 min was allowed for the medication to exert its HR lowering effect. Another limitation is related to the observational design where all factors that could have affected the HR response between R and NR could not have been controlled. Nonetheless, this study was conducted in a high volume center specialized in coronary CTA, with dedicated nursing staff and experienced technologists who utilize a systematic approach to optimize all aspects from patient evaluation to image acquisition [11]. On the other hand, caution should be taken when generalizing these results to less experienced centers with lower coronary CTA volume, where the HR control strategy may not be as standardized or effective. In addition, we have not investigated the ethnic

background of our patients, a factor that could have influenced our results [14]. Finally, we used only one type of multidetector CT scanner and results in terms of image quality and radiation dose may not be applicable to other scanner types.

Conclusion

Approximately 58% of patients who do not achieve the target HR of < 60 bpm prior to coronary CTA with oral metoprolol do not respond to additional IV metoprolol. Alternative strategies to achieve target heart rate need to be explored. In addition, our experience reinforces the knowledge that coronary CTA examinations in patients who do not achieve the target HR are associated with higher radiation dose and decreased image quality in comparison to patients in whom the target HR was reached.

References

1. Taylor AJ, Cerqueira M, Hodgson JM et al (2010) ACCF/SCCT/ACR/AHA/ASE/ASNC/NASCI/SCAI/SCMR 2010 Appropriate Use Criteria for Cardiac Computed Tomography. A Report of the American College of Cardiology Foundation Appropriate Use Criteria Task Force, the Society of Cardiovascular Computed Tomography, the American College of Radiology, the American Heart Association, the American Society of Echocardiography, the American Society of Nuclear Cardiology, the North American Society for Cardiovascular Imaging, the Society for Cardiovascular

Angiography and Interventions, and the Society for Cardiovascular Magnetic Resonance. J Cardiovasc Comput Tomogr 4:407.e1-407.33

2. Abbara S, Arbab-Zadeh A, Callister TQ et al (2009) SCCT guidelines for performance of coronary computed tomographic angiography: a report of the Society of Cardiovascular Computed Tomography Guidelines Committee. J Cardiovasc Comput Tomogr 3:190-204
3. Halliburton SS, Abbara S, Chen MY et al (2011) SCCT guidelines on radiation dose and dose-optimization strategies in cardiovascular CT. J Cardiovasc Comput Tomogr 5:198-224
4. Pannu HK, Alvarez W,Jr, Fishman EK (2006) Beta-blockers for cardiac CT: a primer for the radiologist. AJR Am J Roentgenol 186:S341-5
5. Maffei E, Palumbo AA, Martini C et al (2009) "In-house" pharmacological management for computed tomography coronary angiography: heart rate reduction, timing and safety of different drugs used during patient preparation. Eur Radiol 19:2931-40
6. Degertekin M, Gemici G, Kaya Z et al (2009) Safety and efficacy of patient preparation with intravenous esmolol before 64-slice computed tomography coronary angiography. Coron Artery Dis 19:33-36
7. Mahabadi AA, Achenbach S, Burgstahler C, et al (2010) Safety, efficacy, and indications of beta-adrenergic receptor blockade to reduce heart rate prior to coronary CT angiography. Radiology 257:614-623
8. Roberts WT, Wright AR, Timmis JB, Timmis AD (2009) Safety and efficacy of a rate control protocol for cardiac CT. Br J Radiol 82:267-271
9. Reiter MJ (2004) Cardiovascular drug class specificity: beta-blockers. Prog Cardiovasc Dis 47:11-33

10. Torres FS, Jeddiyan S, Jimenez-Juan L, Nguyen ET (2011) Beta-blockers to control heart rate during coronary CT angiography. Radiology 259:615-6; author reply 616-7
11. Torres FS, Crean AM, Nguyen ET, Paul N (2010) Strategies for radiation-dose reduction and image-quality optimization in multidetector computed tomographic coronary angiography. Can Assoc Radiol J 61:271-279
12. Austen WG, Edwards JE, Frye RL et al (1975) A reporting system on patients evaluated for coronary artery disease. Report of the Ad Hoc Committee for Grading of Coronary Artery Disease, Council on Cardiovascular Surgery, American Heart Association. Circulation 51:5-40
13. Jack DB, Quarterman CP, Zaman R, Kendall MJ (1982) Variability of beta-blocker pharmacokinetics in young volunteers. Eur J Clin Pharmacol 23:37-42
14. Zhou HH, Koshakji RP, Silberstein DJ, Wilkinson GR, Wood AJ (1989) Altered sensitivity to and clearance of propranolol in men of Chinese descent as compared with American whites. N Engl J Med 320:565-570
15. Brodde OE (2008) Beta-1 and beta-2 adrenoceptor polymorphisms: functional importance, impact on cardiovascular diseases and drug responses. Pharmacol Ther 117:1-29
16. de Graaf FR, Schuijf JD, van Velzen JE et al (2010) Evaluation of contraindications and efficacy of oral Beta blockade before computed tomographic coronary angiography. Am J Cardiol 105:767-772
17. Pannu HK, Sullivan C, Lai S, Fishman EK (2008) Evaluation of the effectiveness of oral Beta-blockade in patients for coronary computed tomographic angiography. J Comput Assist Tomogr 32:247-251

18. Shapiro MD, Pena AJ, Nichols JH et al (2008) Efficacy of pre-scan beta-blockade and impact of heart rate on image quality in patients undergoing coronary multidetector computed tomography angiography. Eur J Radiol 66:37-41
19. Regardh CG, Johnsson G (1980) Clinical pharmacokinetics of metoprolol. Clin Pharmacokinet 5:557-569
20. Beck AT SR (1990) Manual for the Beck Anxiety Inventory. San Antonio, TX: The Psycological Corporation
21. Wang Y, Vidan E, Bergman GW (1999) Cardiac motion of coronary arteries: variability in the rest period and implications for coronary MR angiography. Radiology 213:751-758
22. Rybicki FJ, Otero HJ, Steigner ML et al (2008) Initial evaluation of coronary images from 320-detector row computed tomography. Int J Cardiovasc Imaging 24:535-546
23. Steigner ML, Otero HJ, Cai T et al (2009) Narrowing the phase window width in prospectively ECG-gated single heart beat 320-detector row coronary CT angiography. Int J Cardiovasc Imaging 25:85-90
24. Lee AB, Nandurkar D, Schneider-Kolsky ME et al (2011) Coronary Image Quality of 320-MDCT in Patients With Heart Rates Above 65 Beats per Minute: Preliminary Experience. AJR Am J Roentgenol 196:W729-35
25. Khan M, Cummings KW, Gutierrez FR, Bhalla S, Woodard PK, Saeed IM (2011) Contraindications and side effects of commonly used medications in coronary CT angiography. Int J Cardiovasc Imaging 27:441-449
26. Dewey M, Zimmermann E, Deissenrieder F et al (2009) Noninvasive coronary angiography by 320-row computed tomography with lower radiation

exposure and maintained diagnostic accuracy: comparison of results with cardiac catheterization in a head-to-head pilot investigation. Circulation 120:867-875

Figure Caption

Fig. 1 Heart Rate Results in Responders and Non-Responders [a]

HR, heart rate; IV, intravenous;

[a], see text for definitions of HR groups and Responders and Non-Responders;

[b,c], Pooled two-sample *t* test;

Table 1 Clinical and demographic characteristics of patients requiring IV metoprolol for heart rate control prior to coronary CTA.

Characteristics	All patients	Responders [a]	Non-Responders	p-value
Patients, n (%)	53	22 (41.5)	31 (58.5)	-
Age (years), mean (SD)	56.7 (12.3)	54.7 (13.9)	58 (11)	0.33
Male sex, n (%)	36 (68)	14 (63.6)	22 (71)	0.76
BMI, Kg/m^2, mean (SD)	27.5 (5)	27.1 (5.3)	27.8 (4.8)	0.65
Baseline HR (bpm), mean (SD)	79.2 (10.9)	77.6 (10.5)	80.4 (11.1)	0.37
Prior use of β-blocker, n (%)	9 (17)	3 (13.6)	6 (19.4)	0.72
150mg oral metoprolol [b], n (%)	35 (66)	15 (68.1)	20 (64.5)	0.78
Z axis length, mean (SD)	136.8 (11.3)	140 (11.6)	134.6 (10.7)	0.06
120 kVp, n (%)	43 (81.1)	18 (81.8)	25 (80.7)	1
Tube current mA, mean (SD)	503.8 (58.3)	515 (52.8)	495.8 (61.4)	0.28
Coronary calcium score, mean (SD)	230(780)	318.7 (1195.1)	172.6 (318.3)	0.36

IV, intravenous; CTA, computed tomography angiography; BMI, body mass index; HR, heart rate
[a], Responders correspond to patients with a heart rate of < 60 bpm and Non-Responders to patients with a heart rate ≥ 60 bpm during image acquisition
[b], number of patients who received 150 mg of oral metoprolol for heart rate control prior to the intravenous dose

Table 2 Number of IV doses of metoprolol received by responders and non-responders.

Group	Number of IV doses received [a]				
	1	2	3	4 [b]	Total
Responders, n(%)	4 (18.2)	2 (9.1)	3 (13.6)	13 (59.1)	22
Non-Responders, n(%)	1 (3.2)	2 (6.5)	0	28 (90.3)	31
Total, n (%)	5 (9.4)	4 (7.5)	3 (5.6)	41 (77.4)	53 (100)

IV, intravenous
[a], each dose corresponds to 5 mg of metoprolol
[b], Fisher's exact test p-value = 0.017 for comparison between responders and non-responders

Table 3 Distribution of image quality scores according to the target heart rate during acquisition (responders vs non-responders)

Image Quality Score [a]	Responders [b] (Total=321 segments)	Non-Responders (Total=447 segments)	p-value [c]
1	299 (93.1%)	345 (77.2%)	< 0.001
2	14 (4.4%)	61 (13.6%)	< 0.001
3	8 (2.5%)	41 (9.2%)	< 0.001
1+2 [d]	313 (97.5%)	406 (90.8%)	< 0.001

IV, intravenous
[a], See text for definition of image quality score; data presented as number (%) of coronary segments
[b], Responders were defined as patients with a heart rate < 60 bpm and Non-Responders as patients with a heart rate ≥ 60 bpm during image acquisition
[c], Fisher exact test
[d], Grades 1 and 2 were considered of diagnostic image quality

Table 4 Radiation dose according to target heart rate during acquisition.

	Responders [a]	Non-Responders	p-value
HR (bpm), mean (SD)	55.4 (3.9)	67.4 (5.3)	<0.005
DLP (mGy.cm), mean (SD)	438.7 (160.2)	571.9 (211.8)	0.016
Effective Dose (mSv) [b], mean (SD)	6.1 (2.2)	8.0 (2.9)	0.016
≥2 heart beat scan	2 (9%)	18 (58%)	0.001

HR, heart rate; DLP, dose-length product

[a] Responders were defined as patients with a heart rate < 60 bpm and Non-Responders as patients with a heart rate ≥ 60 bpm during image acquisition

[b] Effective dose was calculated by multiplying the dose-length product for 0.014

Figure 1

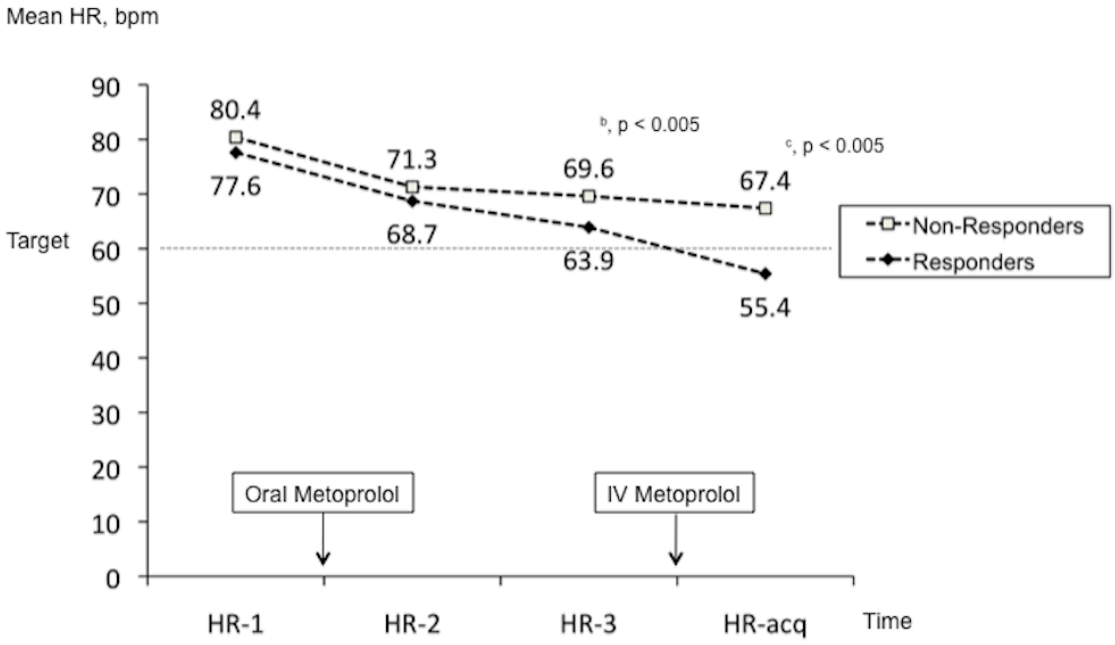
Mean HR, bpm
90
80
70
60
50
40
30
20
10
0
Target
80.4
71.3
69.6
67.4
77.6
68.7
63.9
55.4
b, p < 0.005
c, p < 0.005
Non-Responders
Responders
Oral Metoprolol
IV Metoprolol
HR-1
HR-2
HR-3
HR-acq
Time

8. Artigo Original em Inglês:

Title:

Assessment of Aortic Root Dimensions in Patients with a Bicuspid Aortic Valve Using Cardiovascular Magnetic Resonance Imaging.

Authors:

Felipe S. Torres, MD[1,2], Jonathan D. Windram, BSc (Hons), MBChB, MRCP (UK) [3], Timothy J. Bradley, MBChB[4], Bernd J. Wintersperger, MD[1,5], Ravi Menezes, PhD[1], Andrew M. Crean, MD[1, 3], Sebastian Ley, MD[1], Jack M. Colman,MD[3], Candice K. Silversides, MD[3], Rachel M. Wald, MD[3,4]

[1]Joint Department of Medical Imaging, University Health Network, University of Toronto, Toronto, Ontario, Canada

[2]Postgraduate Studies Program in Cardiology, School of Medicine, Universidade Federal do Rio Grande do Sul, Brazil

[3]Toronto Congenital Cardiac Centre for Adults, Peter Munk Cardiac Centre, University Health Network, University of Toronto, Toronto, Ontario, Canada

[4]Division of Pediatric Cardiology, Hospital for Sick Children, University of Toronto, Toronto, Ontario, Canada.

[5]Department of Clinical Radiology, University Hospitals Munich, Ludwig-Maximilians-University Munich, Munich, Germany

ABSTRACT

Background: Accuracy of aortic root measurements using cardiovascular magnetic resonance imaging (CMR) in patients with a bicuspid aortic valve (BAV) has not been well elucidated. We sought to evaluate the reproducibility of CMR-derived aortic root measurements in relation to standard transthoracic echocardiographic measurements.

Methods and Results: Steady-state free precession cine CMR images in 68 consecutive patients (65% male) with BAV were analyzed. Cross-sectional aortic root measurements at the level of the aortic sinuses from CMR, in systole and diastole, were made and included cusp-commissure diameters, cusp-cusp diameters and aortic root areas. Values obtained from CMR were compared to standard echocardiographic root measurements from contemporary studies, when available. The degree of aortic root asymmetry on CMR was expressed using the coefficient of variance of the root diameters in each dimension for an individual (CoeffVi) as compared with the median of the entire population (CoeffVp). Asymmetry of the aortic root was defined as CoeffVi > CoeffVp. Excellent intra-reader (intra-class correlation coefficient [ICC] ≥ 0.98) and moderate inter-reader (ICC range 0.37-0.95) reproducibility were observed for all CMR measurements. Aortic root areas produced the most reproducible results (inter and intra-reader ICC ≥ 0.94). Despite reasonable agreement between CMR and echocardiography, echocardiography systematically underestimated aortic root dimensions (1-3.9 mm) in comparison to CMR, particularly in asymmetric roots.

Conclusion: CMR-derived aortic root dimensions are reproducible. The aortic root area has the best reproducibility within and between readers.

Echocardiography underestimates maximum aortic root diameter; aortic root asymmetry further decreases the agreement between CMR and echocardiographic measurements.

Keywords: aorta, magnetic resonance imaging, echocardiography, congenital heart disease, bicuspid aortic valve

INTRODUCTION

A bicuspid aortic valve (BAV) is the most common form of congenital heart disease (1) and results in a significant burden of illness, particularly in adulthood. Nearly 1 out of every 4 patients with a BAV will experience an adverse cardiovascular event in their lifetime (2). The aortopathy seen in the context of a BAV may be manifest in the aortic root, the ascending aorta, or both (3). Precise measurements of aortic dimensions are critical, as size is well recognized as a strong predictor of dissection, rupture and mortality (4). Therefore, accurate and reproducible aortic measurements are crucial as absolute aortic size and/or progressive aortic enlargement are key determinants of suitability and appropriate timing for surgical intervention (5, 6).

Although cardiovascular magnetic resonance imaging (CMR) is well suited for evaluation of extent of aortopathy and has been identified as a key imaging modality for surveillance of aortic dimensions over time (7), reproducibility of the various aortic root measurements provided by CMR is largely unknown. Furthermore, there has been no published systematic comparison between CMR-derived measurements and transthoracic echocardiography (TTE), although current guidelines to direct surgical intervention in dilated aortas are derived primarily from echocardiographic measurements (4, 6).

Echocardiographic assessment of the aortic root is generally limited to the parasternal long axis window, considered the standard view for aortic root measurements (8), despite the fact visualization is not cross-sectional. Therefore, TTE may fail to adequately demonstrate details aortic root

morphology and size, particularly in the setting of a BAV, where aortic dimensions are often asymmetric (9). Given the superior imaging capabilities of CMR, and the high reproducibility of CMR measurements (10), we hypothesized that CMR would afford good reproducibility for evaluation of the aortic root in patients with BAV and that aortic root asymmetry would have a negative impact on the agreement between CMR and TTE measurements. The objective of this study was to evaluate the reproducibility of CMR derived aortic root measures and to relate these to standard 2D TTE dimensions in patients with a BAV.

METHODS

Study Population

The study is a retrospective cohort analysis of consecutive patients with a diagnosis of BAV referred for CMR imaging at our institution between January 2006 and December 2008. Candidates were identified from an existing cardiovascular database. Patients were included if they had no prior history of surgery involving the aortic root and if imaging included adequate steady-state free precession cine acquisitions (cine-SSFP) across the aortic root in cross-section. Available TTE studies were included for analysis if performed within 6 months of the CMR examination. The Research Ethics Board of our institution approved this study and, based on the retrospective study design, the requirement for written informed consent was waived.

Cardiovascular Magnetic Resonance Imaging (CMR)

CMR studies were performed on one of two commercially available 1.5

Tesla whole body scanners (Signa EXCITE, GE Healthcare, Waukesha, WI, USA or MAGNETOM Avanto, Siemens Healthcare, Erlangen, Germany) with a dedicated phased array surface coil. For each patient, a stack of contiguous retrospectively gated cine-SSFP acquisitions in cross-section across the aortic root were obtained following prescription derived from two complimentary views, the coronal localizer and on the left ventricular outflow tract 3-chamber view (Figure 1). Specifically, a plane perpendicular to the aortic root in each of the aforementioned views defined the aortic root cine-SSFP plane of acquisition and coverage extended from the distal left ventricular outflow tract to the ascending aorta. Cine-SSFP images were obtained during an end-expiratory breath-hold (8-12 seconds) with a typical in-plane spatial resolution of 1.3 x 2.6 mm, a slice thickness of 5-6mm and a temporal resolution adjusted at ≤50 msec.

Image Analysis

All images were transferred to a dedicated workstation and measurements were made using calipers placed from one blood-wall interface to the opposite blood-wall interface (internal aortic diameter) using commercially available software (Advantage Workstation 4.4, GE Medical Systems). The morphology of aortic valve, including the presence and number of raphae, was determined using CMR cross-sectional aortic root imaging according to the classification system described by Sievers et al (11).

For each aortic root cine-SSFP acquisition, the frames demonstrating maximal systolic and diastolic distension at the aortic sinus level were visually selected and measurements were obtained for each frame by an experienced

reader. In aortic roots with 3 distinct cusps, 2-dimensional measurements were drawn from one blood-wall interface to another (12), from cusp-to-opposite-commissure (3 cusp-commissure measurements: from right, left and non-coronary cusps to respective opposite commissures) and from cusp-to-cusp (3 cusp-cusp measurements: right-left coronary cusp, right-non coronary cusp and left-non coronary cusp), in addition to the cross sectional area of the aortic root (Figure 2). All measurements were carefully drawn from the interface between the aortic wall and blood pool at the sinus level (12) in an attempt to provide the largest systolic and diastolic measurements. In the presence of a root with only 2 distinct cusps (a “pure” BAV), 2-dimensional measurements were limited to cusp-cusp and commissure-commissure dimensions only (2 measurements, Figure 2); aortic root area was measured in the same manner as described above. Measurements were repeated by the same reader following an interval of at least 2 weeks. A second experienced reader, blinded to the measurements of the first reader, independently selected the appropriate systolic and diastole frames and repeated the same set of measurements in a randomly selected sample of patients with 3 distinct cusps (25% of the total population) and in all patients with ”pure” BAV morphology. The average of 2 measurements performed by each reader in each dimension was used for analysis.

Groups reflecting relative root asymmetry were created through calculation of the coefficient of variance of the CMR measurements in each dimension (cusp-commissure and cusp-cusp dimensions) for an individual (CoeffVi), which was compared to the median coefficient of variance for the entire population (CoeffVp). Two groups were generated for each dimension

in systole and also in diastole: those with ‘symmetric’ (CoeffVi ≤ CoeffVp) aortic roots and those with ‘asymmetric’ (CoeffVi > CoeffVp) aortic roots. Example of a symmetric and of an asymmetric aortic root is demonstrated (Figure 3).

Transthoracic Echocardiography (TTE)

Measurements of the aortic root on TTE were recorded by an experienced echocardiographer blinded to the corresponding CMR measurements. According to accepted practice guidelines set out by the American Society of Echocardiography and the European Society of Cardiology (8), measurements were made in the parasternal long axis acoustic window, perpendicular to the long axis of the vessel, in the plane and phase demonstrating the largest diameter of the sinuses of Valsalva (with measurement calipers placed from inner edge to inner edge).

Statistical Analysis

Descriptive analyses were used to summarize patient demographics and aortic root measurements. Continuous variables were described using means (± standard deviation [SD]) or medians (with ranges), as appropriate, while categorical variables were described using frequencies and percentages.

Intra- and inter-observer reproducibilities, for systolic and diastolic aortic root CMR measurements, were explored using the intra-class correlation coefficient (ICC). Agreement between the TTE and CMR measurements was assessed using Bland and Altman plots generated for the

entire population as well as for subgroups based on aortic root asymmetry. The paired t-test was used to compare the difference between TTE and the largest CMR measurement according to symmetry versus asymmetry of the aortic root. A p-value of < 0.05 was considered statistically significant.

RESULTS

A total of 101 patients were identified, however 33 patients were excluded (due to lack of adequate cross-sectional views of the aortic root [n=27] and prior aortic root intervention [n=6]). A total of 68 patients (44 males [65%], mean age 31.8±10.5 years) were studied. Contemporary TTE imaging was available in 48 patients (71%) with median of 62 days (range 0-179) between CMR and TTE. All CMR and TTE studies were deemed technically adequate for image analysis.

Associated diagnoses included current or previous aortic coarctation (n=46, 68%), hypoplastic aortic arch (n=6, 9%), patent ductus arteriosus (n=6, 9%), ventricular septal defect (n=2, 3%) and Shone complex (n=2, 3%). Morphology of the BAV, as determined by CMR, was most commonly right-left coronary cusp fusion (n=42, 62%), followed by
right-non coronary cusp fusion (n=8, 12%) and left-non coronary cusp fusion (n=1, 1%). Fusion at 2 commisures was seen in a subset of patients (n=12, 18%) and all had right-left as well as right-non coronary cusp raphae. A “pure” BAV (2 cusps only with no discernable raphae) was present in a minority of patients (n=5, 7%).

CMR and TTE Imaging

On CMR, systolic measurements were consistently larger than corresponding diastolic values (Table 1) and cusp-cusp dimensions were larger than respective cusp-commissure measurements (Table 1). Similar observations were made in the "pure" BAV subset of patients (n=5) with mean systolic and diastolic cusp-cusp measurements 33.4 mm (±4.2) and 32.6 mm (±4.3), respectively; mean systolic and diastolic commissure-commissure measurements 27.5 mm (±2.7) and 24.2 mm (±3.1), respectively; and mean systolic and diastolic aortic root areas 774 mm^2 (±176) and 726 mm (±173), respectively. On TTE, mean aortic root diameter in the parasternal long axis view was 33.7 mm (± 6.2).

Intra- and Inter-observer Reproducibility

Intra and inter-reader reproducibility for aortic root measurements obtained from CMR were calculated for the 63 patients with at least one raphe in one analysis. Due to the small number of patients with a "pure" BAV morphology (5 patients), intra and inter-reader reproducibility could not be reliably calculated for this subset. The intra-reader reproducibility for each of the 6 CMR measurements of aortic root diameter and aortic root area in 63 patients was excellent, with ICC ≥0.986 for all measures (Table 2). Inter-reader reproducibility was moderate for 2D aortic root diameter measurements but was excellent for the aortic root areas, with ICC ≥ 0.944 for the latter (Table 2).

Relationship between CMR and TTE Measurements

There was a statistically significant difference between the TTE and the

largest CMR measurement, with TTE measurements consistently smaller than CMR measurements, irrespective of root symmetry or phase of the cardiac cycle (Table 3). When considering the entire study population (symmetric and asymmetric roots), the systematic error between TTE and CMR for *systolic* cusp-commisure and cusp-cusp measurements was 2.1 and 3.9 mm, respectively; the systematic error between TTE and CMR for *diastolic* cusp-commisure and cusp-cusp measurements was 1.0 and 2.9 mm, respectively (Figure 4). The magnitude of the mean bias and limits of agreement between TTE and CMR values was most affected by root asymmetry but not necessarily by plane of measurement (cusp-commissure or cusp-cusp diameters) or phase of the cardiac cycle (systole or diastole) (Figure 5). Of note, the largest systematic error between TTE and CMR (4.9 mm) was observed for asymmetric roots using cusp-cusp measurements in systole; conversely the smallest bias was observed in symmetric roots with cusp-commissure measurements in diastole (-0.01 mm) (Figure 5).

DISCUSSION

This is the first study to demonstrate that CMR measurements of the aortic root in patients with BAV are highly reproducible, irrespective of measurement type or phase of the cardiac cycle. It is notable, however, that, despite good agreement between CMR and TTE measurements, standard TTE dimensions are almost invariably smaller than those derived from CMR, and we found that differences were most striking in those with asymmetric aortic roots. This novel observation may have important implications when determining suitability and timing for surgery on the aorta, as management

guidelines are based on thresholds of aortic size that are predominantly derived from echocardiographic data. Finally, the emergence of the aortic root area as the most reliable measurement within and between observers suggests that this value may be a robust parameter for longitudinal evaluation of progressive enlargement of the aortic root in patients with BAV.

The term “bicuspid aortic valve” encompasses a broad spectrum of aortic valve morphologic phenotypes unified by the common feature that the valve does not fully open to 3 commissures. Although the “pure” form of BAV is composed of only 2 completely developed cusps, 2 sinuses of Valsalva and 2 commissures, the most frequently encountered phenotype consists of 3 cusps and 3 sinuses of Valsalva with 1 or 2 malformed or obliterated commissures, giving rise to a fibrous ridge called a raphe (12). It is not surprising, therefore, that an asymmetric aortic root can arise from a malformed cusp (and corresponding sinus of Valsalva) which tends to be larger than the others. Consequently, measurements of root diameter may vary considerably depending on orientation of the measurement plane. Relative asymmetry of the aortic root, with relatively small right-non cusp dimensions, has been described recently in a normal population of adults using CMR imaging (12), and is similarly the smallest measured value in our study (Table 1). Notably, ours is the first study to systematically apply a statistically derived measure of aortic root asymmetry, the co-efficient of variance, to the BAV population.

Measurements obtained from TTE can result in erroneous under-estimation of the true maximal dimension of the aortic root, not only because the standard imaging plane only displays 2 cusps, but the cusps visualized

are typically the right and non-coronary which tend to manifest smaller dimensions as compared with the remainder of the aortic root (12). In contrast, given the multiplanar capabilities of CMR, cross-sectional imaging of the aortic root at the level of the sinuses of Valsalva can be readily obtained enabling evaluation of the morphology of all cusps with subsequent selection of the largest cusp-cusp or cusp-commissure diameter. It is not surprising, therefore, that the greatest discrepancy between TTE and CMR in our study occurred in the valves with the greatest degree of asymmetry.

In this study, we demonstrate that TTE measures of the aortic root diameter are consistently smaller than those provided by CMR, irrespective of measurement type (cusp-cusp or cusp-commissure) or phase in the cardiac cycle (systole or diastole). Furthermore, we observe that the smallest degree of systematic bias between modalities occurs in symmetric valves, during diastole, using cusp-commissure measurements. This finding is in keeping with recent data from a population of normals, which determined that diastolic cusp-commissure measurements corresponded most closely with “reference” echocardiographic root measurements (recorded in the Framingham cohort) (12). Similarly, we determined that the intra- and inter-reader ICC values for 2-dimensional measures (cusp-cusp and cusp-commissure) were generally better for diastolic measurements as compared with their respective systolic counterparts; we speculate that this may be due to less flow artifact in diastole allowing for more precise vessel wall-blood pool definition as compared with the systolic phase which may demonstrate significant spin dephasing in the context of a stenotic valve with accelerated. Given the striking ICC values for diastolic aortic root area measurements for inter-reader and intra-reader

reproducibility (ICC 0.950 and 0.998, respectively), we hypothesize that this measure may be the optimal surveillance parameter for determination of progressive aortic root enlargement.

An increase in CMR utilization for evaluation of aortopathy has occurred in recent years given increased availability and general improvements in spatial and temporal resolution allowing for superior visualization of valve and arch morphology. CMR is currently regarded as the reference standard for evaluation of aortic dimensions and is indicated for evaluation of aortopathy (valve and ascending aorta) as well as monitoring of disease progression over time (6, 7, 13). Nonetheless, there is a surprising paucity of data regarding interpretation and incorporation of CMR-derived measurements into clinical decision making processes for patients with aortopathy related to BAV. In a cohort of 80 patients referred for aortic valve replacement (importantly only 32 patients with BAV), Joziasse et al (14) demonstrated that CMR may be more sensitive but less specific than TTE for the delineation of BAV morphology and that TTE underestimates aortic arch dimensions (specifically the ascending aorta) in comparison to CMR but that a single maximal root measurement at the sinuses of Valsalva on CMR was not significantly different than the TTE measurement. Of note, only limited information regarding orientation or location of the acquired CMR measurements was provided in their study (14). In contrast, with detailed cross-sectional measurements of the aortic root in short axis using CMR (cusp-cusp and cusp-commissure orientations), we found a consistent discrepancy between CMR and TTE values. Additionally, we exclusively evaluated adults with BAV, unlike the Joziasse study where the majority of

patients did not have BAV and, therefore, the effect of aortic root asymmetry in patients with BAV in relation to CMR and TTE measurements may have been diluted within the larger study population (14).

Electrocardiographic-gated multidetector computed tomography (MDCT) has also been increasingly used to evaluate the aortic root due to its excellent spatial resolution and multiplanar reformat capability. In line with our findings, studies using MDCT have described discrepancies between short axis measurements of the oval-shaped aortic annulus and TTE-derived measurements (15) and have also demonstrated differences in aortic root dimensions related to the phase of the cardiac cycle (i.e., systole or diastole) (16). The major disadvantages of CT in comparison to MR imaging are the use of iodinated contrast media and ionizing radiation. Long term surveillance of aortic root dimensions in a relatively young population of patients with BAV may be problematic given the concerns related to the long term effects of cumulative exposure to ionizing radiation due to repeated CT examinations (17).

Precision of aortic measurement is paramount for optimal management of patients with aortopathy related to BAV. This is because criteria which may invoke surgical intervention include aortic root/ ascending aorta dimensions > 50 mm and/or rapid expansion of the aorta > 5 mm/year (6, 13). As shown in this study, CMR can not only provide reproducible data in the context of a BAV, but can also demarcate asymmetry and increased root size at the level of the sinuses of Valsalva, which can be masked by standard TTE views. Despite these apparent strengths, caution should be applied when interpreting CMR-derived root dimensions, because current management algorithms,

which incorporate absolute aortic measures, have been created primarily from data derived from echocardiography (4). If and how CMR-measurements can be incorporated into clinical management strategies has not yet been elucidated. It seems that CMR imaging would provide useful additional data if an aorta was found to be enlarged on screening echocardiography. However, further research initiatives with a prospective construct could better clarify the role of CMR in determination of appropriate timing for surgical intervention.

The present study has some limitations, which should be recognized. In this retrospective study, TTE studies contemporaneous with CMR studies were not available in all patients, although they were available in the majority (n=48, 71%). TTE and CMR were generally not performed on the same day but instead within a 6-month time frame which was deemed clinically acceptable by the study investigators (median time difference between CMR and TTE studies was 62 days). Although the time difference between CMR and TTE studies may have introduced a minor degree of error, we believe that this would have negligible impact given that the average rate of progression for the BAV population is 0.2 mm/year (2). Additionally, given the relatively low number of patients with valve morphology other than right-left or right-non coronary raphe, the reproducibility of each measurement could not be related to the specific subtype of BAV. Similarly, it was not possible to stratify the correlation between TTE and CMR measurements based on valve morphology. As well, due to the lack of a standardized definition of aortic root asymmetry, we developed a novel, statistically derived, expression of asymmetry, the co-efficient of variance, so that the aortic root diameters of an individual can be related to the remainder of the population. Consequently,

no single cut-off value could be generated for application to other populations. It should also be recognized that there is no accepted “gold standard” for aortic dimensions with which to compare TTE and CMR measurements. Finally, the evaluation of patients with a broader spectrum of disease, such as those with larger aortic roots than the ones studied here, those with BAV not associated with other aortic pathology, and/or those with other forms of aortopathy with higher risk for dissection, such as Marfan or Loeys-Dietz syndrome, would likely be very informative.

CONCLUSIONS

In adults with BAV, CMR derived measurements of the aortic root dimensions, from cusp-to-commissure and from cusp-to-cusp show excellent intra-observer and moderate inter-observer reproducibility. Aortic root area measurements have excellent intra- and inter-observer reproducibility and as such, may be ideal for longitudinal evaluation of patients with BAV. Although there is relatively good agreement between CMR and TTE derived measurements of the aortic root at the level of the sinuses of Valsalva, TTE consistently underestimates maximum aortic root diameter as compared with CMR, and aortic root asymmetry further decreases the agreement between CMR and TTE measurements. Minimal systematic bias between modalities occurs measurements are made from cusp-to-opposite commissure, in symmetric valves, during diastole. These observations may have relevance for determination of timing for surgical intervention for aortic root dilation.

FUNDING SOURCES: None.

DISCLOSURES: None.

REFERENCES

1. Siu SC, Silversides CK. Bicuspid Aortic Valve Disease. J Am Coll Cardiol. 2010;55:2789–800.

2. Tzemos N, Therrien J, Yip J, Thanassoulis G, Tremblay S, Jamorski MT, Webb GD, Siu SC. Outcomes in adults with bicuspid aortic valves. JAMA. 2008;300:1317-1325.

3. Zanotti G, Vricella L, Cameron D. Thoracic aortic aneurysm syndrome in children. Semin Thorac Cardiovasc Surg Pediatr Card Surg Annu. 2008;11:11-21.

4. Davies RR, Goldstein LJ, Coady MA, Tittle SL, Rizzo JA, Kopf GS, Elefteriades JA. Yearly rupture or dissection rates for thoracic aortic aneurysms: simple prediction based on size. Ann Thorac Surg. 2002;73:17-27.

5. David TE. Surgical Treatment of Ascending Aorta and Aortic Root Aneurysms. Prog Cardiovasc Dis. 2010;52:438-444.

6. Bonow RO, Carabello BA, Kanu C, de Leon AC Jr, Faxon DP, Freed MD, Gaasch WH, Lytle BW, Nishimura RA, O'Gara PT, O'Rourke RA, Otto CM, Shah PM, Shanewise JS, Smith SC Jr, Jacobs AK, Adams CD, Anderson JL, Antman EM, Faxon DP, Fuster V, Halperin JL, Hiratzka LF, Hunt SA, Lytle

BW, Nishimura R, Page RL, Riegel B. ACC/AHA 2006 Guidelines for the Management of Patients With Valvular Heart Disease: A Report of the American College of Cardiology/American Heart Association Task Force on Practice Guidelines (Writing Committee to Revise the 1998 Guidelines for the Management of Patients With Valvular Heart Disease): Developed in Collaboration With the Society of Cardiovascular Anesthesiologists: Endorsed by the Society for Cardiovascular Angiography and Interventions and the Society of Thoracic Surgeons. Circulation. 2006;114:e84-231.

7. Pennell DJ, Sechtem UP, Higgins CB, Manning WJ, Pohost GM, Rademakers FE, van Rossum AC, Shaw LJ, Yucel EK; Society for Cardiovascular Magnetic Resonance; Working Group on Cardiovascular Magnetic Resonance of the European Society of Cardiology. Clinical indications for cardiovascular magnetic resonance (CMR): Consensus Panel report. Eur Heart J. 2004;25:1940-1965.

8. Lang RM, Bierig M, Devereux RB, Flachskampf FA, Foster E, Pellikka PA, Picard MH, Roman MJ, Seward J, Shanewise JS, Solomon SD, Spencer KT, Sutton MS, Stewart WJ; Chamber Quantification Writing Group; American Society of Echocardiography's Guidelines and Standards Committee; European Association of Echocardiography. Recommendations for Chamber Quantification: A Report from the American Society of Echocardiography's Guidelines and Standards Committee and the Chamber Quantification Writing Group, Developed in Conjunction with the European Association of Echocardiography, a Branch of the European Society of Cardiology. J Am Soc

Echocardiogr. 2005;18:1440-1463.

9. Braverman AC, Güven H, Beardslee MA, Makan M, Kates AM, Moon MR. The Bicuspid Aortic Valve. Curr Probl Cardiol. 2005;30:470-522.

10. Groth M, Henes FO, Müllerleile K, Bannas P, Adam G, Regier M. Accuracy of thoracic aortic measurements assessed by contrast enhanced and unenhanced magnetic resonance imaging. Eur J Radiol. 2011 Feb 8. [Epub ahead of print]

11. Sievers HH, Schmidtke C. A classification system for the bicuspid aortic valve from 304 surgical specimens. J Thorac Cardiovasc Surg. 2007;133:1226-1233.

12. Burman ED, Keegan J, Kilner PJ. Aortic root measurement by cardiovascular magnetic resonance: specification of planes and lines of measurement and corresponding normal values. Circ Cardiovasc Imaging. 2008;1:104-113.

13. Hiratzka LF, Bakris GL, Beckman JA, Bersin RM, Carr VF, Casey DE Jr, Eagle KA, Hermann LK, Isselbacher EM, Kazerooni EA, Kouchoukos NT, Lytle BW, Milewicz DM, Reich DL, Sen S, Shinn JA, Svensson LG, Williams DM; American College of Cardiology Foundation/American Heart Association Task Force on Practice Guidelines; American Association for Thoracic Surgery; American College of Radiology; American Stroke Association;

Society of Cardiovascular Anesthesiologists; Society for Cardiovascular Angiography and Interventions; Society of Interventional Radiology; Society of Thoracic Surgeons; Society for Vascular Medicine. 2010 ACCF/AHA/AATS/ACR/ASA/SCA/SCAI/SIR/STS/SVM Guidelines for the Diagnosis and Management of Patients With Thoracic Aortic Disease: A Report of the American College of Cardiology Foundation/American Heart Association Task Force on Practice Guidelines, American Association for Thoracic Surgery, American College of Radiology, American Stroke Association, Society of Cardiovascular Anesthesiologists, Society for Cardiovascular Angiography and Interventions, Society of Interventional Radiology, Society of Thoracic Surgeons, and Society for Vascular Medicine. Circulation. 2010;121;e266-369.

14. Joziasse IC, Vink A, Cramer MJ, van Oosterhout MF, van Herwerden LA, Heijmen R, Sieswerda GT, Mulder BJ, Doevendans PA. Bicuspid stenotic aortic valves: clinical characteristics and morphological assessment using MRI and echocardiography. Neth Heart J. 2011;19:119-125.

15. Ng AC, Delgado V, van der Kley F, Shanks M, van de Veire NR, Bertini M, Nucifora G, van Bommel RJ, Tops LF, de Weger A, Tavilla G, de Roos A, Kroft LJ, Leung DY, Schuijf J, Schalij MJ, Bax JJ. Comparison of aortic root dimensions and geometries before and after transcatheter aortic valve implantation by 2- and 3-dimensional transesophageal echocardiography and multislice computed tomography. Circ Cardiovasc Imaging. 2010;3:94-102.

16. de Heer LM, Budde RP, Mali WP, de Vos AM, van Herwerden LA, Kluin J. Aortic root dimension changes during systole and diastole: evaluation with ECG-gated multidetector row computed tomography. Int J Cardiovasc Imaging. 2011;27:1195-1204.

17. Brenner DJ, Hall EJ. Computed tomography-an increasing source of radiation exposure. N Engl J Med. 2007;357:2277-2284.

Figure Legends:

Figure 1. The short axis oblique cine-SSFP view of the aortic root, at the sinus level (C), was obtained based on a prescription derived from two complimentary views, the coronal localizer SSFP image (A) and on the left ventricular outflow tract 3-chamber cine-SSFP view (B).

Figure 2. Single short axis oblique cine-SSFP diastolic (A, C) and systolic (B, D) frames of the aortic root at the sinus level. Cusp-cusp (dashed lines) and cusp-commissure (solid lines) measurements in the aortic root with 3 distinct cusps (A, B) and cusp-cusp (solid lines) and commissure-commissure (solid lines) measurements in the "pure" bicuspid aortic valve (C,D).

Figure 3. Single short axis oblique cine-SSFP systolic (A,C) and diastolic (B,D) frames of the aortic root at the sinus level demonstrating a symmetric (CoeffVi < CoeffVp) (A,B) and an asymmetric (CoeffVi > CoeffVp) (C,D) aortic roots for both cusp-commissure and cusp-cusp dimensions.
CoeffVi, coefficient of variance for an individual; CoeffVp, coefficient of variance for the entire population.

Figure 4. Bland and Altman plots of the difference in aortic root diameter derived from transthoracic echocardiography (TTE) and cardiovascular magnetic resonance imaging (CMR) as a function of average measurements (symmetric and asymmetric roots) in 48 patients. TTE versus maximal systolic

(top row) and maximal diastolic (bottom row) cusp-to-commissure (left column) and cusp-to-cusp (right column) CMR measurements.

Figure 5. Bland and Altman plot of the difference in aortic root diameter between transthoracic echocardiography (TTE) and cardiovascular magnetic resonance imaging (CMR) as a function of the average of systolic (top two rows) and diastolic (bottom two rows) measurements in symmetric (left column) and asymmetric (right column) aortic roots in 48 patients.

Table 1. Cusp-cusp, cusp-commissure and aortic root area measurements derived from CMR*.

Measurement	Systole	Diastole
RCC-LCC (mm)	34.2 ± 5.8	32.9 ± 5.4
LCC-NCC (mm)	37.1 ± 5.9	35.9 ± 5.8
NCC-RCC (mm)	36.5 ± 6.0	35.2 ± 5.7
RCC-commissure (mm)	32.9 ± 5.4	30.7 ± 5.1
LCC-commissure (mm)	34.2 ± 5.6	32.1 ± 5.3
NCC-commissure (mm)	35.5 ± 5.6	34.3 ± 5.5
Aortic Root Area (mm^2)	982 ± 301	893 ± 277

Data presented as mean ± SD

*, 63 patients with at least one raphe.

CMR, cardiovascular magnetic resonance; RCC, right coronary cusp; LCC, left coronary cusp; NCC, non coronary cusp;

Table 2. Intra and inter-reader reproducibility of CMR measurements of the aortic root.

	Intra-reader Reproducibility *		Inter-reader Reproducibility †	
Measurement	**ICC (CI 95%)**	**ICC (CI 95%)**	**ICC (CI 95%)**	**ICC (CI 95%)**
	Systole	**Diastole**	**Systole**	**Diastole**
LCC – Com	0.997 (0.995, 0.998)	0.998 (0.996, 0.999)	0.831 (0.227, 0.951)	0.872 (0.688, 0.952)
RCC – Com	0.995 (0.992, 0.997)	0.997 (0.995, 0.998)	0.368 (-0.141, 0.717)	0.819 (0.576, 0.930)
NCC – Com	0.993 (0.989, 0.996)	0.998 (0.996, 0.999)	0.643 (-0.079, 0.892)	0.697 (0.135, 0.896)
LCC- NCC	0.997 (0.996, 0.998)	0.988 (0.981, 0.993)	0.619 (-0.093, 0.888)	0.869 (0.087, 0.968)
RCC- NCC	0.997 (0.995, 0.998)	0.997 (0.995, 0.998)	0.643 (-0.059, 0.908)	0.620 (0.048, 0.862)
RCC- LCC	0.997 (0.995, 0.998)	0.986 (0.977, 0.991)	0.883 (0.643, 0.959)	0.731 (0.408, 0.893)
Aortic Root Area	0.999 (0.998, 0.999)	0.998 (0.997, 0.999)	0.944 (0.449, 0.986)	0.950 (0.870, 0.981)

*, 63 patients with a least one raphe;

†, 17 patients.

CMR, cardiovascular magnetic resonance; Com, opposite commissure; ICC, intra-class correlation coefficient; LCC, left coronary cusp; NCC, non-coronary cusp; RCC, right coronary cusp.

Table 3. Comparison between CMR and TTE measurements of the aortic root in systole and diastole according to root asymmetry *, †.

Mean difference between CMR and TTE measurements	All Mean (95% CI)	Symmetric ‡ Mean (95% CI)	Asymmetric Mean (95% CI)	*P* value §
Systole (mm)	3.9 (3.2, 4.6)	3.3 (2.5, 4.2)	4.4 (3.2, 5.7)	< 0.001
Diastolie (mm)	2.8 (2.1, 3.7)	2.3 (1.3, 3.4)	3.4 (2.2, 4.6)	< 0.001

*, 48 patients;

†, see text for definition of aortic root asymmetry using the co-efficient of variance;

‡, number of symmetric aortic roots in systole (n=26) and in diastole (n=28);

§ , paired t-test, for comparison between symmetric and asymmetric aortic roots.

CMR, cardiovascular magnetic resonance imaging; TTE, transthoracic echocardiography.

Figure 1.

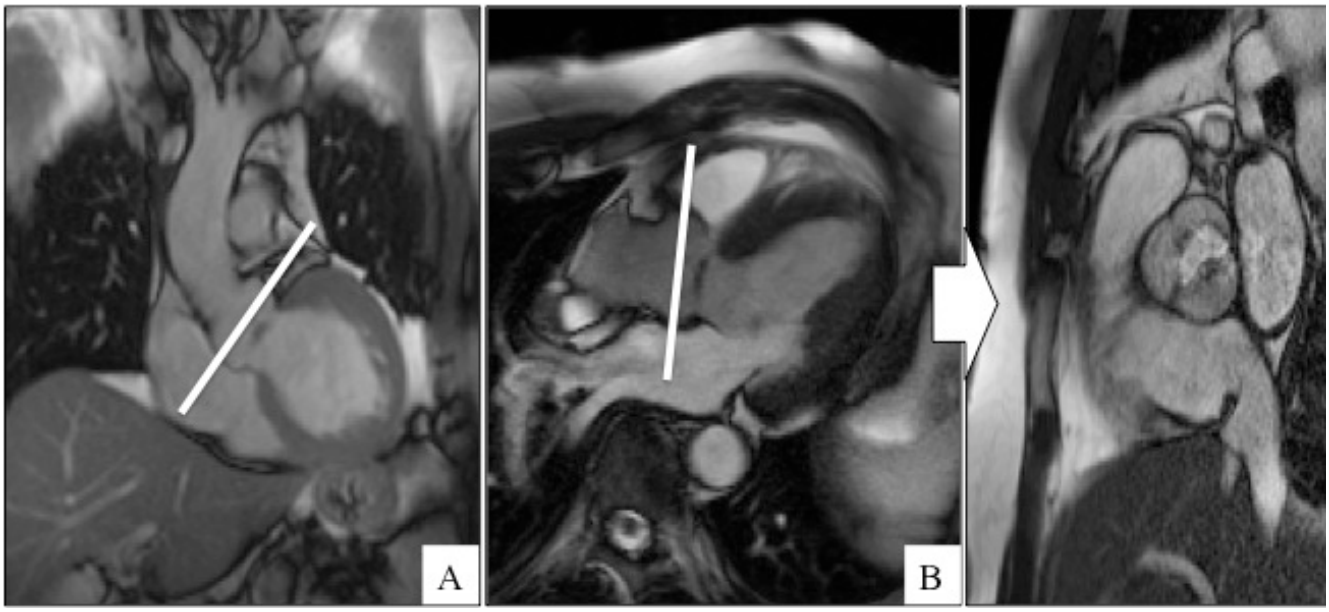

Figure 2.

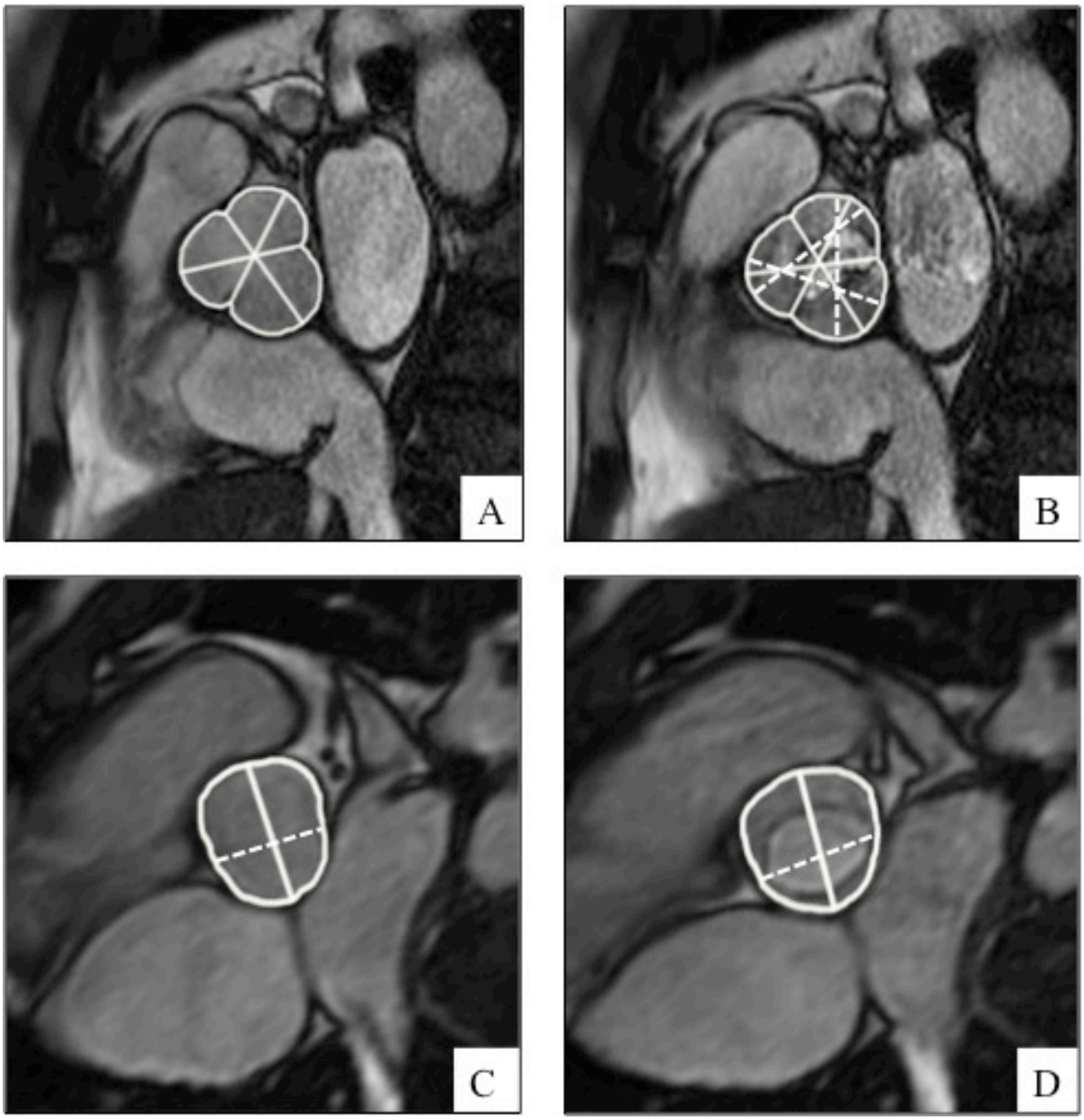

Figure 3.

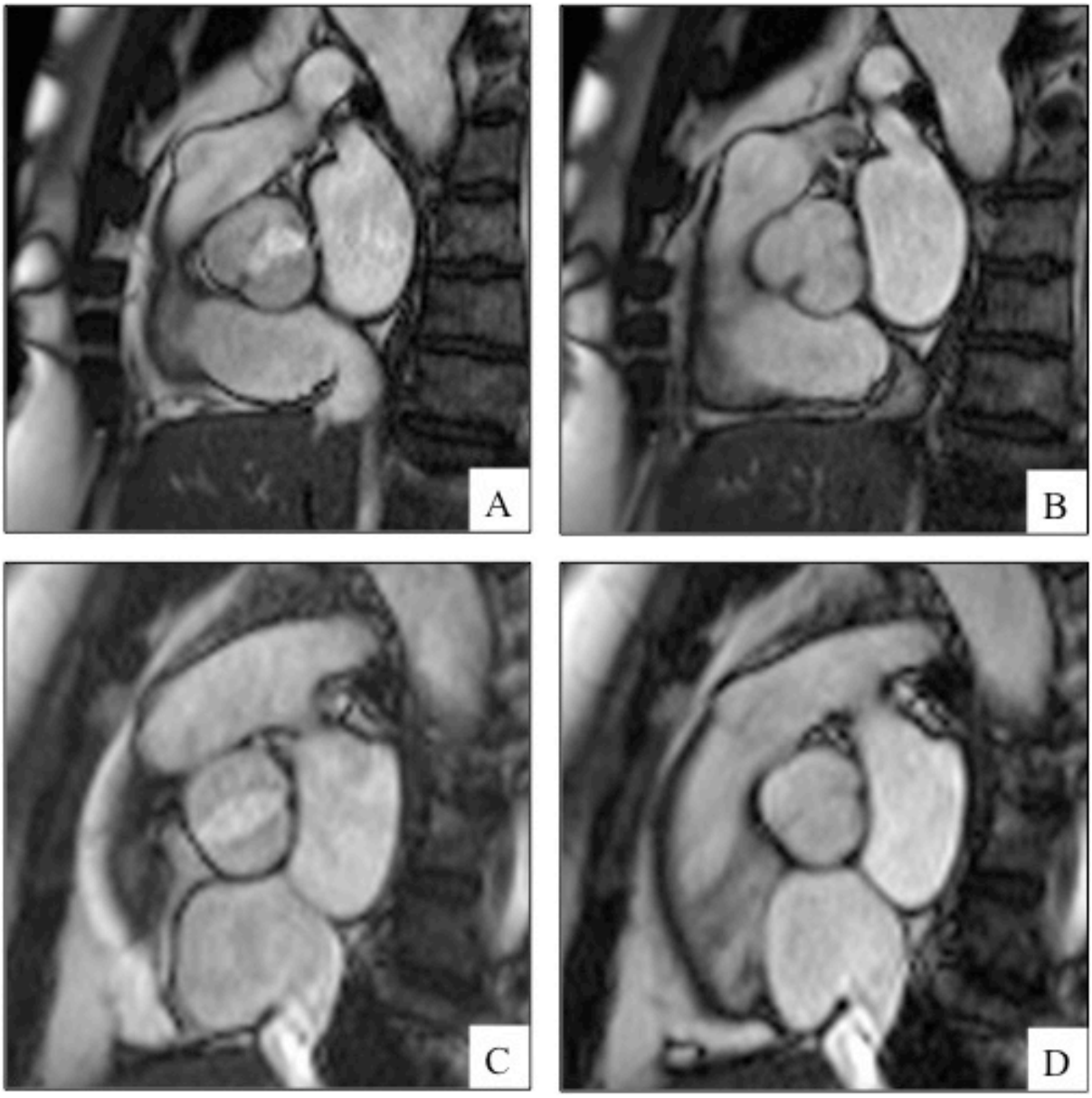

Figure 4.

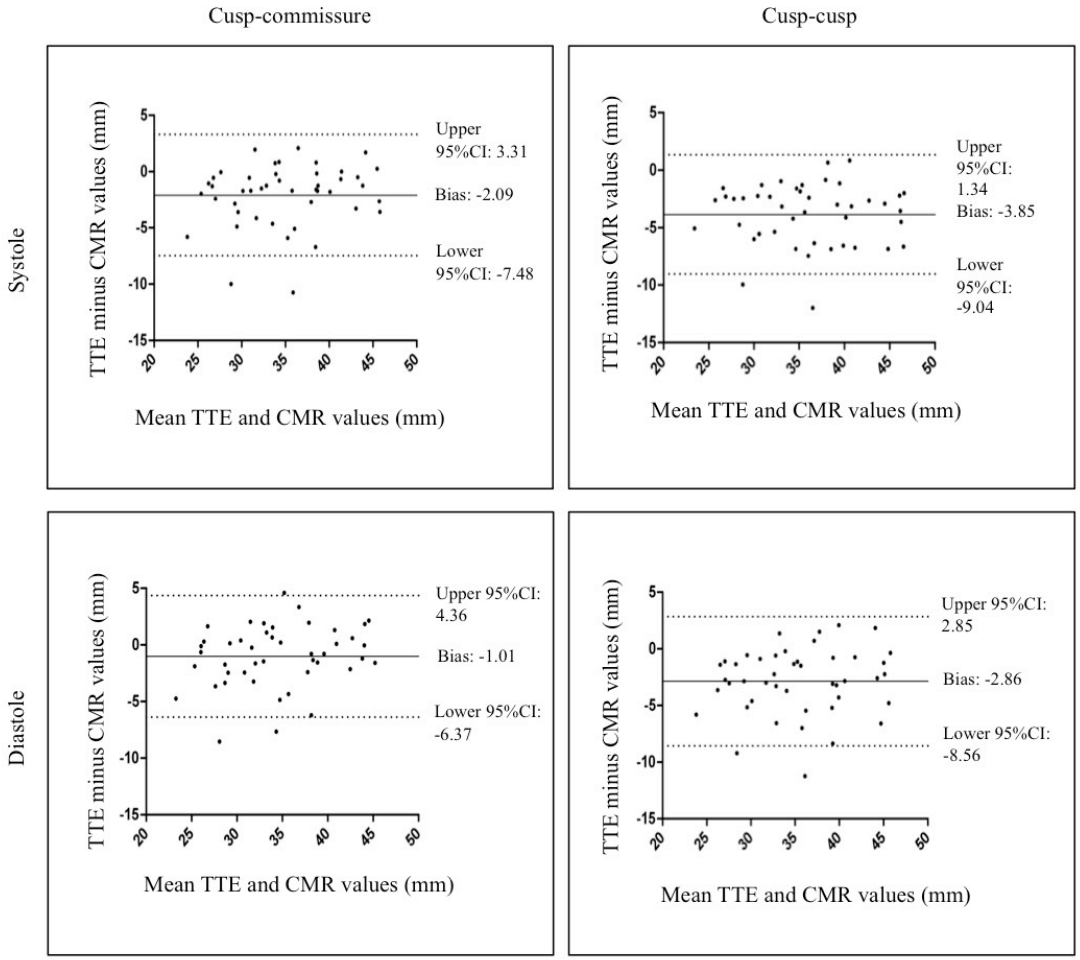
Cusp-commissure
Cusp-cusp
Systole
Diastole
TTE minus CMR values (mm)
Mean TTE and CMR values (mm)
Upper 95%CI: 3.31
Bias: -2.09
Lower 95%CI: -7.48
Upper 95%CI: 1.34
Bias: -3.85
Lower 95%CI: -9.04
Upper 95%CI: 4.36
Bias: -1.01
Lower 95%CI: -6.37
Upper 95%CI: 2.85
Bias: -2.86
Lower 95%CI: -8.56

Figure 5.

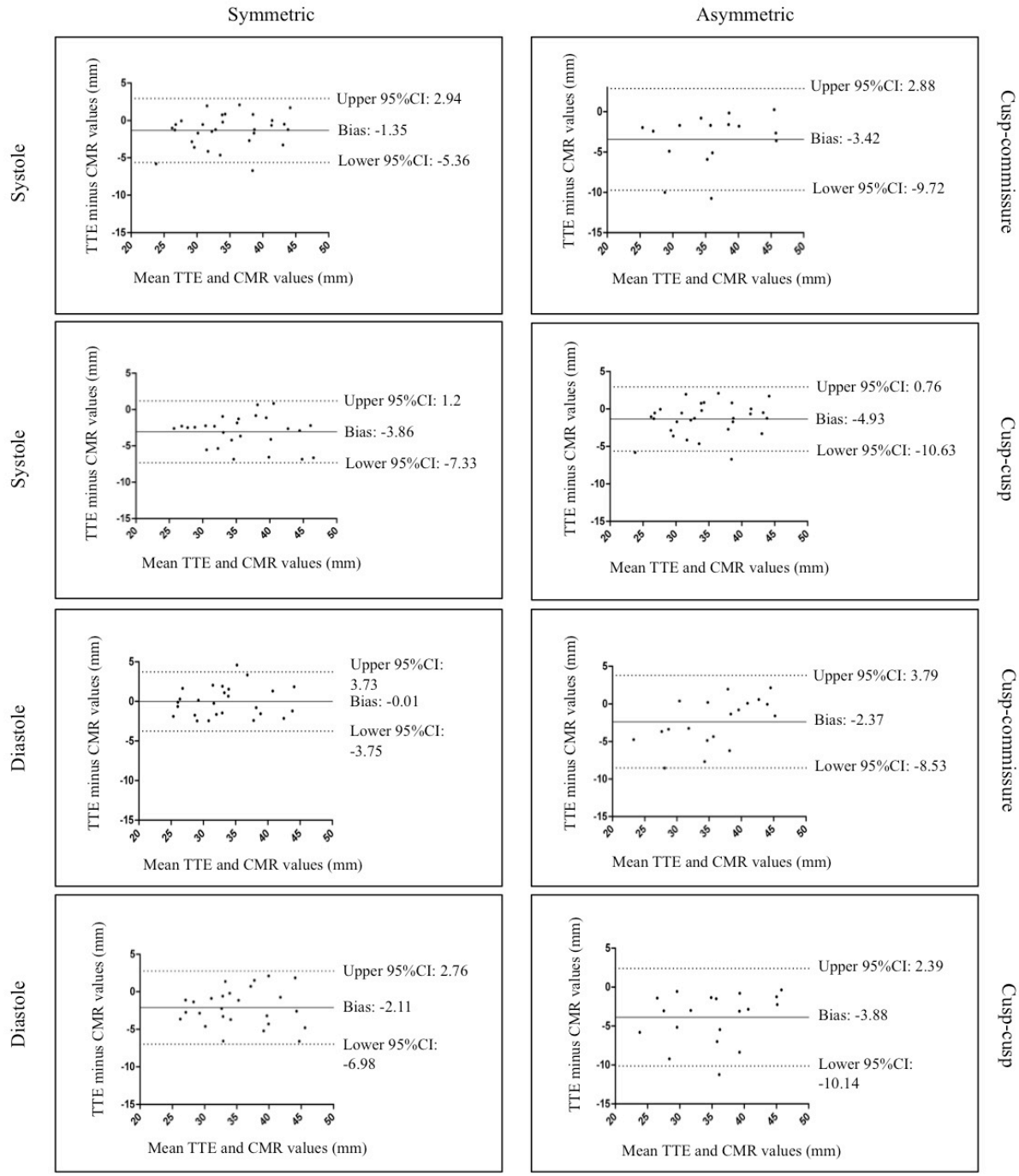
Symmetric
Asymmetric
Systole
Diastole
Cusp-commissure
Cusp-cusp
TTE minus CMR values (mm)
Mean TTE and CMR values (mm)
Upper 95%CI: 2.94
Bias: -1.35
Lower 95%CI: -5.36
Upper 95%CI: 2.88
Bias: -3.42
Lower 95%CI: -9.72
Upper 95%CI: 1.2
Bias: -3.86
Lower 95%CI: -7.33
Upper 95%CI: 0.76
Bias: -4.93
Lower 95%CI: -10.63
Upper 95%CI: 3.73
Bias: -0.01
Lower 95%CI: -3.75
Upper 95%CI: 3.79
Bias: -2.37
Lower 95%CI: -8.53
Upper 95%CI: 2.76
Bias: -2.11
Lower 95%CI: -6.98
Upper 95%CI: 2.39
Bias: -3.88
Lower 95%CI: -10.14